

ISSN 0280-5316
ISRN LUTFD2/TFRT--5553--SE

Adaptive Control of Systems with Backlash

David Angeli

Department of Automatic Control
Lund Institute of Technology
February 1996

Department of Automatic Control Lund Institute of Technology P.O. Box 118 S-221 00 Lund Sweden		<i>Document name</i> MASTER THESIS	
		<i>Date of issue</i> February 1996	
		<i>Document Number</i> ISRN LUTFD2/TFRT--5553--SE	
<i>Author(s)</i> David Angeli		<i>Supervisors</i> K. J. Åström	
		<i>Sponsoring organisation</i>	
<i>Title and subtitle</i> Adaptive Control of Systems with Backlash.			
<i>Abstract</i> <p>Backlash is often present in mechanical transmission systems and can be one of the main causes that severely limit control systems performances. In this work are presented a number of adaptive algorithms that through a proper feedforward nonlinear action try to compensate the backlash. Due to the nonlinear nature of the problem, convergency proofs are very difficult; nevertheless simulations showed a good behavior in most parameters settings both with the explicit and the implicit approach.</p>			
<i>Key words</i>			
<i>Classification system and/or index terms (if any)</i>			
<i>Supplementary bibliographical information</i>			
<i>ISSN and key title</i> 0280-5316			<i>ISBN</i>
<i>Language</i> English	<i>Number of pages</i> 84	<i>Recipient's notes</i>	
<i>Security classification</i>			

Contents

1. Introduction	3
2. Backlash and Backlash inverse	7
2.1 Systems and their properties	7
2.2 Backlash definition	8
2.3 Backlash inverse	12
3. Adaptive backlash inversion	14
3.1 Plant and Controller structure	14
3.2 Backlash inverse estimation	15
3.3 Plant and backlash estimate: implicit approach	26
3.4 Plant and backlash estimate: explicit approach	39
4. Adaptive backlash inversion through a dynamic system	46
4.1 Backlash inversion through a dynamic block	46
4.2 Plant and Controller structure	48
4.3 Dynamic backlash inversion: implicit approach	49
4.4 Non linear observer	62
4.5 Dynamic backlash inversion: explicit approach	68
A. RLS continuous time implementation	80
B. Related works and future research	82
C. Bibliography	84

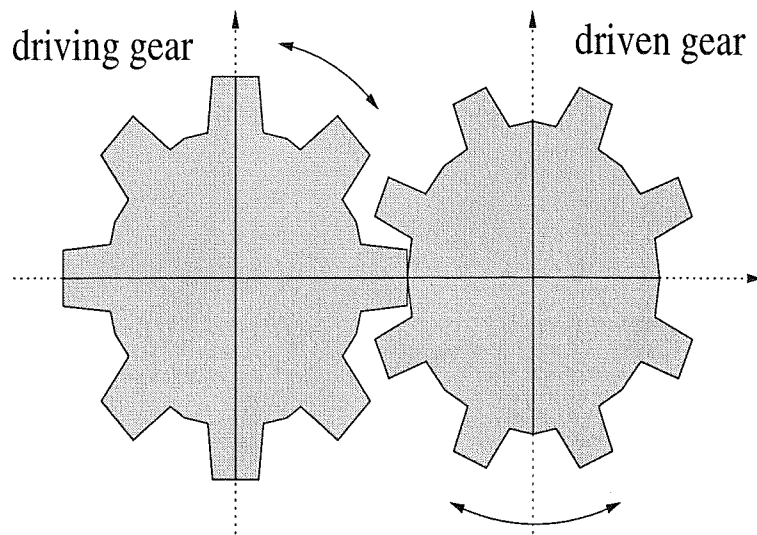


Figure 1.1 Gears with backlash

1. Introduction

Real-world control systems are often affected by a number of non-linear *parasitic effects*. Such effects can include:

- Noise
- Friction
- *Backlash*
- Hysteresis
- Unmodeled resonances
- Time delay
- Saturation
- Dead-zones

These effects are present to some extent in most systems. Whether they are significant and what to do about them is often the question. The most optimistic course is simply to ignore them; a more prudent approach is to include the parasitic effects that might be troublesome in the simulation model of the plant and run the simulation enough times to convince yourself that they are really negligible.

If, on the contrary, they result to affect in a significant way the control system performances, there are some general measures that can be adopted, but the most appropriate remedies are usually tailored to the specific parasitics.

Backlash often occurs in transmission systems. It is caused by the small gaps which exist in a transmission mechanism. In gear trains, there always exist small gaps between a pair of mating gears, due to unavoidable errors in manufacturing and assembly. Figure 1.1 illustrates a typical situation. As a result of the gaps, when the driving gear inverts its rotation the driven gear does not move until the two cuts are newly in contact. Therefore, if the

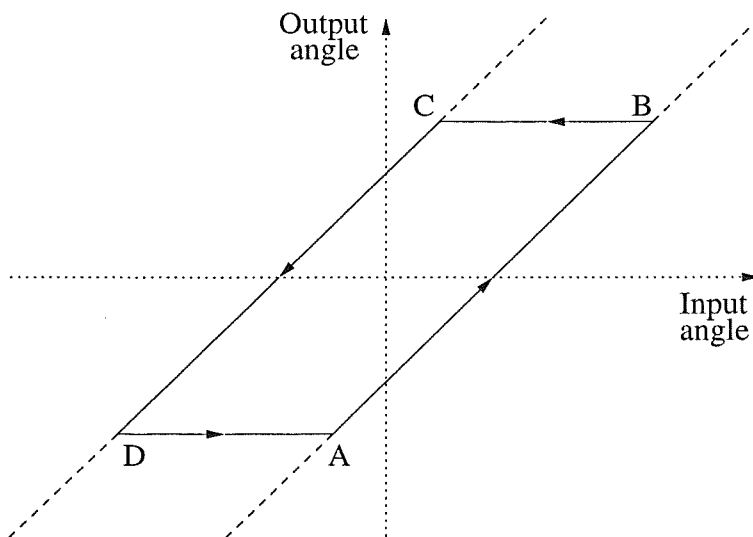


Figure 1.2 A backlash nonlinearity

driving gear is in periodic motion, the driven gear will move along the closed path shown in Figure 1.2.

A rigorous definition of the backlash is presented in the next chapter; here we just want to point out some of its main properties in order to understand the kind of impact it can have on a close-loop system.

A critical feature of backlash is its multi-valued nature. Corresponding to each input we have a closed interval of possible output values, depending on the history of the input. Multi-valued nonlinearities, like backlash and hysteresis usually lead to energy storage in the system. Energy storage is a frequent cause of instability and self-sustained oscillations.

Another way to figure out this effect is considering its frequency domain behavior. As already said, the backlash output at a certain t depends on the input history; in particular a suitable choice for a rigorous backlash definition is to consider its output as a state. Even if these features are in general typical of dynamic systems, still the backlash is a *static* model, in the sense that a rescaling of the temporal axis for the input results in an equal rescaling for the output. In particular this is reflected into the backlash describing function, being the latest *frequency independent*.

The most dangerous feature of backlash with regard to a control system is the time delay introduced by the *deadzone*. It causes in fact a nonzero phase shift on the first harmonic of the output (up to 90°), and this is mainly the effect that can lead the close-loop system to limit cycles and instability.

In Figure 1.3 are plotted the Nyquist diagrams of a second order system $1/(s^2 + 2\xi s + 1)$ for growing values of ξ together with $-1/N(A)$, (where N is the backlash describing function). It is clear that even for open-loop stable system with pronounced resonances the backlash can have some kind of impact on the control performance.

Consider the following open loop system with a stable pole, plus an integral action: $P(s) = K/[s(s+p)]$. We can have two different situations, just varying the gain K . For low gain, we have the phase plane diagram shown in Figure 1.4. Basically the equilibrium point, due to the presence of the backlash dead-zone has become a segment, and we observe self-sustained oscillations with

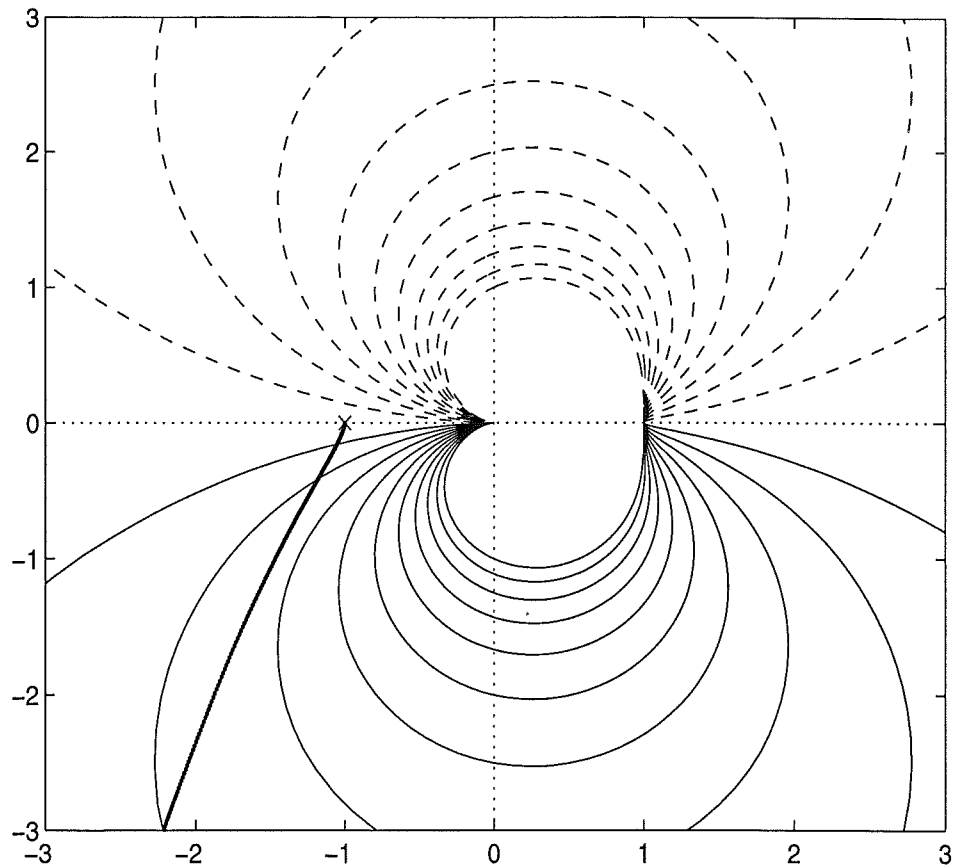


Figure 1.3 *Nyquist diagram of a closed-loop system with backlash*

decreasing frequency along this segment ¹ (see Figure 1.5).

If we increase the gain we have stable limit cycles around the origin; the corresponding phase plane diagram is shown in Figure 1.4. When the open-loop system is unstable, the situation is always more critical; in general, instead of achieving asymptotical tracking of constant references, we see stable limit cycles around the set-up point. In Figure 1.6 is shown this particular effect, for two different backlash widths (namely equal to the 5% and 15% of the backlash input amplitude).

It would be interesting to have control algorithms who can provide some kind of non-linear compensation, in order to improve the performances of our controller, rather than looking for more accurate mechanical components, which in general are very expensive.

There are several features of backlash, and of parasitics in general, that naturally lead to the adoption of an adaptive strategy for the controller. Backlash parameters in fact:

- are often unknown or poorly known;
- vary with tear, wear and temperature;

¹The Figure is just a section of the states space, since we did not plot the backlash internal state.

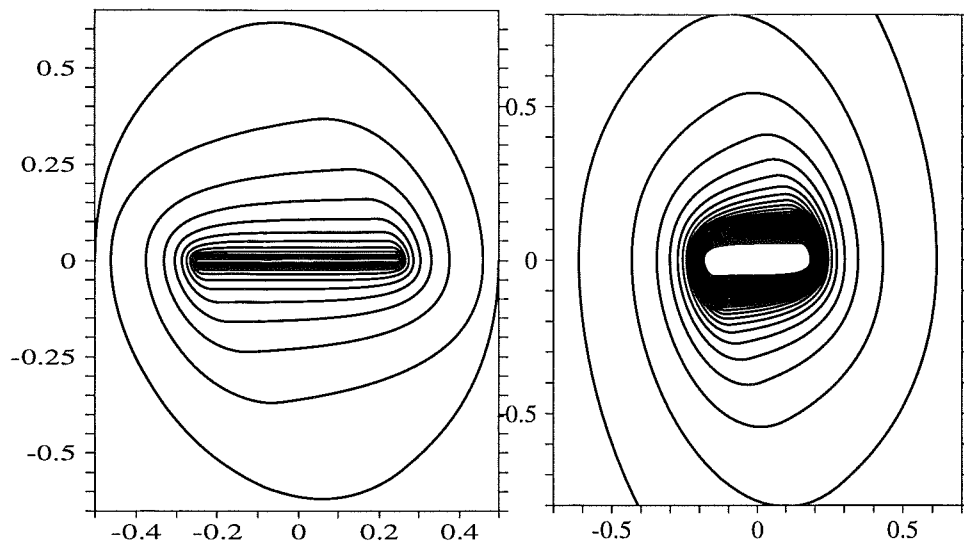


Figure 1.4 *Phase plane diagrams of systems with backlash*

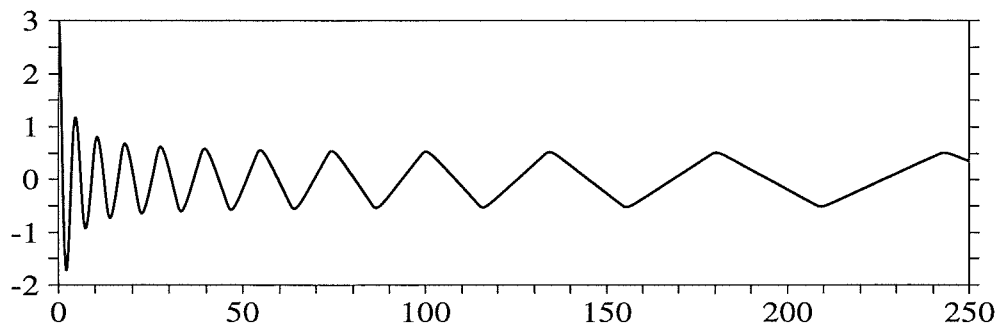


Figure 1.5 *Self-sustained oscillations*

- vary from component to component.

However most adaptive control results are for linear plants or plants with differentiable nonlinearities, and are not applicable to nondifferentiable nonlinearities. With the present work we intend to propose some possible algorithm to adaptively control systems with backlash.

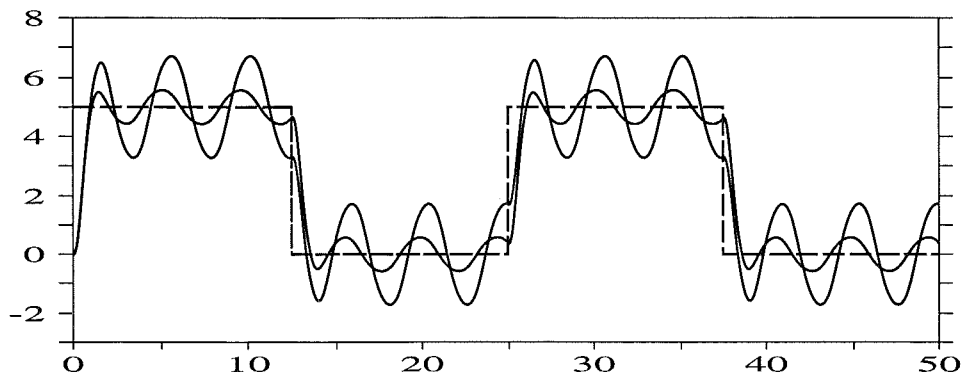


Figure 1.6 *Limit cycles*

2. Backlash and Backlash inverse

Backlash is a complicated phenomenon. Krasnoselsky has developed a mathematical machinery to describe backlash and other hysteresis phenomena (see [4]). In this chapter we introduce his ideas and try to exploit them to define a left backlash inverse (see [1], [2]).

2.1. Systems and their properties

Nonlinearities of backlash type can be regarded as a particular kind of system.

System definition

A system is a mathematical model with a variable input $v(t)$ and a variable output $u(t)$. The evolution of the output of the system is completely determined when it is known the initial state of the system and the input signal.

Short memory system

If the state of a system can be uniquely determined by the values of $\{v(t), u(t)\}$ then the system will be called *short memory system*. We can use a simple notation to denote the output dependence from the initial state and from the input $v(t)$:

$$u(t) = B[t_0, v_0, u_0]v(t)$$

where v_0, u_0 is the system state at t_0 and $B[t_0, v_0, u_0]$ is a functional¹ depending on the initial time and state. If the system is a short memory one then the following *semigroup identity* is true $\forall t_0, t_1, t$ such that $t_0 \leq t_1 \leq t$:

$$B[t_0, v_0, u_0]v(t) = B[t_1, v(t_1), B[t_0, v_0, u_0]v(t_1)]v(t)$$

Autonomous system

Assume that the admissibility of the input $v(t)$ ($t \geq t_0$) at the state $\{v_0, u_0\}$ implies that the input $\bar{v}(t) = v(t - \tau)$ ($t \geq t_0 + \tau$) is admissible at the same state and the equality

$$B[t_0 + \tau, v_0, u_0]\bar{v}(t + \tau) = B[t_0, v_0, u_0]v(t) \quad (t \geq t_0)$$

holds. Then the system B is called *autonomous*. In other words, a system is autonomous if its properties are time-invariant.

¹If we denote with \mathcal{V} the set of admissible inputs, and with \mathcal{U} the set of admissible outputs, then a system is a function $B : \mathcal{V} \longrightarrow \mathcal{U}$. Assume $v \in \mathcal{V}$, then $B[t_0, v_0, u_0]v$ denotes the corresponding $B(v) \in \mathcal{U}$, it is therefore an output signal, while $B[t_0, v_0, u_0]v(t)$ denotes the output signal evaluated at t .

Static system

A system is called *static* if it is autonomous and if the following implication is true $\forall \alpha > 0$:

$$\left. \begin{aligned} \bar{v}(t) &\doteq v(\alpha t + (1 - \alpha)t_0) \\ u(t) &\doteq B[t_0, v_0, u_0]v(t) \\ \bar{u}(t) &\doteq B[t_0, v_0, u_0]\bar{v}(t) \end{aligned} \right\} \Rightarrow \bar{u}(t) = u(\alpha t + (1 - \alpha)t_0)$$

In particular, the system will be static in the case of any function $u = f(v)$.

Controllable system

A static, deterministic system B is *controllable* if for any pair of the feasible states $\{v_0, u_0\}$, $\{v_1, u_1\}$ there exists an input $u(t)$ ($t_0 \leq t \leq t_1$) which is admissible at the initial state $\{v_0, u_0\}$, such that $v(t_0) = v_0$, $v(t_1) = v_1$ and $B[t_0, v_0, u_0]v(t_1) = u(t_1)$.

2.2. Backlash definition

Monotonous input

Let us consider the following strip in \mathbb{R}^2 :

$$\Sigma = \left\{ (v, u) \in \mathbb{R}^2 \text{ such that } v - C_r \leq u \leq v - C_l \right\}$$

where C_l and C_r are two real numbers such that $C_l < C_r$ (see Figure 2.1). Σ is the set of feasible states for the backlash $\mathcal{B}(C_l, C_r)$. In order to define rigorously the backlash output we can first define its output for monotonous input signals. Let $(v_0, u_0) \in \Sigma$ with $v(t)$ monotonous and such that $v(t_0) = v_0$, then we can define

$$B[t_0, v_0, u_0]v(t) \doteq \begin{cases} u_0 & \forall t \text{ such that } u_0 + C_l \leq v(t) \leq u_0 + C_r \\ v(t) - C_l & \forall t \text{ such that } v(t) \leq u_0 + C_l \\ v(t) - C_r & \forall t \text{ such that } v(t) \geq u_0 + C_r \end{cases} \quad (2.1)$$

Notice that this definition satisfies the semi-group identity.

Piecewise monotonous input

For piecewise monotonous inputs, operator B can be defined by using the semi-group identity. To this purpose, the domain of the input $u(t)$ is to be divided into intervals $[t_0, t_1], [t_1, t_2], \dots, [t_{i-1}, t_i], \dots$ of its monotonicity. On the interval $[t_0, t_1]$ we define the output $u(t)$ by the relation 2.1, next we take the pair $\{v(t_1), u(t_1)\}$ as a new initial state and again, by using 2.1 we define the output on $[t_1, t_2]$.

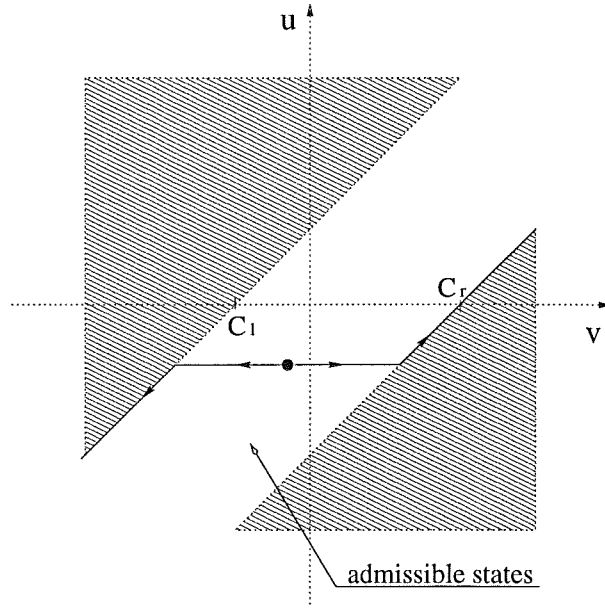


Figure 2.1 Backlash output for a monotonous input.

Continuous inputs

In order to define the backlash output for all continuous inputs we need some estimates for the operator W , with piecewise monotonous inputs. The following estimates hold (see [4]):

Lemma 1

Let the input $v(t)$ ($t_0 \leq t \leq T$) be piecewise monotonous and

$$\{v(t_0), u_0\} \in \Sigma, \quad a \leq v(t) \leq b \quad (t_0 \leq t \leq T).$$

Then

$$\min\{u_0, a - C_l\} \leq B[t_0, v(t_0), u_0]v(t) \leq \max\{u_0, b - C_r\}$$

Lemma 2

Assume piecewise monotonous inputs $v(t)$ and $w(t)$ satisfy the conditions

$$\{v(t_0), u_0\}, \{w(t_0), u_0\} \in \Sigma$$

$$a \leq v(t) \leq b, \quad a \leq w(t) \leq b \quad (t_0 \leq t \leq T)$$

Then

$$\left| B[t_0, v(t_0), u_0]v(t) - B[t_0, w(t_0), u_0]w(t) \right| \leq \sup_{\tau \in [t_0, t]} |v(\tau) - w(\tau)|$$

Proof.

Assume that the assertion of the lemma is not correct, there would exist $\tau_0, \tau_1 \in [t_0, T]$ such that

$$|x(\tau_0) - y(\tau_0)| = \sup_{\tau \in [t_0, \tau_0]} |v(\tau) - w(\tau)| \quad (2.2)$$

and

$$|x(t) - y(t)| > \sup_{\tau \in [t_0, t]} |v(\tau) - w(\tau)| \quad (\tau_0 < t \leq \tau_1) \quad (2.3)$$

where

$$x(t) \doteq B[t_0, v(t_0), u_0]v(t)$$

$$y(t) \doteq B[t_0, w(t_0), u_0]w(t)$$

With no loss of generality one can assume that the functions $v(t)$ and $w(t)$ are monotonous on $[\tau_0, \tau_1]$. For definiteness, let $x(t) > y(t)$ for $\tau_0 < t < \tau_1$. Consider only the case of a non-decreasing input $v(t)$ on $[\tau_0, \tau_1]$ (an analogous treatment would also apply to the case of a non-increasing input). At first, let $x(\tau_0) = v(\tau_0) - C_r$. Then $x(t) = v(t) - C_r$ ($\tau_0 \leq t \leq \tau_1$) and, by the obvious inequality $y(t) \geq w(t) - C_r$ ($\tau_0 \leq t \leq \tau_1$), the estimate

$$x(t) - y(t) \leq v(t) - w(t) \quad (\tau_0 \leq t \leq \tau_1) \quad (2.4)$$

follows, implying that

$$|x(t) - y(t)| \leq |v(t) - w(t)| \quad (\tau_0 \leq t \leq \tau_1) \quad (2.5)$$

The previous relation contradicts 2.3, thus the inequality $x(\tau_0) > v(\tau_0) - C_r$ is true. Consequently, for the values t which are close to τ_0 and larger, the output signal $x(t)$ assumes the constant value $x(\tau_0)$. By 2.3 and 2.2 it follows that the function $y(t)$ is non-increasing and for the same range of time instants t it assumes values less than $y(\tau_0)$. This means that the function $w(t)$ is non-increasing and $y(t) = w(t) - C_l$ ($\tau_0 \leq t \leq \tau_1$). Hence, in view of the obvious inequality $x(t) \leq v(t) - C_l$ ($\tau_0 \leq t \leq \tau_1$), the estimate 2.4 follows, yielding also 2.5 which contradicts 2.3.

□

Let $v_*(t)$ ($t \geq t_0$) be a continuous input and $(v_*(t_0), u_0) \in \Sigma$. Consider any arbitrary sequence $v_n(t)$ ($t \geq t_0$) of piecewise monotonous continuous inputs which converge to $v_*(t)$ uniformly on any finite interval $[t_0, T]$ and satisfy the condition $\{v_n(t_0), u_0\} \in \Sigma$. Let

$$u_n(t) \doteq B[t_0, v_n(t_0), u_0]v_n(t) \quad (t \geq t_0; n = 1, 2, \dots)$$

Due to Lemma 2 we have

$$\|u_n(t) - u_m(t)\|_\infty \leq \|v_n(t) - v_m(t)\|_\infty$$

on any interval $[t_0, T]$. Therefore $u_n(t)$ is a Cauchy sequence and it converges uniformly to some function $u_*(t)$ ($t_0 \leq t \leq T$). We define

$$B[t_0, v(t_0), u_0]v_*(t) \doteq u_*(t)$$

Figure 2.2 shows the input-output characteristic of backlash.

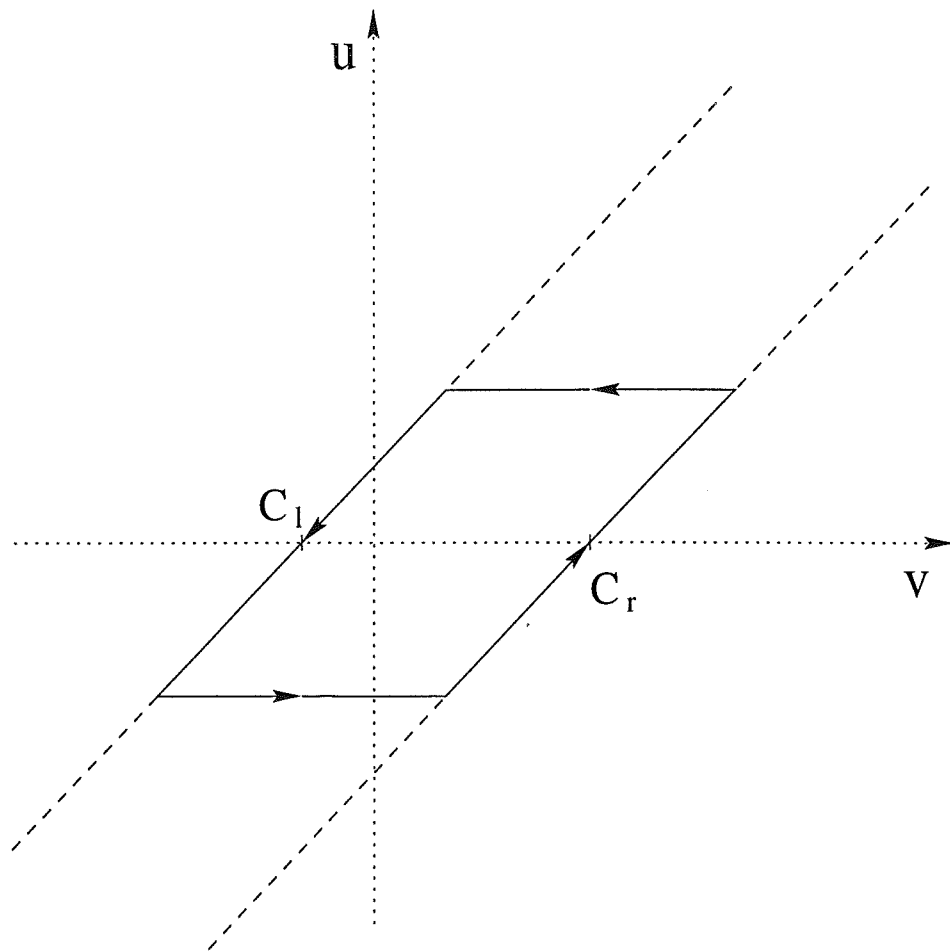


Figure 2.2 *Backlash*

Theorem

The backlash, defined for all continuous inputs, is a *short-memory, static and controllable system*.

2.3. Backlash inverse

The most damaging effect of backlash on system performance is the delay corresponding to the time needed to traverse the inner horizontal segment. This causes a kind of irreversibility which implies that the system cannot be inverted. In order to achieve the backlash inversion we must basically prevent it from operating in the dead-zone.

$$v(t) \doteq u_d(t) + \omega(t) \quad (2.6)$$

where

$$\omega(t) \doteq \begin{cases} C_r & \text{if } \dot{u}_d > 0 \\ C_l & \text{if } \dot{u}_d < 0 \\ \omega(t_-) & \text{if } \dot{u}_d = 0 \end{cases}$$

If we look at the previous definition we see that, whenever the input derivative changes its sign the output signal jumps with the amplitude $C_r - C_l$, corresponding to the backlash width. The following Lemma holds:

Backlash inverse lemma

Equation 2.6 defines the inverse $BI(\cdot)$ of the backlash $B(\cdot)$, in the sense that

$$B[BI[u_d(t_0)]] = u_d(t_0) \Rightarrow B[BI[u_d(t)]] = u_d(t) \quad \forall t \geq t_0$$

for any piecewise continuous $u_d(t)$.

We can define a backlash inverse that handle discontinuities in the following way.

Let $u_d(t)$ be discontinuous at t_ω , define the sequence of continuous functions

$$u_n(t) \doteq \begin{cases} u_d(t), & t < t_n^l \\ u_d(t_n^l) + (t - t_n^l) \frac{u_d(t_n^l) - u_d(t_\omega)}{t_n^l - t_\omega}, & t_n^l \leq t < t_\omega \\ u_d(t_n^r) + (t - t_n^r) \frac{u_d(t_n^r) - u_d(t_\omega)}{t_n^r - t_\omega}, & t_\omega < t \leq t_n^r \\ u_d(t), & t > t_n^r \end{cases}$$

where t_n^l and t_n^r are two arbitrary temporal sequences, such that

$$t_n^l < t_\omega < t_n^r, \quad t_n^l \rightarrow t_\omega, \quad t_n^r \rightarrow t_\omega$$

The following equality holds :

$$\lim_{n \rightarrow +\infty} u_n(t) = u_d(t)$$

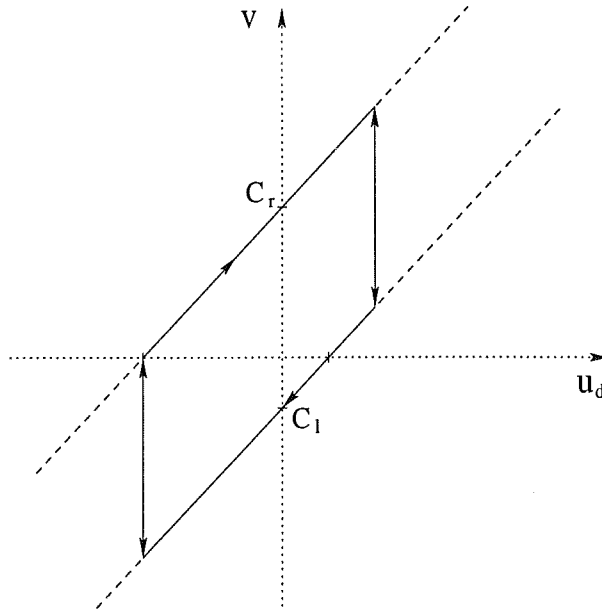


Figure 2.3 *Backlash inverse*

Then we can define the backlash inverse output as

$$BI[u_d(t)] \doteq \lim_{n \rightarrow +\infty} BI[u_n(t)]$$

The backlash inverse characteristic is shown in Figure 2.3.

Notice that the backlash inverse needs the knowledge of the derivative $\dot{u}_d(t)$; it is in some sense a kind of non proper system. When we employ the backlash inverse within a control loop we must be sure that the loop is well-posed. If the plant is strictly proper, we can easily guarantee well-posedness assuming to have feedbacks of the same order of the plant. An alternative is to approximate the derivative operator s with the following filter: $\dot{u}_d(t)$:

$$\dot{u}_d(t) \approx \frac{s}{\tau s + 1} u_d(t)$$

In the following chapters we will always assume $s = \frac{d}{dt}$.

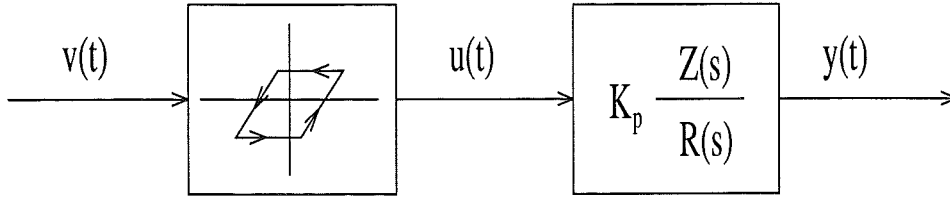


Figure 3.1 Plant structure.

3. Adaptive backlash inversion

Backlash non-linearities in real components are often poorly known, increase with wear and tear, and vary from component to component. It is therefore appealing to have some adaptive strategy to recognize and compensate the damaging effects of backlash on the control loop. In this chapter it is attempted to find control laws that can deal with a backlash with unknown parameters.

3.1. Plant and Controller structure

The structure of the plant that we consider is shown in Figure 3.1. Here we have an ordinary backlash, with unity slope. Let C_r and C_l respectively denote the right and left abscissas of the two intersections with the X axis. The linear part of the plant is described by the strictly causal transfer function $P(s) = K_p Z(s)/R(s)$ where

- $Z(s)$ and $R(s)$ are assumed, without loss of generality, to be monic polynomials, with $\partial R(s) = n$, $\partial Z(s) = m < n$
- K_p is the high frequency gain

We now turn to consider our controller structure (see Figure 3.2). The dynamics of the backlash is canceled by the backlash inverse in front of it, while the resulting linear plant $P(s)$ is controlled with a model reference approach. In order to do that we have to make the following assumptions:

- $Z(s)$ is a Hurwitz polynomial;
- the model reference is $W_m(s) = K_m/R_m(s)$, where $R_m(s)$ is a monic Hurwitz polynomial; furthermore we define $y_m(t) \doteq W_m(s)r(t)$
- the order of $R_m(s)$ is equal to the relative degree of the plant;

If the previous hypotheses are satisfied the controller parameters can be taken so that the closed-loop transfer function equals the model. Technically this is done by solving the following Diophantine equation:

$$\theta_u(s)R(s) + K_p\theta_y(s)Z(s) = \Lambda(s)[R(s) - R_m(s)Z(s)]$$

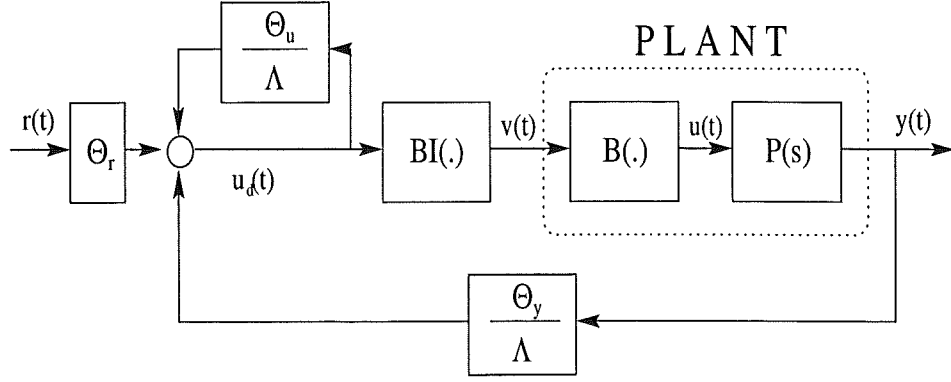


Figure 3.2 Close loop system.

where $\Lambda(s)$ is a stable polynomial of degree n . According to standard control theory if we let $\theta_r = K_m/K_p$ then the following control law:

$$u_d(t) = \frac{\theta_u(s)}{\Lambda(s)} u_d(t) + \frac{\theta_y(s)}{\Lambda(s)} y(t) + \theta_r r(t)$$

gives a vanishing tracking error, i. e.

$$\lim_{t \rightarrow +\infty} y(t) - y_m(t) = 0$$

The problem now is that the backlash is a kind of parasitic effect which is not known a priori, or at least is not exactly known. It is therefore interesting to have an adaptive algorithm which estimates the backlash width. This implies that we only have an approximate inverse of the backlash in the feedback loop.

3.2. Backlash inverse estimation

Output error parametrization

In order to develop an adaptive algorithm we have to see how the output error depends on the error of the backlash parameters estimate. Let us define some indicator¹ functions:

- $\hat{\chi}_r(t) \doteq \chi[u_d(t), v(t)]$ on the upward side of \hat{BI}
- $\hat{\chi}_l(t) \doteq \chi[u_d(t), v(t)]$ on the downward side of \hat{BI} ²
- $\chi_r(t) \doteq \chi[v(t), u(t)]$ on the upward side of backlash]
- $\chi_l(t) \doteq \chi[v(t), u(t)]$ on the downward side of backlash]
- $\chi_s(t) \doteq \chi[v(t), u(t)]$ in the dead zone of backlash]³

$$^1\chi[\text{condition}] = \begin{cases} 1 & \text{when condition is true} \\ 0 & \text{when condition is false} \end{cases}$$

$$^2\hat{\chi}_r(t) + \hat{\chi}_l(t) = 1$$

$$^3\chi_r(t) + \chi_l(t) + \chi_s(t) = 1$$

With this notation it follows that

$$u(t) = \chi_r(t)[v(t) - C_r] + \chi_l(t)[v(t) - C_l] + \chi_s(t)u_s \quad (3.1)$$

where u_s is the value of $u(t)$ when the backlash enters the dead zone. In order to compute the difference $u(t) - u_d(t)$ we must solve for $u_d(t)$ the backlash inverse equation 2.6. After some calculations we get

$$u_d(t) = \hat{\chi}_r(t)[v(t) + \hat{C}_r] + \hat{\chi}_l(t)[v(t) + \hat{C}_l] \quad (3.2)$$

From equations 3.1 and 3.2 we obtain

$$u(t) - u_d(t) = \hat{\chi}_r(t)[\hat{C}_r - C_r] + \hat{\chi}_l(t)[\hat{C}_l - C_l] + d_0(t) \quad (3.3)$$

where

$$d_0(t) = [\chi_r(t) - \hat{\chi}_r(t)][v(t) - C_r] + [\chi_l(t) - \hat{\chi}_l(t)][v(t) - C_l] + \chi_s(t)u_s$$

Introduce

$$\theta_b(t) \doteq \begin{pmatrix} \hat{C}_r \\ \hat{C}_l \end{pmatrix} \quad \theta_b^* \doteq \begin{pmatrix} C_r \\ C_l \end{pmatrix} \quad \omega_b(t) \doteq \begin{pmatrix} \hat{\chi}_r(t) \\ \hat{\chi}_l(t) \end{pmatrix}$$

the equation 3.3 becomes

$$u(t) - u_d(t) = [\theta_b(t) - \theta^*]^T \omega_b(t) + d_0(t) \quad (3.4)$$

The following proposition holds:

Proposition.

The unparametrizable part $d_0(t)$ of the control error $u(t) - u_d(t)$ is bounded for any t .

Proof.

There are three different cases to be examined:

1. if $\chi_l(t) = 1, \chi_r(t) = 0, \chi_s(t) = 0$, then

$$d_0(t) = \begin{cases} 0 & \text{for } \hat{\chi}_l = 1, \hat{\chi}_r = 0 \\ C_r - C_l, & \text{for } \hat{\chi}_l = 0, \hat{\chi}_r = 1; \end{cases}$$

2. if $\chi_l(t) = 0, \chi_r(t) = 1, \chi_s(t) = 0$, then

$$d_0(t) = \begin{cases} 0 & \text{for } \hat{\chi}_l = 0, \hat{\chi}_r = 1 \\ C_l - C_r, & \text{for } \hat{\chi}_l = 1, \hat{\chi}_r = 0; \end{cases}$$

3. if $\chi_l(t) = 0, \chi_r(t) = 0, \chi_s(t) = 1$, then

$$d_0(t) = \begin{cases} u_s - v(t) + C_l, & \text{for } \hat{\chi}_l = 1, \hat{\chi}_r = 0 \\ u_s - v(t) + C_r, & \text{for } \hat{\chi}_l = 0, \hat{\chi}_r = 1 \end{cases}$$

Since $\{v(t) - u_s\} \in [C_l, C_r]$ it follows that $d_0(t)$ is always bounded.

□

An upper bound for d_0 is given by the following inequality:

$$|d_0(t)| \leq |\hat{W} - W|$$

where

$$W \doteq C_r - C_l \quad \hat{W} \doteq \hat{C}_r - \hat{C}_l$$

It follows from standard control theory that the output error of the closed loop system can be expressed as

$$e(t) = H(s) \left[(\theta_b(t) - \theta_b^*)^T \omega_b(t) + d_0(t) \right] \quad (3.5)$$

where

$$H(s) \doteq \frac{K_p}{R_m(s)} \left(1 - \frac{\theta_u(s)}{\Lambda(s)} \right)$$

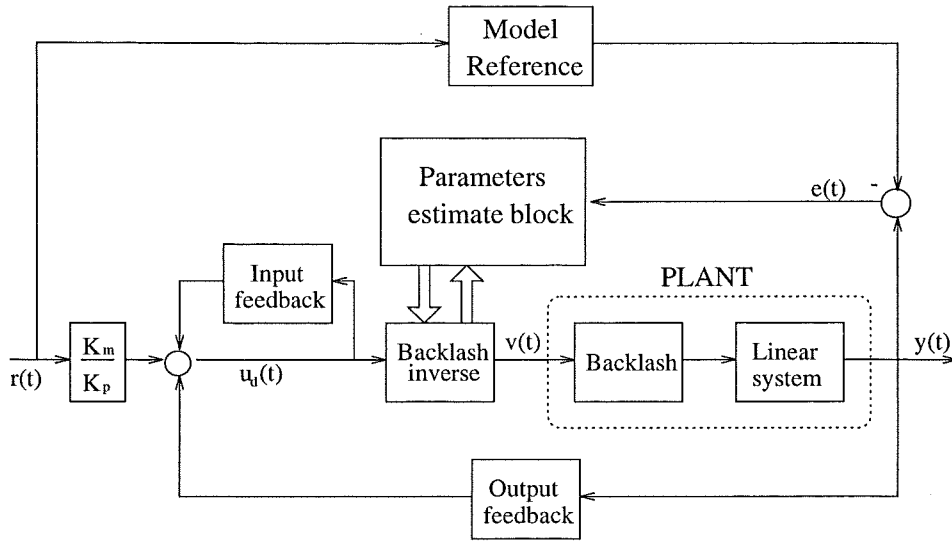


Figure 3.3 The structure of the adaptive controller.

Adaptive law

The linear parametrization of the output error given by equation 3.5 allows us to implement an adaptive law with the augmented error technique. Some robustification is useful to take care of disturbances. The parameters estimate can be updated using the following law:

$$\begin{aligned}\zeta(t) &\doteq H(s) [\omega_b(t)] \\ \xi(t) &\doteq \theta_b(t)^T \zeta(t) - H(s) [\theta_b(t)^T \omega_b(t)] \\ z(t) &\doteq 1 + \zeta(t)^T \zeta(t) + \xi(t)^2\end{aligned}$$

$$\dot{\theta}_b(t) = -\Gamma \zeta(t) \frac{e(t) + \xi(t)}{z(t)} \quad (3.6)$$

Since we have the noise $d_0(t)$ it is not clear that this algorithm produces asymptotic tracking or convergence of the estimates to their matching values. However the boundedness of $d_0(t)$ allows us to prove (*Key technical lemma*) the boundedness of all the signals in the closed-loop system (see [2]). Some simulations results will be given to illustrate what may happen.

We are dealing with a non-linear identification problem, so, it is not a priori clear what kind of "persistent excitation" condition should be imposed to guarantee that the estimates converge or that the tracking error goes to zero. Let us consider a simple backlash model with slope k and width $2b$. If the input is a sine wave $A \sin(\omega t)$ the output is the one shown in Figure 3.4. Let $w(t)$ be the output of the backlash; we can then calculate the phase and amplitude of the first harmonic of this signal in the following way:

$$a_1 = \frac{1}{\pi} \int_{-\pi}^{\pi} w(t) \cos(\omega t) d(\omega t) \quad b_1 = \frac{1}{\pi} \int_{-\pi}^{\pi} w(t) \sin(\omega t) d(\omega t)$$

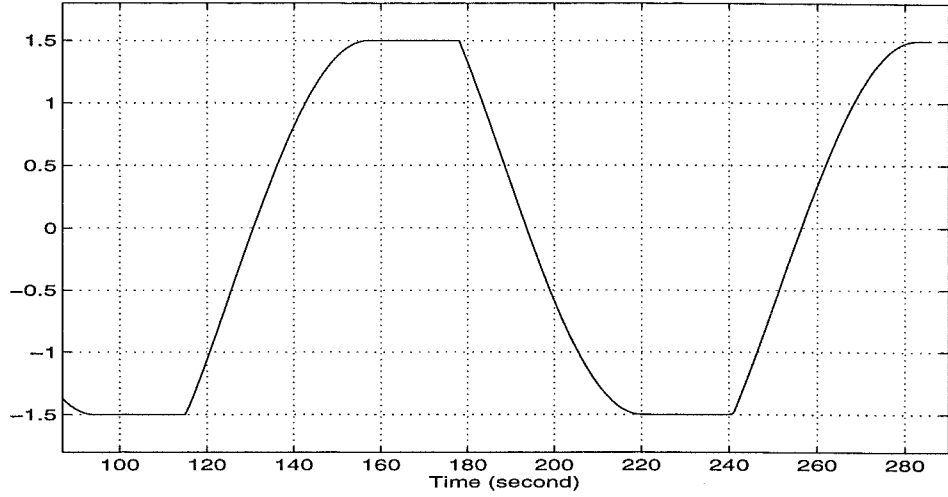


Figure 3.4 Backlash output for a sine wave input.

Then the describing function of the backlash is

$$N(A, \omega) = \frac{b_1 + ja_1}{A}$$

In our case we have

$$a_1 = \frac{4kb}{\pi} \left(\frac{b}{A} - 1 \right)$$

$$b_1 = \frac{Ak}{\pi} \left(\frac{\pi}{2} - \arcsin \left(\frac{2b}{A} - 1 \right) - \left(\frac{2b}{A} - 1 \right) \sqrt{1 - \left(\frac{2b}{A} - 1 \right)^2} \right)$$

$$|N(A)| = \sqrt{a_1^2 + b_1^2}$$

$$\angle N(A) = \arctan \left(\frac{a_1}{b_1} \right)$$

Figures 3.5 and 3.6 show the graphs of the amplitude and of the phase shift of a symmetric backlash with slope and width equal to 1. It is not difficult to see that the first harmonic of the output signal has all the information required to estimate the backlash parameters. From the phase shift it is possible to compute the backlash width. Notice that the phase shift is independent of the slope k . If the width is already known the slope can be computed from the amplitude.

The situation is completely different if the input signal is a square wave. The output is then also a square wave with the same phase as the input signal

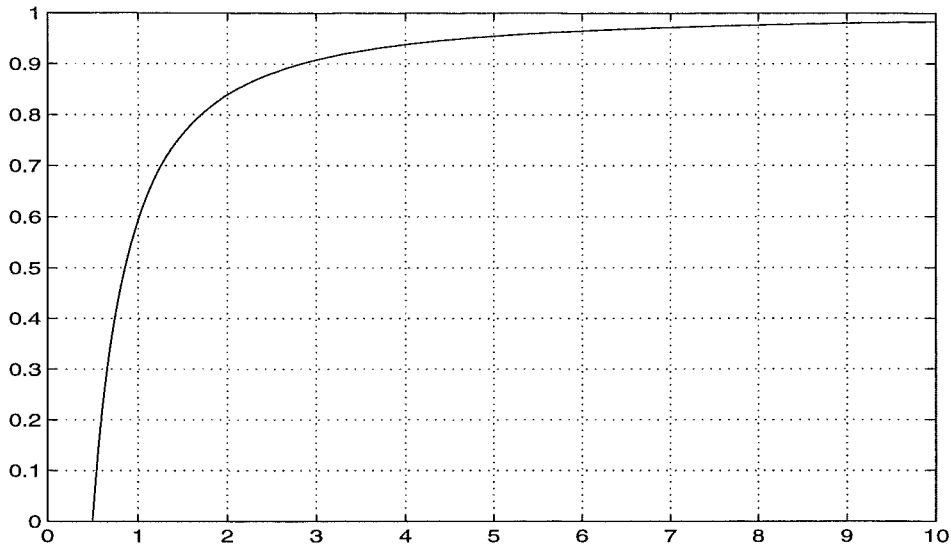


Figure 3.5 *Amplitude of the describing function of backlash*

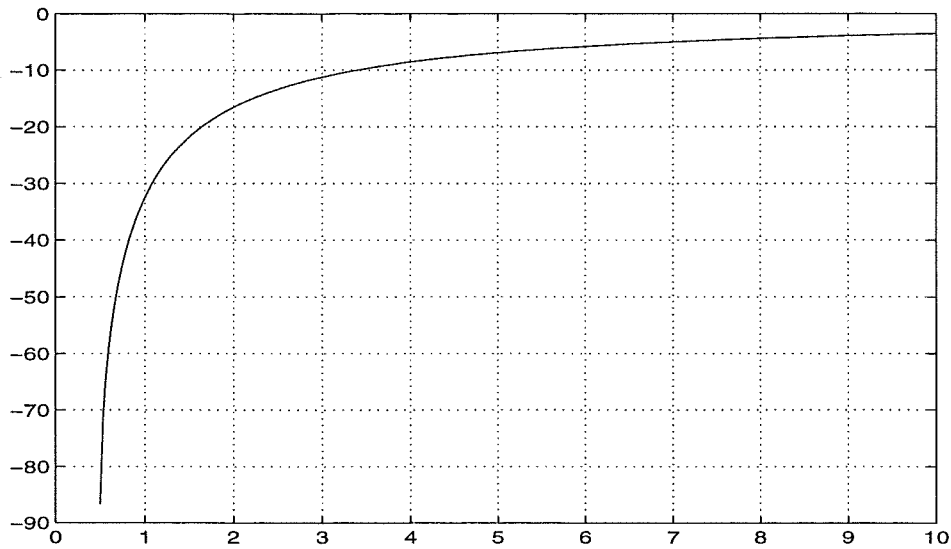


Figure 3.6 *Phase of the describing function of backlash*

but with a different amplitude. In particular the amplitude W of the output signal is given by

$$W = k(A - b)$$

Since we do not have any other “phase shift information” we are not able to explicit the backlash parameters in terms of A and W . This simple observation clearly shows that a square wave is not a “persistently exciting signal” for the system we have been considering. This is true whenever you need to estimate the backlash width together with a static gain.

Simulation results

The first algorithm that we have tested is exactly the same suggested by Kokotovic in [1]; the main difference with respect to the algorithm proposed in this section is that it estimates both the width and the slope of the backlash. Without loss of generality we can include the backlash slope in the high frequency gain of the linear system.

Example 1

Hereby we are considering a second order unstable system. In the absence of a proper backlash compensation we would have limit cycles around the reference signal. In particular Example 1 refers to the following situation:

Linear plant model	$P(s) = \frac{1}{(s-1.5)(s+1)}$
Reference model	$W_m(s) = \frac{\omega^2}{s^2 + 2\xi\omega s + \omega^2} \quad \begin{matrix} \omega = 3 \\ \xi = 0.7 \end{matrix}$
Input signal	$2\sin(2\pi\nu_0 t) \quad \nu_0 = 0.3$
Backlash parameters	$C_r = 2 \quad C_l = -2 \quad slope = 1$
Adaptive law gain	$\Gamma = \begin{pmatrix} 5 & 0 & 0 \\ 0 & 0 & 0 \\ 0 & 0 & 5 \end{pmatrix}$
Feedback polynomial	$\Lambda(s) = (s + 3)^2$

The results are shown in Figure 3.7. The output error, after a brief transient, tends to zero very quickly and the parameters estimates are tuned to their real values. Notice that in this first example we have for simplicity chosen a unitary backlash slope and that the corresponding parameters of the adaptation law has been initialized to its real value. Besides the gain Γ has been set to a low value in order to let clearly understand from the plottings how do the backlash and its adaptive inverse operate.

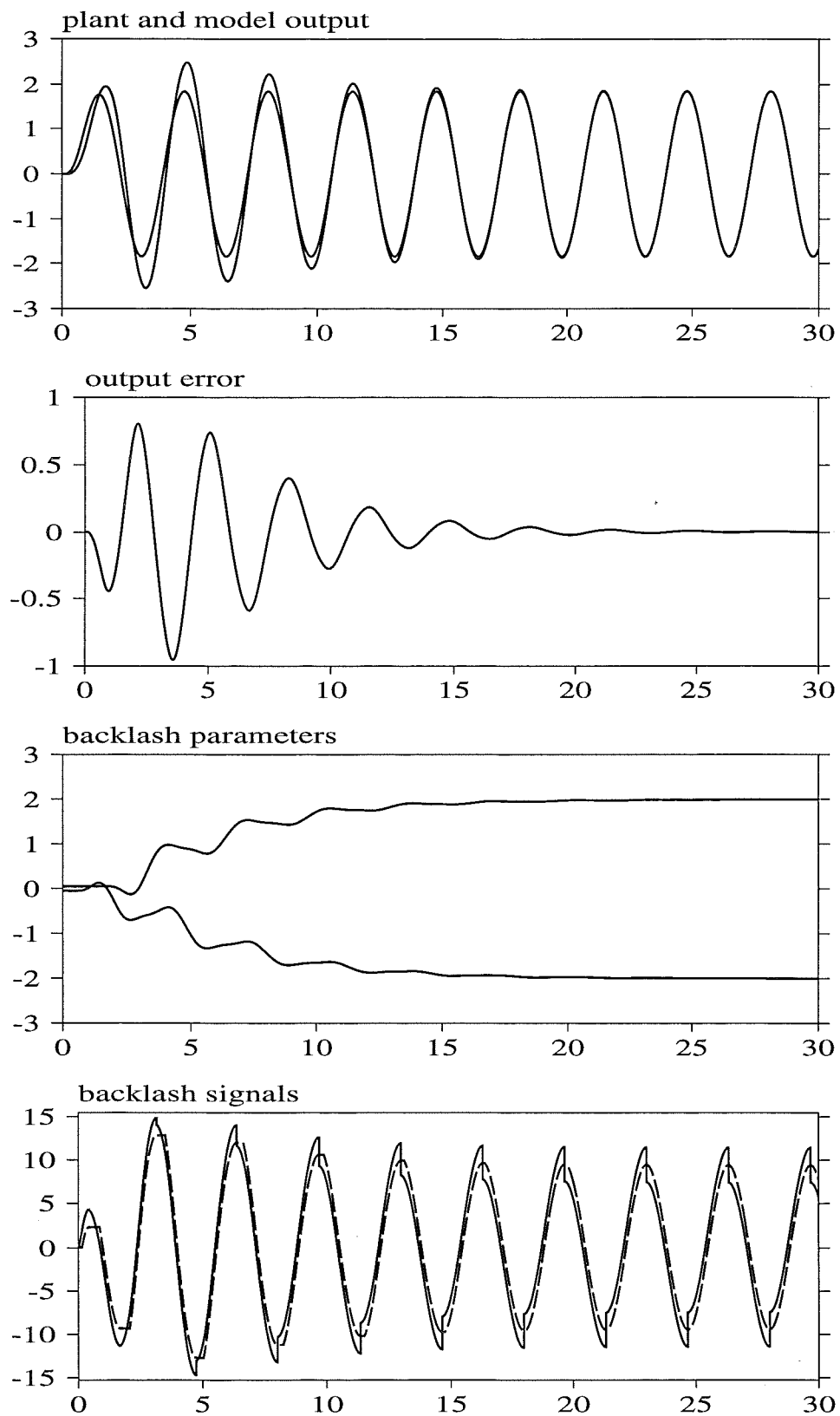


Figure 3.7 *Simulation of Example 1*

Example 2

The second example refers to a different situation, where the backlash width has been decreased and the signal amplitude has been increased. Besides we are now estimating also the slope of the backlash.

Linear plant model	$P(s) = \frac{1}{(s-1.5)(s+1)}$
Reference model	$W_m(s) = \frac{1}{(s+2)(s+3)}$
Input signal	$3 \sin(2\pi\nu_0 t) \quad \nu_0 = 0.3$
Backlash parameters	$C_r = 1 \quad C_l = -1 \quad slope = 3$
Adaptive law gain	$\Gamma = \begin{pmatrix} 5 & 0 & 0 \\ 0 & 5 & 0 \\ 0 & 0 & 5 \end{pmatrix}$
Feedback polynomial	$\Lambda(s) = (s + 3)^2$

Even with very bad initial values for the backlash and gain estimates the convergence has proved to be fast and precise (see Figure 3.8). Notice that as long as we have a phase-shift between the input and the output we are not able to correctly estimate the slope.

Example 3

We have then tried with other wave forms , such as squarewaves, to see if the convergence was equally achieved; the results are shown in Figure 3.9.

Linear plant model	$P(s) = \frac{1}{(s-1.5)(s+1)}$
Reference model	$W_m(s) = \frac{\omega^2}{s^2 + 2\xi\omega s + \omega^2} \quad \begin{matrix} \omega = 3 \\ \xi = 0.7 \end{matrix}$
Input signal	$2.5 + 2.5\text{sign}(\sin(2\pi\nu_0 t)) \quad \nu_0 = 0.1$
Backlash parameters	$C_r = 0.5 \quad C_l = -0.5 \quad slope = 1$
Adaptive law gain	$\Gamma = \begin{pmatrix} 15 & 0 & 0 \\ 0 & 5 & 0 \\ 0 & 0 & 15 \end{pmatrix}$

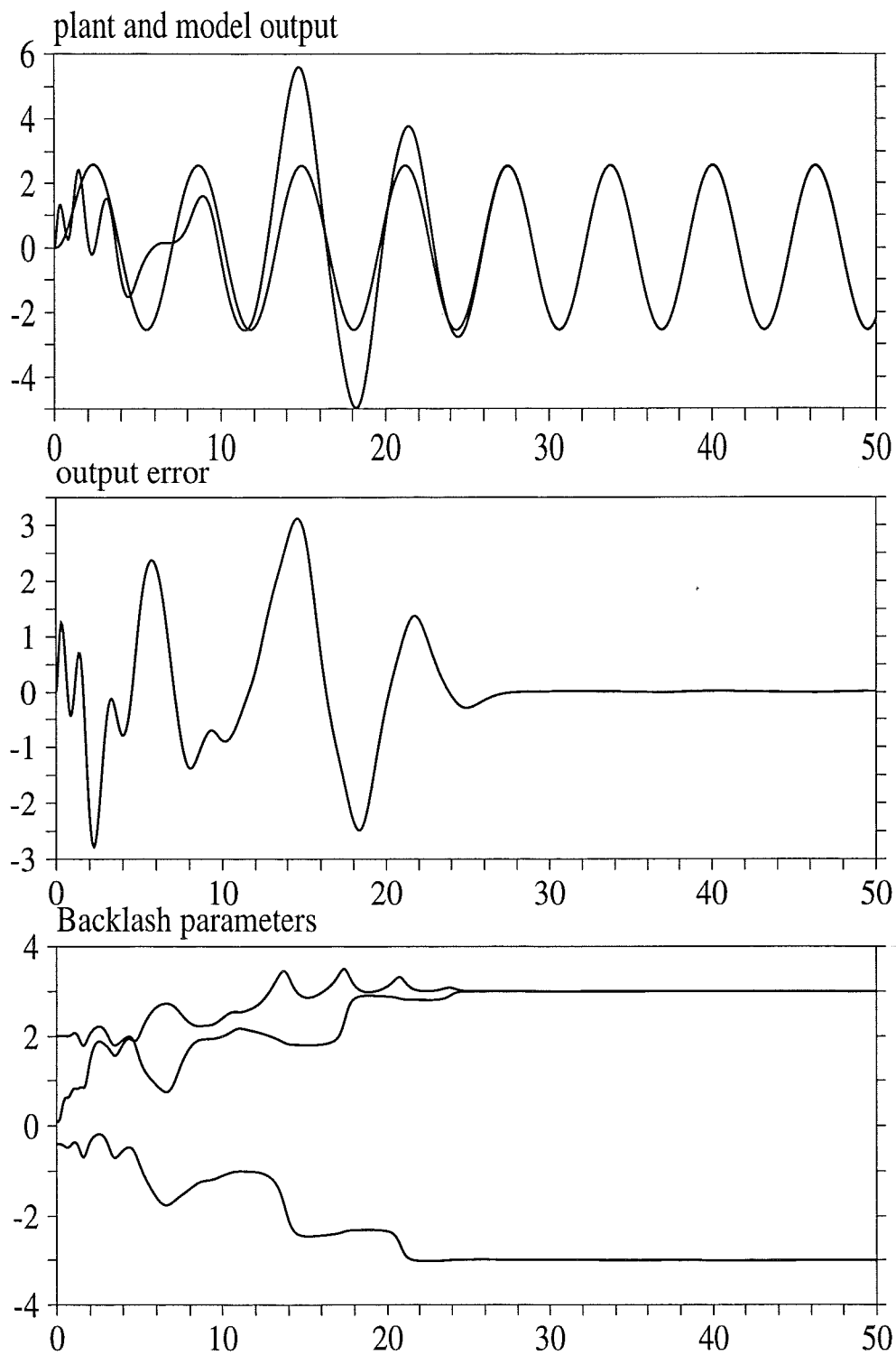


Figure 3.8 Simulation of Example 2

Even if there is not analytical proof of the convergence of this algorithm the simulation results clearly indicates that with sufficient “rich” signals, both asymptotic tracking and estimates convergence is achieved.

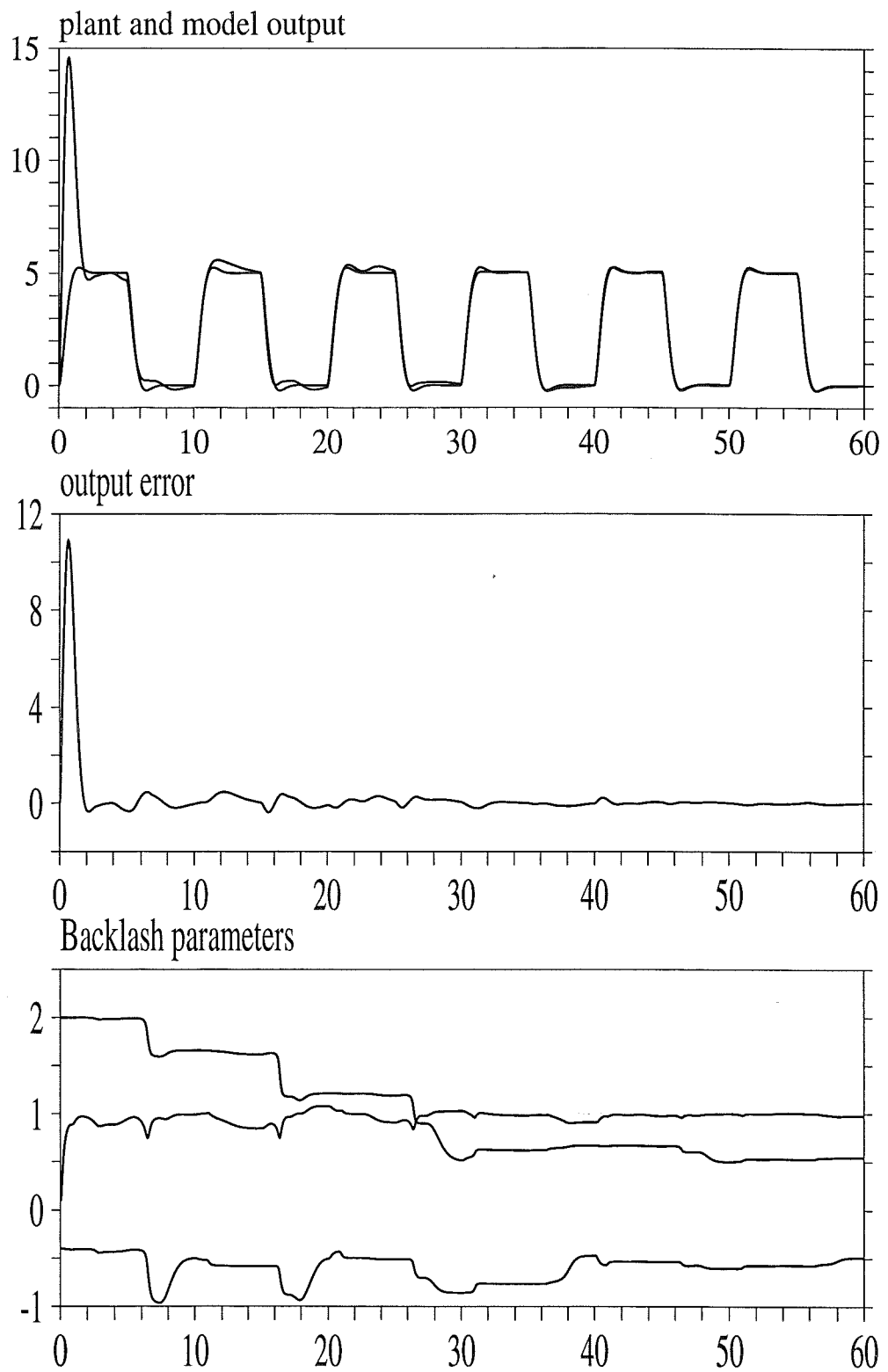


Figure 3.9 Simulation of Example 3

3.3. Plant and backlash estimate: implicit approach

Output error parametrization

One possible direction in which we can generalize Kokotovic algorithm is to consider unknown plant and backlash at the same time. One way to deal with that problem (for the discrete time case) is described in [2]. There are two main limitations of this approach for continuous time systems:

- the controller has many unknown parameters which sometimes are redundant;
- there are algebraic loops that can give chattering and high frequency switching of the backlash inverse;

The large number of parameters employed was mainly motivated by the desire to keep a linear-like parametrization of the output error. Still the presence of a residual noise due to the intrinsic non-linear nature of this problem, makes convergence proofs very difficult. The first approach we have followed can be seen as a variant of the standard MRAC for linear plants. The controller structure is the same described in Section 3, with the difference that the polynomials $\theta_u(s), \theta_y(s)$ and the scalar gain θ_r are estimated by the adaptation law. If a smaller number of parameters is used we loose the possibility to have a linear-like output error equation; it still leads to a pseudo-regression model that had good convergency properties in most simulations. Let θ_u^*, θ_y^* denote the solution of the following diophantine equation:

$$\theta_u^T \vec{d}(s) R(s) + K_p \theta_y^T \vec{d}(s) Z(s) = \Lambda(s) [R(s) - R_m(s) Z(s)] \quad (3.7)$$

where

$$\vec{d}(s) = (1 \ s \ s^2 \ \dots \ s^{n-1})^T$$

and let $\theta_r^* = K_m/K_p$, if we denote with $\theta_u(t), \theta_y(t), \theta_r(t)$ their estimate at time t then for a closed-loop linear plant the MRC approach gives the following output error:

$$e(t) = \frac{K_p}{R_m(s)} \{ [\theta_u(t) - \theta_u^*]^T \vec{d}(s) u(t) + [\theta_y(t) - \theta_y^*]^T \vec{d}(s) y(t) + [\theta_r(t) - \theta_r^*] r(t) \}$$

Our non-linear system can be seen as a linear plant where a noise $n(t)$ enters the closed loop in front of the block $P(s)$. In particular the noise $n(t)$ can be expressed as a linear function of the backlash parameters estimates errors plus a bounded disturbance $d_0(t)$.

$$n(t) = [\theta_b(t) - \theta_b^*]^T \omega_b(t) + d_0(t)$$

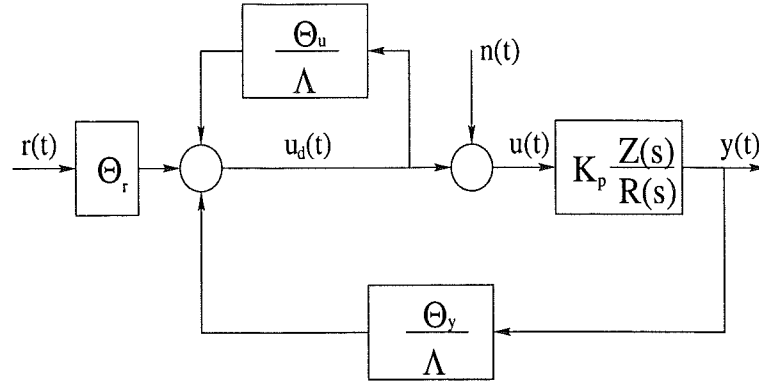


Figure 3.10 *Linear equivalent of the close loop system.*

From the controller structure it follows that

$$u_d(t) = \frac{\theta_u(s)}{\Lambda(s)} u_d(t) + \frac{\theta_y(s)}{\Lambda(s)} y(t) + \theta_r(t) r(t)$$

If we substitute $y(t) = \left(K_p Z(s) / R(s) \right) u(t)$ into the previous equality we obtain the following expression:

$$\left[1 - \frac{\theta_u(s)}{\Lambda(s)} - K_p \frac{\theta_y(s) Z(s)}{\Lambda(s) R(s)} \right] u_d(t) = K_p \frac{\theta_y(s) Z(s)}{\Lambda(s) R(s)} n(t) + \theta_r r(t)$$

Define the errors on the estimates, $\tilde{\theta}_u(s) \doteq \theta_u(s) - \theta_u^*(s)$ and $\tilde{\theta}_y(s) \doteq \theta_y(s) - \theta_y^*(s)$ and use the Diophantine equation 3.7 we obtain the expression

$$R_m(s) \frac{Z(s)}{R(s)} u_d = \tilde{\theta}_u(s) \Lambda(s) u_d + K_p \frac{\tilde{\theta}_y(s) Z(s)}{\Lambda(s) R(s)} u_d + K_p \frac{\theta_y^*(s) Z(s)}{\Lambda(s) R(s)} n + \theta_r r \quad (3.8)$$

Since $u(t) = u_d(t) + n(t)$ we have

$$K_p \frac{\tilde{\theta}_y(s) Z(s)}{\Lambda(s) R(s)} u_d(t) + K_p \frac{\theta_y^*(s) Z(s)}{\Lambda(s) R(s)} n(t) = \frac{\tilde{\theta}_y(s)}{\Lambda(s)} y(t) + K_p \frac{\theta_y^*(s) Z(s)}{\Lambda(s) R(s)} n(t)$$

and

$$R_m(s) \frac{Z(s)}{R(s)} u_d(t) = R_m(s) \frac{Z(s)}{R(s)} u(t) - R_m(s) \frac{Z(s)}{R(s)} n(t)$$

If we substitute the last two expressions in equation 3.8 and divide both the members by $R_m(s)$ we set

$$\begin{aligned} \frac{Z(s)}{R(s)} u(t) &= \frac{1}{R_m(s)} \frac{\tilde{\theta}_u(s)}{\Lambda(s)} u_d(t) + \frac{1}{R_m(s)} \frac{\tilde{\theta}_y(s)}{\Lambda(s)} y(t) + \\ &\quad \frac{Z(s)}{R(s)} \left(\frac{K_p \theta_y^*(s)}{R_m(s) \Lambda(s)} + 1 \right) n(t) + \frac{1}{R_m(s)} \theta_r(t) r(t) \end{aligned} \quad (3.9)$$

Using the Diophantine equation now gives

$$\frac{Z(s)}{R(s)} \left(\frac{K_p \theta_y^*}{\Lambda(s) R_m(s)} + 1 \right) = \frac{1}{K_p} H(s)$$

The *output error* is given by

$$e(t) \doteq y(t) - y_m(t) = K_p \frac{Z(s)}{R(s)} u(t) - K_p \frac{\theta_r^*}{R_m(s)} r(t)$$

It follows from equation 3.9 the expression of the output error:

$$\frac{e(t)}{K_p} = \frac{1}{R_m(s)} [\Theta(t) - \Theta^*]^T \Omega(t) + J(s) [\theta_b(t) - \theta_b^*]^T \omega_b(t) + J(s) d_0(t) \quad (3.10)$$

where we have defined $J(s) \doteq H(s)/K_p$. Further more:

$$\Theta(t) \doteq \begin{pmatrix} \theta_u(t) \\ \theta_y(t) \\ \theta_r(t) \end{pmatrix} \quad \Theta^* \doteq \begin{pmatrix} \theta_u^* \\ \theta_y^* \\ \theta_r^* \end{pmatrix} \quad \Omega(t) \doteq \begin{pmatrix} \omega_u(t) \\ \omega_y(t) \\ \omega_r(t) \end{pmatrix}$$

$$\omega_u(t) = \frac{\vec{d}(s)}{\Lambda(s)} u(t) \quad \omega_y(t) = \frac{\vec{d}(s)}{\Lambda(s)} y(t) \quad \omega_r(t) = r(t)$$

There are essentially two contributions to the output error. One term is due to the error of the parameters estimate, which can be computed in the same way as for linear plants; the other is due to the error of the backlash estimates which is computed as in the case of a known plant.

Adaptive law

Expression 3.10 is not a standard parametrization of the output error since two different stable transfer functions are involved, namely $J(s)$ and $1/R_m(s)$. In addition one of the transfer functions depends on the parameters vector θ_u^* . We can implement an *extended stochastic gradient* algorithm, with the augmented-error technique in the following way. Let

$$\zeta(t) \doteq \frac{1}{R_m(s)} \Omega(t) \quad \zeta_b(t) \doteq \hat{J}(s) \omega_b(t)$$

where $\hat{J}(s)$ is the transfer function $J(s)$ with θ_u^* substituted by its estimate $\theta_u(t)$. Define now the *auxiliary error* $\xi(t)$ as

$$\xi(t) \doteq \Theta(t)^T \zeta(t) - \frac{1}{R_m(s)} \Theta(t)^T \Omega(t) + \theta_b(t)^T \zeta_b(t) - \hat{J}(s) \theta_b(t)^T \omega_b(t)$$

The *augmented error* $\varepsilon(t)$ is given by

$$\varepsilon(t) \doteq e(t) + k(t)\xi(t) \quad (3.11)$$

Using the *normalizing factor* $z(t) \doteq 1 + \zeta(t)^T \zeta(t) + \zeta_b(t)^T \zeta_b(t) + \xi^2(t)$ the adaptation law can be chosen as

$$\begin{aligned} \dot{\Theta}(t) &= -\text{sign}(K_p) \Gamma_1 \zeta(t) \frac{\varepsilon(t)}{z(t)} \\ \dot{\theta}_b(t) &= -\text{sign}(K_p) \Gamma_2 \zeta_b(t) \frac{\varepsilon(t)}{z(t)} \\ \dot{k}(t) &= -\gamma_3 \xi(t) \frac{\varepsilon(t)}{z(t)} \end{aligned} \quad (3.12)$$

Simulation results

The behavior of the algorithm described in this Section will now be investigated by simulations.

Example 4

In the first example we have the following data:

Linear plant model	$P(s) = \frac{1}{(s-1.5)(s+1)}$
Model reference	$W_m(s) = \frac{\omega^2}{s^2 + 2\xi\omega s + \omega^2} \quad \begin{matrix} \xi = 0.7 \\ \omega = 3 \end{matrix}$
Backlash parameters	$C_r = 2 \quad C_l = -2$
Input signal	<i>squarewave</i> <i>frequency 0.1 Hz</i> <i>amplitude 5</i>
Matching parameters values	$\theta_u^* = \begin{pmatrix} -41.05 \\ -4.7 \end{pmatrix}$ $\theta_y^* = \begin{pmatrix} -156.075 \\ -132.875 \end{pmatrix}$ $\theta_r^* = 9$
Feedback polynomial	$\Lambda(s) = (s + 3)^2$

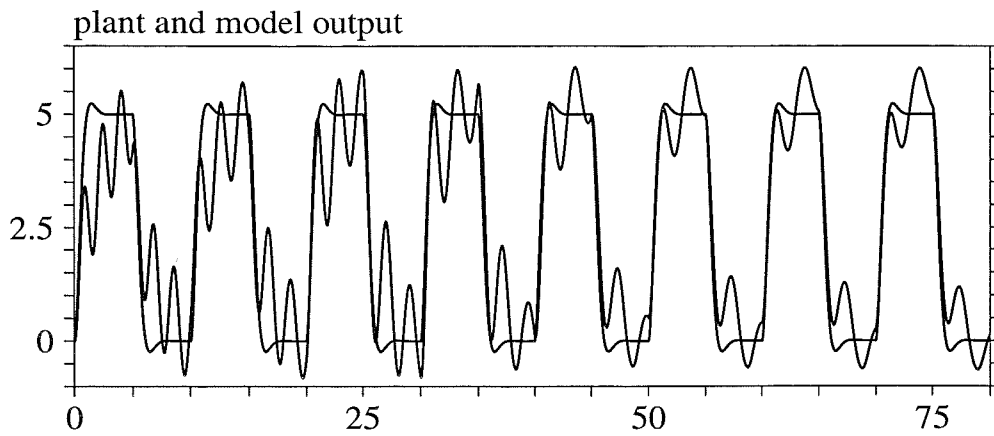


Figure 3.11 Simulation of Example 4

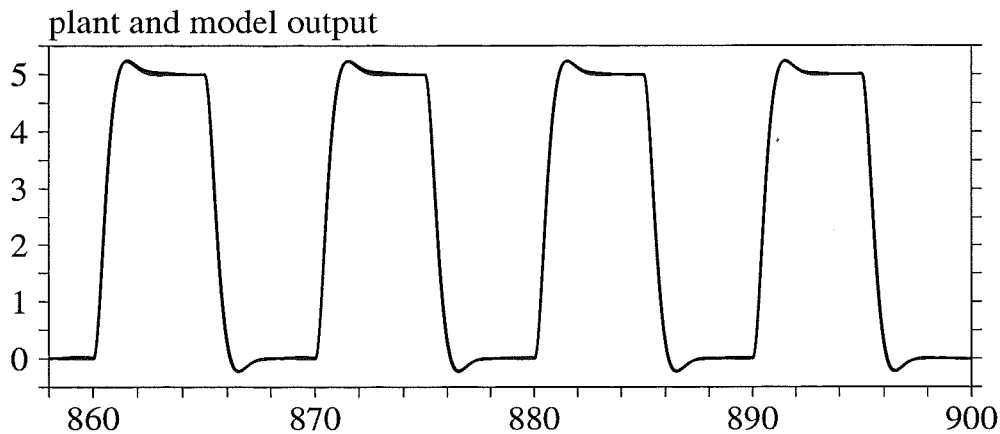


Figure 3.12 Simulation of Example 4

Figure 3.11 shows the model and the plant outputs in the transient phase. In Figure 3.12 we see the same quantities after 858 seconds. Figures 3.13 and 3.14 show the evolution of the output error. We can see how the convergence becomes quite slow after the initial transient. This is mostly due to the slow convergence of the linear controller parameters. Figure 3.15 shows that the backlash parameters have almost converged, while Figure 3.16 shows that $\theta_u(t)$ and $\theta_y(t)$ have a saturated behavior though quite far from their matching

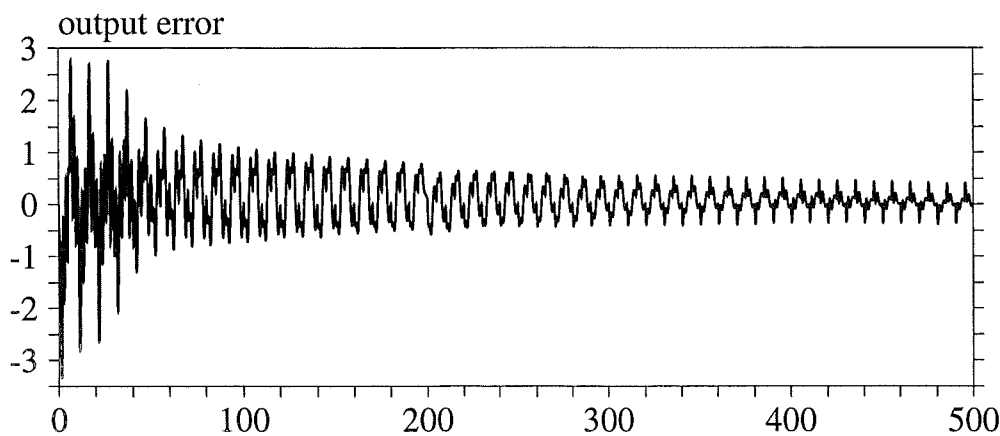


Figure 3.13 Simulation of Example 4

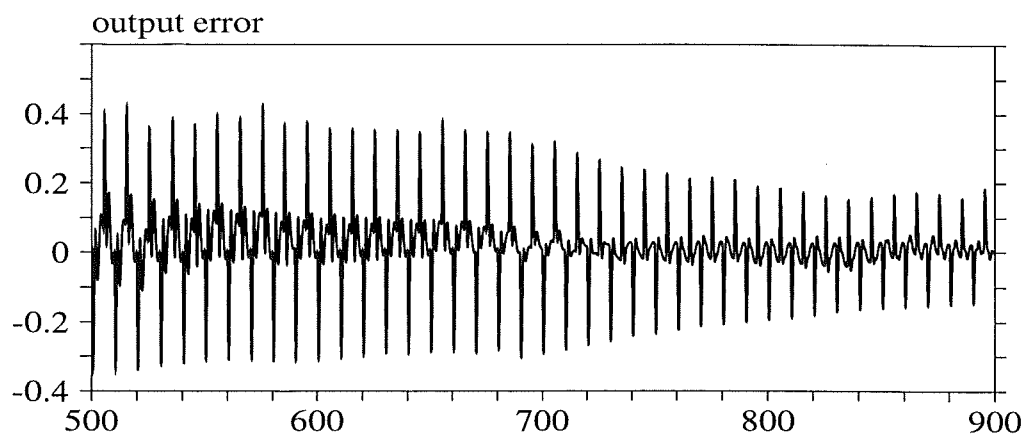


Figure 3.14 Simulation of Example 4

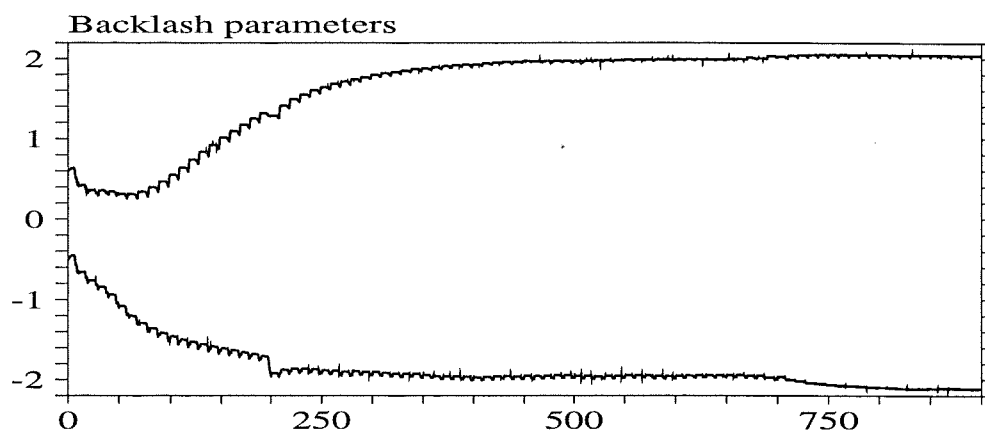


Figure 3.15 Simulation of Example 4

values θ_u^* , θ_y^* . Figure 3.17 shows the control signal $v(t)$ and the backlash output $u(t)$ after the backlash inverse is tuned.

In order to have a faster convergence of the linear controller parameters, we tried to use input signals with richer harmonic contents. In particular we have used linear combinations of sine waves as reference signal. Different

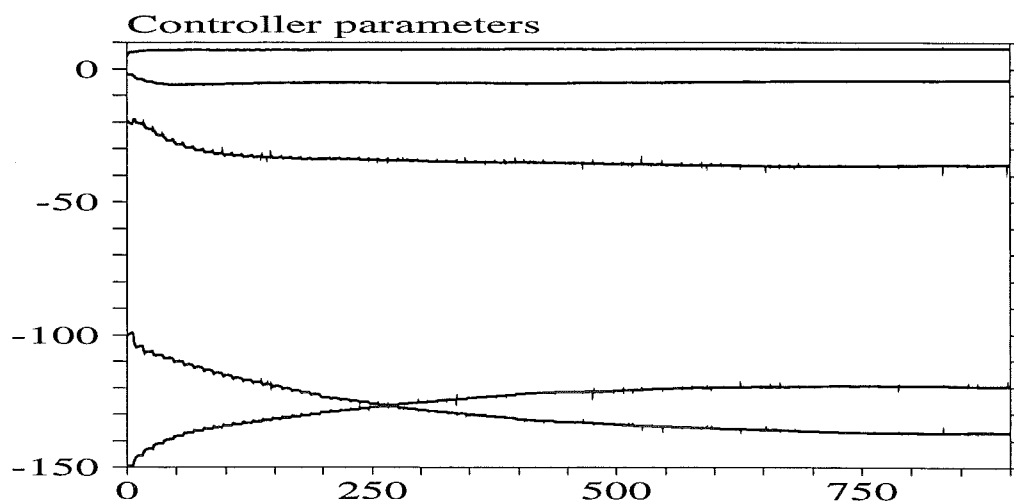


Figure 3.16 Simulation of Example 4

results were obtained with periodic or quasi-periodic signals: the convergence speed of the output error to zero was slightly higher for periodic signals, but this slowed down the convergence rate.

In this case we have the same data of Example 4. The only difference is in the reference signal. Here we are using a linear combination of sine wave.

Linear plant model	$P(s) = \frac{1}{(s-1.5)(s+1)}$
Model reference	$W_m(s) = \frac{\omega^2}{s^2 + 2\xi\omega s + \omega^2}$ $\xi = 0.7$ $\omega = 3$
Backlash parameters	$C_r = 2$ $C_l = -2$
Input signal	$\sum_{i=1}^4 5 \sin(2\pi\nu_i t)$ $\nu_1 = 0.05$ $\nu_2 = 0.1$ $\nu_3 = 0.2$ $\nu_4 = 0.4$

32

Example 6

The convergency speed depends critically on the specifications. The convergence is faster if we relax our model requirements by decreasing ω . This is illustrated in the next example, where we have chosen a marginally stable plant and relaxed our constraints taking $\omega = 2$. The Figures refer to the following settings:

Linear plant model	$P(s) = \frac{1}{s(s+1)}$
Model reference	$W_m(s) = \frac{\omega^2}{s^2 + 2\xi\omega s + \omega^2}$ $\xi = 0.7$ $\omega = 2$
Backlash parameters	$C_r = 0.5$ $C_l = -0.5$
Input signal	<i>squarewave</i> <i>frequency 0.1Hz</i> <i>amplitude 1</i>

If we look at the plottings of the plant output or of the output error, we clearly see how the control system achieves a satisfactory performance within the first 50 seconds of transient. Afterwards the convergence of the controller parameters is very slow and the output error becomes almost periodic. However this residual output error does not compromise the backlash compensation and only leads to small oscillations of the backlash parameters around their matching values. Notice also that in this last example we used a different parametrization⁴ of the backlash, defining a width W and a bias v_0 as

$$W \doteq C_r - C_l$$

$$v_0 \doteq \frac{C_r + C_l}{2}$$

This can turn out to be helpful for the tuning of the adaptation law gains; in general it is convenient to have a higher gain for the width parameter and a low gain for the bias, at least in all the situations in which we expect to have an almost symmetric backlash. This differentiation of the tuning is not obviously possible with the parametrization in terms of C_l and C_r as long as we wish to have a diagonal gain matrix. This also explain the almost constant plot of the bias in Figure 3.19.

⁴A regressor expression for this new parametrization is given in Section 3.4

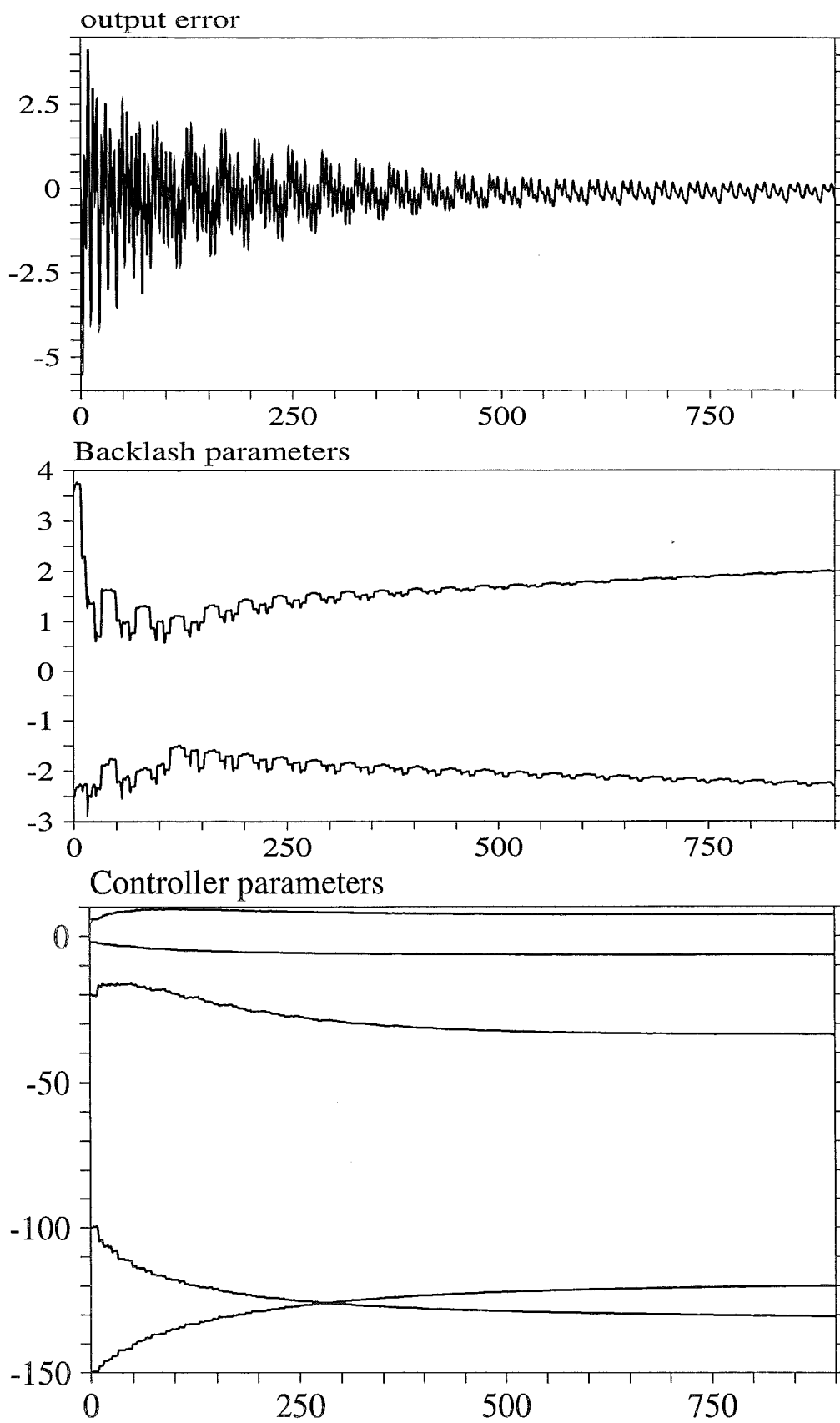


Figure 3.18 *Simulation of Example 5*

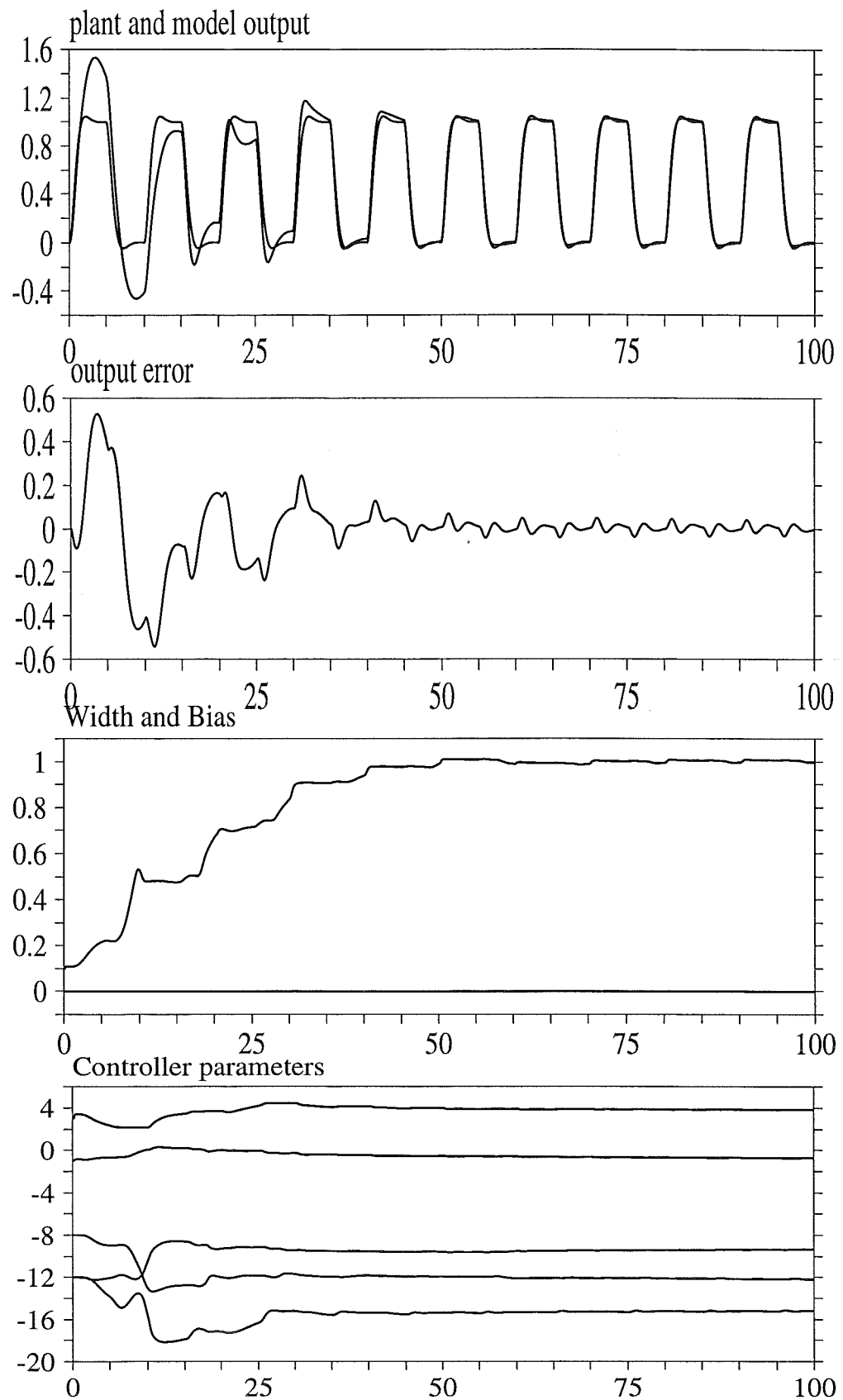


Figure 3.19 Simulation of Example 6

Recursive Least Square version

One possible way to speed up the convergence of the controller parameters is to use an RLS algorithm. In order to obtain a proper regressor for the algorithm we have to use the *augmented error*. In particular, if we refer to the following error model:

$$e(t) = K_p \sum_{i=1}^n W_i(s) [(\theta_i(t) - \theta_i^*)^T \omega_i(t)] \quad (3.13)$$

we can define the auxiliary errors as

$$\zeta_i(t) \doteq W_i(s) [\omega_i(t)]$$

$$\xi_i(t) \doteq \theta_i(t)^T \zeta_i(t) - W_i(s) [\theta_i(t)^T \omega_i(t)]$$

The augmented error becomes

$$\varepsilon(t) \doteq e(t) + \varphi(t) \xi(t)$$

where

$$\xi(t) \doteq \sum_{i=1}^n \xi_i(t)$$

The augmented error can also be written as

$$\varepsilon(t) = \tilde{\Theta}^T(t) \Phi(t) \quad (3.14)$$

where the following notations have been used:

$$\tilde{\Theta}(t) \doteq \begin{pmatrix} \theta_1(t) - \theta_1^* \\ \theta_2(t) - \theta_2^* \\ \vdots \\ \theta_n(t) - \theta_n^* \\ \varphi(t) - K_p \end{pmatrix} \quad \Phi(t) \doteq \begin{pmatrix} W_1(s) \omega_1(t) \\ W_2(s) \omega_2(s) \\ \vdots \\ W_n(s) \omega_n(t) \\ \xi(t) \end{pmatrix}$$

Equation 3.14 is a regression model for the augmented error. We can now implement a standard continuous time RLS algorithm with exponential forgetting in the following way:

$$\dot{\tilde{\Theta}}(t) = -\text{sign}(K_p) P(t) \Phi(t) \varepsilon(t) \quad (3.15)$$

$$\dot{P}(t) = \alpha P(t) - P(t) \Phi(t) \Phi^T(t) P(t)$$

If we consider the backlash output error expression, it is evident that the previous laws can be used for our adaptive control. The differences, with respect to the scheme described so far, are the presence of the disturbance

$d_0(t)$ and the dependence of one of the transfer functions on the parameter θ_u^* . Simulation results showed a good convergence both of the backlash and controller parameters. The major improvement with respect to the 'gradient' algorithm is the almost constant convergence rate of $\Theta(t)$, even in the presence of a very small output error. Unfortunately the numerical solution of the differential equations requires a substantial computational effort. There are also problems with ill-conditioning.

Example 7

The simulation results shown in Figure 3.20 refer to data almost equal to Example 6. The only difference is that we are using a RLS algorithm to estimate the controller parameters. If we compare Figure 3.19 and 3.20 we see that a slightly longer transient is seen for the RLS algorithm, probably due to a more pronounced oscillation of the bias estimate that we could avoid in the SG algorithm thank to a correct choose of the adaptation gain Γ . Afterwards the tuning of the RLS becomes clearly more accurate, and a smaller output error is shown.

Linear plant model	$P(s) = \frac{1}{s(s+1)}$
Model reference	$W_m(s) = \frac{\omega^2}{s^2 + 2\psi\omega s + \omega^2}$ $\psi = 0.7$ $\omega = 2$
Backlash parameters	$C_r = \frac{1}{2} \quad C_l = -\frac{1}{2}$
Input signal	<i>squarewave</i> <i>frequency 0.1Hz</i> <i>amplitude 1</i>
Matching parameters values	$\theta_u^* = \begin{pmatrix} -9.4 \\ -1.8 \end{pmatrix}$ $\theta_y^* = \begin{pmatrix} -16 \\ -13.8 \end{pmatrix}$ $\theta_r^* = 4$
Feedback polynomial	$\Lambda(s) = (s + 2)^2$

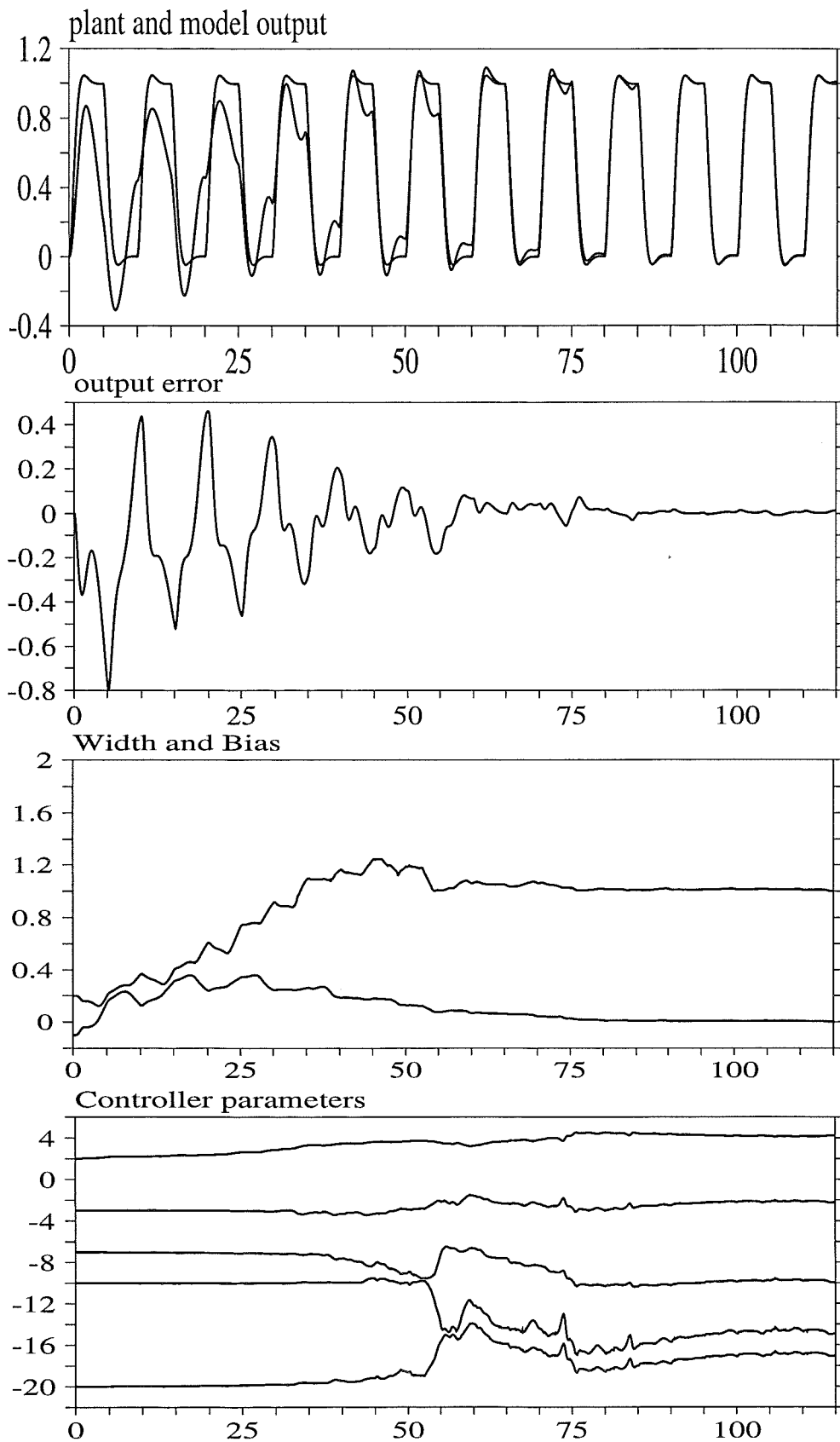


Figure 3.20 Simulation of Example 7

3.4. Plant and backlash estimate: explicit approach

Output parametrization

We will now use an explicit approach to the problem. Our aim is to define an adaptive law to estimate an explicit model of the plant. Afterwards the estimated model is used to design a controller. Consider the simple plant structure shown in Figure 3.1. We will use a different notation, since we need a different parametrization of the plant. Assume that $P(s) = B(s)/A(s)$ where

$$\begin{aligned} A(s) &= s^n + a_1 s^{n-1} + a_2 s^{n-2} + \dots + a_n \\ B(s) &= b_0 s^m + b_1 s^{m-1} + \dots + b_m \end{aligned}$$

with $m \leq n$. Consider a stable polynomial $\Upsilon(s)$, with degree $\geq n$. Let $\Delta_i(s)$ denote the following transfer functions:

$$\Delta_i(s) \doteq \frac{s^i}{\Upsilon(s)} \quad \text{for } i = 0 \dots n$$

A filtered version of the plant output $y_{\Upsilon} \doteq \Delta_n(s)y(t)$ can be computed with the following linear regression model:

$$\begin{aligned} y_{\Upsilon} = & -a_1 \Delta_{n-1}(s)[y(t)] - a_2 \Delta_{n-2}(s)[y(t)] - \dots - a_n \Delta_0(s)[y(t)] + \\ & + b_0 \Delta_m(s)[u(t)] + b_1 \Delta_{m-1}(s)[u(t)] + \dots + b_m \Delta_0(s)[u(t)] \end{aligned} \quad (3.16)$$

Consider the expression of the backlash output

$$u(t) = \chi_r(t)[v(t) - C_r] + \chi_l(t)[v(t) - C_l] + \chi_s(t)u_s$$

If the backlash is parametrized in terms of a width W and a bias v_0 we have

$$W \doteq C_r - C_l$$

$$v_0 \doteq \frac{C_r + C_l}{2}$$

$$u(t) = v(t) - v_0 + \frac{\chi_l(t) - \chi_r(t)}{2} W + \chi_s(t)[u_s - v(t)]$$

If we substitute the previous expression for $u(t)$ in eqn. 3.16 we obtain

$$\begin{aligned} y_{\Upsilon} = & -a_1 \Delta_{n-1}y(t) - a_2 \Delta_{n-2}y(t) - \dots - a_n \Delta_0 y(t) + \\ & + b_0 W \Delta_m \rho(t) + b_1 W \Delta_{m-1} \rho(t) + \dots + b_m W \Delta_0 \rho(t) + \\ & + b_0 \Delta_m v(t) + \dots + b_m \Delta_0 v(t) - \frac{b_m v_0}{\Upsilon(0)} + d(t) \end{aligned} \quad (3.17)$$

where we defined

$$\begin{aligned} \rho(t) &\doteq \frac{\chi_l(t) - \chi_r(t)}{2} \\ d(t) &\doteq \frac{B(s)}{\Upsilon(s)} [\chi_s(u_s - v(t))] \end{aligned}$$

Let us notice that $\rho(t)$ is in general not known. In order to write a linear regression model of the plant, we need all the quantities in the regressor to be accessible. Define $\hat{\rho}(t)$ as

$$\hat{\rho}(t) \doteq \frac{\hat{\chi}_l(t) - \hat{\chi}_r(t)}{2}$$

Eqn. 3.17 then becomes

$$\begin{aligned} y_{\Upsilon} = & -a_1 \Delta_{n-1} y(t) - a_2 \Delta_{n-2} y(t) - \dots - a_n \Delta_0 y(t) + \\ & + b_0 W \Delta_m \hat{\rho}(t) + b_1 W \Delta_{m-1} \hat{\rho}(t) + \dots + b_m W \Delta_0 \hat{\rho}(t) + \\ & + b_0 \Delta_m v(t) + \dots + b_m \Delta_0 v(t) - \frac{b_m v_0}{\Upsilon(0)} + \bar{d}(t) \end{aligned} \quad (3.18)$$

where

$$\bar{d}(t) = d(t) + \frac{B(s)}{\Upsilon(s)} [\rho(t) - \hat{\rho}(t)] W$$

Introduce the following vectors :

$$\theta_a \doteq \begin{pmatrix} a_1 \\ a_2 \\ . \\ . \\ a_n \end{pmatrix} \quad \phi_a(t) \doteq \begin{pmatrix} -\Delta_{n-1}[y(t)] \\ -\Delta_{n-2}[y(t)] \\ . \\ . \\ -\Delta_0[y(t)] \end{pmatrix}$$

$$\theta_b \doteq \begin{pmatrix} b_0 \\ b_1 \\ . \\ . \\ b_m \end{pmatrix} \quad \phi_b(t) \doteq \begin{pmatrix} \Delta_m[v(t)] \\ \Delta_{m-1}[v(t)] \\ . \\ . \\ \Delta_0[v(t)] \end{pmatrix}$$

$$\theta_w \doteq W \theta_b \quad \phi_w(t) \doteq \begin{pmatrix} \Delta_m[\hat{\rho}(t)] \\ \Delta_{m-1}[\hat{\rho}(t)] \\ . \\ . \\ \Delta_0[\hat{\rho}(t)] \end{pmatrix}$$

Let θ and $\phi(t)$ denote the vectors

$$\theta \doteq \begin{pmatrix} \theta_a \\ \theta_b \\ \theta_w \\ \frac{b_m v_0}{\Upsilon(0)} \end{pmatrix} \quad \phi(t) \doteq \begin{pmatrix} \phi_a(t) \\ \phi_b(t) \\ \phi_w(t) \\ -1 \end{pmatrix}$$

then eqn. 3.18 can be rewritten as

$$y_{\Upsilon} = \theta^T \phi(t) + \bar{d}(t) \quad (3.19)$$

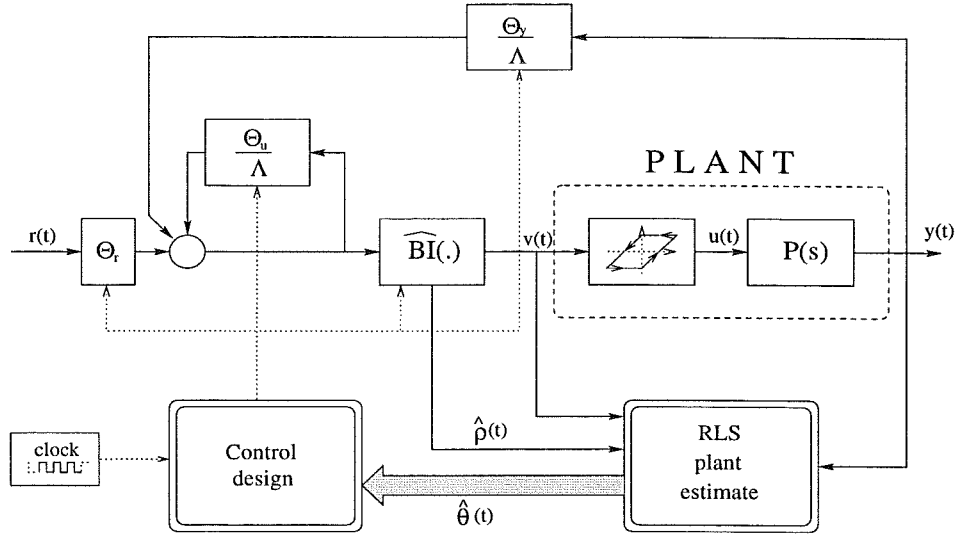


Figure 3.21 The structure of the controller

Adaptive law

We have obtained a linear regression model for our plant. The RLS algorithm with exponential forgetting becomes

$$\begin{aligned} \frac{d}{dt} \hat{\theta}(t) &= P(t) \phi(t) e(t) \\ e(t) &= y_r(t) - \phi^T(t) \hat{\theta}(t) \\ \frac{d}{dt} P(t) &= \alpha P(t) - P(t) \phi(t) \phi^T(t) P(t) \end{aligned} \quad (3.20)$$

Control design

The controller must be updated at discrete times according to some direct synthesis method. First we can choose the backlash inverse parameters in the following way⁵ :

$$\begin{aligned} \hat{v}_0 &\doteq \frac{\Upsilon(0)}{\hat{b}_m} \hat{\theta}^T \vec{e}_{n+2m+1} \\ \hat{w} &\doteq \arg \min_{W \in \mathbb{R}} [\hat{\theta}_w - W \hat{\theta}_b]^T Q [\hat{\theta}_w - W \hat{\theta}_b] \end{aligned} \quad (3.21)$$

where Q is an $m \times m$ positive definite matrix. Using the previous expression and equating the derivative to zero we obtain

$$\hat{w} = \frac{\hat{\theta}_b^T Q \hat{\theta}_w}{\hat{\theta}_b^T Q \hat{\theta}_b}$$

It can be shown that

$$\lim_{\hat{\theta}(t) \rightarrow \theta} \hat{w}(t) = W \quad \lim_{\hat{\theta}(t) \rightarrow \theta} \hat{v}_0(t) = v_0$$

⁵ \vec{e}_j is the j -th element of the canonical base. Here $\hat{\theta}^T(t) \vec{e}_{n+2m+1}$ is the last element of vector $\hat{\theta}(t)$

The MRC approach can be used to design a stabilizing controller for the estimated plant. Introduce

$$\begin{aligned}\hat{A}(s) &\doteq s^n + \hat{a}_1 s^{n-1} + \hat{a}_2 s^{n-2} + \dots + \hat{a}_n \\ \hat{B}(s) &\doteq \hat{b}_0 s^m + \hat{b}_1 s^{m-1} + \dots + \hat{b}_m\end{aligned}$$

the controller parameters are then obtained by solving the following Diophantine equation:

$$\theta_u(s)\hat{A}(s) + \theta_y(s)\hat{B}(s) = \Lambda(s)[\hat{A}(s) - \frac{1}{\hat{b}_0}\hat{B}(s)R_m(s)] \quad (3.22)$$

where we have chosen as a reference model $W_m(s) = K_m/R_m(s)$. The feed-forward gain is given by

$$\theta_r = \frac{K_m}{\hat{b}_0}$$

Simulation results

Example 8

Hereby we consider a second-order plant with integral action. In the absence of a proper backlash inversion this leads to self-sustained oscillations or to limit cycles, according to the closed-loop gain. More in detail we are referring to the following settings:

Linear plant model	$P(s) = \frac{1}{s(s+1)}$
Backlash parameters	$C_l = -0.3 \quad C_r = 0.7$
Reference model	$W_m(s) = \frac{\omega^2}{s^2 + 2\xi\omega s + \omega^2} \quad \begin{matrix} \xi = 0.7 \\ \omega = 2 \end{matrix}$
Feedback polynomial	$\Lambda(s) = (s + 2)^2$
Clock interval	3 sec.
Forgetting factor	$\alpha = 0.15$
RLS polynomial	$\Upsilon(s) = (s + 3)^2$

The convergence is very fast compared with the corresponding Example 6 of the previous chapter. This is partially due to the use of an RLS algorithm, but most it is due to the fact that a different approach is used. Notice that all the algorithms presented need some acknowledgments in order to prevent the system to operate with a negative estimate of the backlash width. This is particularly evident in “width and bias” of Figure 3.22.

Example 9

The convergence speed of this algorithm is essentially independent from the control requirements. In this example we have in fact chosen a more critical plant model, with unstable dynamics. We are also considering more severe requirements, having increased ω to 3. Notice that in both simulation we did not assume to have any a priori information about the magnitude of the plant parameters. All the estimates are in fact initialized to zero. Still the convergence was very fast and precise. Figure 3.23 refer to the following settings:

Linear plant model	$P(s) = \frac{1}{(s-1.5)(s+1)}$
Backlash parameters	$C_l = -0.3 \quad C_r = 0.7$
Reference model	$W_m(s) = \frac{\omega^2}{s^2 + 2\xi\omega s + \omega^2} \quad \begin{matrix} \xi = 0.7 \\ \omega = 3 \end{matrix}$
Feedback polynomial	$\Lambda(s) = (s + 2)^2$
Clock interval	3 sec.
Forgetting factor	$\alpha = 0.15$
RLS polynomial	$\Upsilon(s) = (s + 3)^2$

Notice that this last Example can be somehow compared with Example 4, where an implicit approach is used. The only difference is in the backlash parameters. It is quite evident that the two algorithms really have different convergence rates. We should not forget at the same time that this is achieved thank to a bigger computational effort.

Besides we must mention that the explicit approach requires an additional step, that is the control design block. The convergency speed of the open-loop plant estimates is therefore filtered by the sensitivities involved in the control design. This means that even if the plant estimates do not depend on the control requirements, this dependence is somehow reintroduced when considering the control loop as a whole. The solution of Diophantine equations leads in fact to higher sensitivities to parameters variations when we are dealing with more severe requirements.

The algorithm was convergent, (for low order examples) also with a sinusoidal reference. The backlash itself and the discrete updating of the control law generate higher order harmonics and provide *persistent excitation* to the system. It should be noticed also that in both examples there were no zeroes to estimate, and the $B(s)$ polynomial was reduced to a scalar coefficient. It is possible that some lack of excitation is met when dealing with higher order models or with zeroes in plant dynamics.

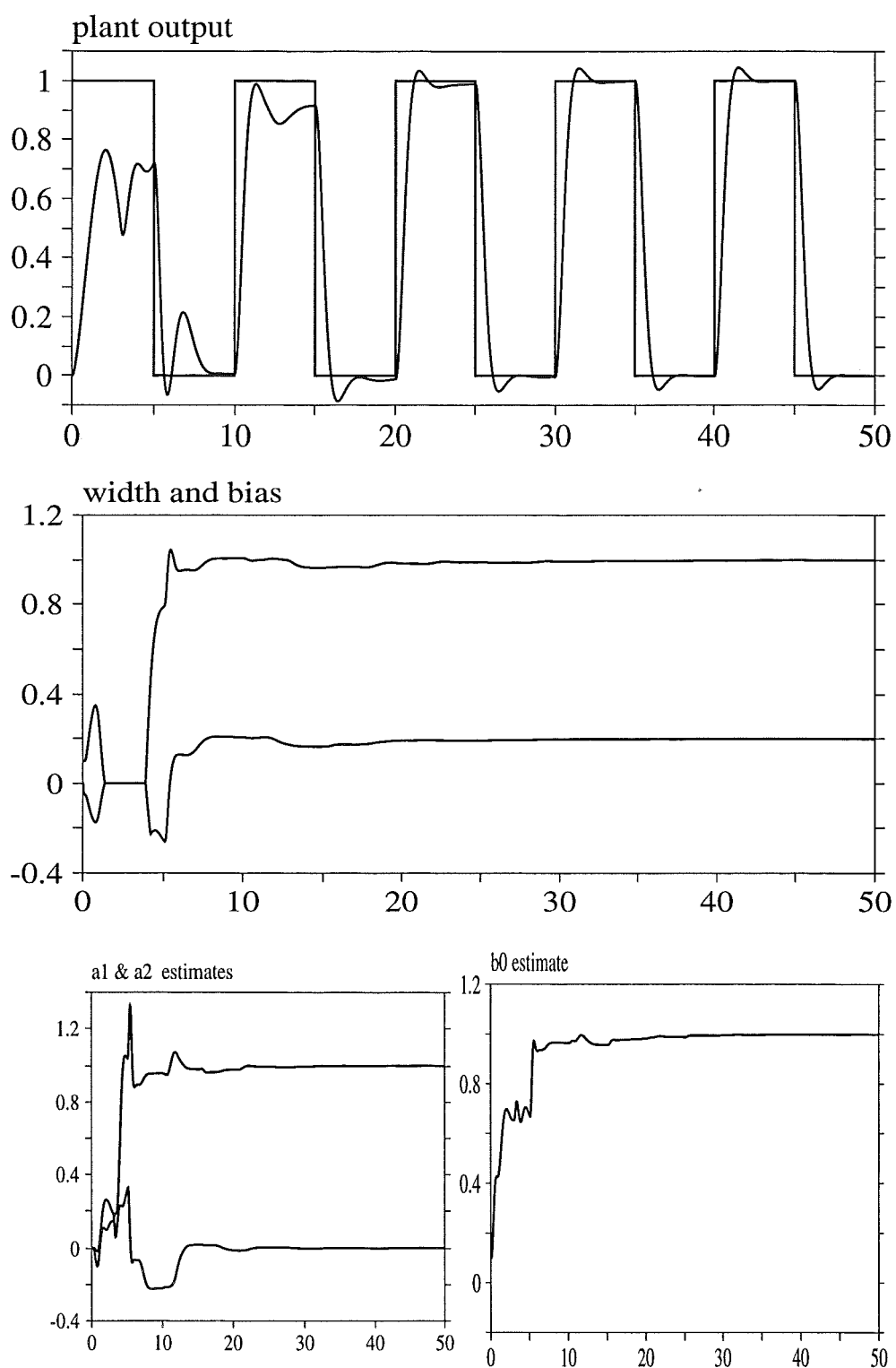


Figure 3.22 *Simulation of Example 8*

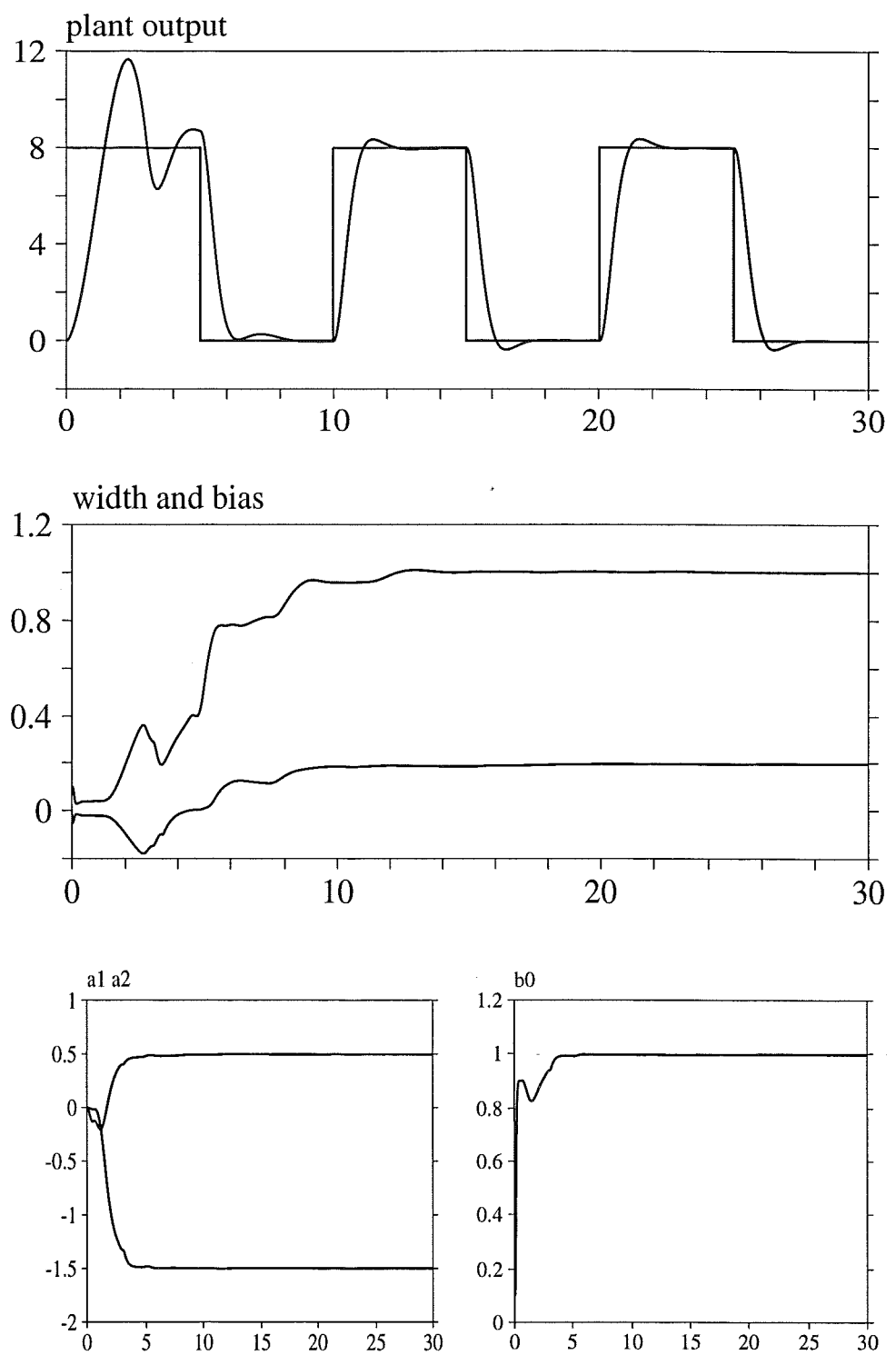


Figure 3.23 Simulation of Example 9

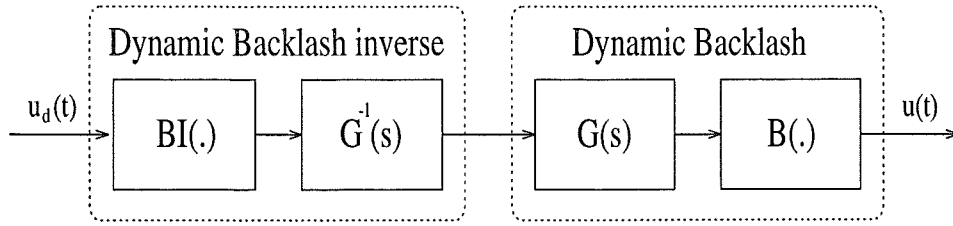


Figure 4.1 Backlash inversion through a stably invertible system

4. Adaptive backlash inversion through a dynamic system

A more complex situation arises if the backlash nonlinearity is preceded by a dynamic system. The aim of backlash inversion through a dynamic system is to some extent similar to the problem of tracking a square wave reference. Therefore, an exact backlash inversion is not possible for continuous time systems. Still, if we control the dynamic block to a sufficiently ready model, we can prevent the backlash from operating in the dead-zone for too long time.

4.1. Backlash inversion through a dynamic block

An interesting point left open by Kokotovic is the backlash inversion through a dynamical system. If the transfer function of the dynamic block is stably invertible, an easy way to invert the backlash is shown in Figure 4.1. This kind of scheme provides *asymptotic backlash inversion*, i. e.

$$\lim_{t \rightarrow \infty} u(t) - u_d(t) = 0$$

On the contrary if the transfer function of the dynamic block is not stably invertible even the objective of asymptotic backlash inversion is not achievable. Let us consider a *minimum phase* transfer function $G(s) \doteq K_g Z_g(s)/R_g(s)$ with *relative degree* ≥ 1 .

Since we are trying to invert the backlash dynamics for control aims, what we are really interested in, is not actually the “backlash inversion”; it will be sufficient to have a sort of “backlash linearization”. This means essentially that we would like to have

$$\lim_{t \rightarrow \infty} u(t) = G_m(s)[u_d(t)]$$

where $G_m(s)$ is a linear transfer function. Let us denote with $u_d(t)$ the dynamic backlash inverse input (see Figure 4.2). We define

$$DBI[u_d(t)] \doteq u_d(t) + \delta(t)$$

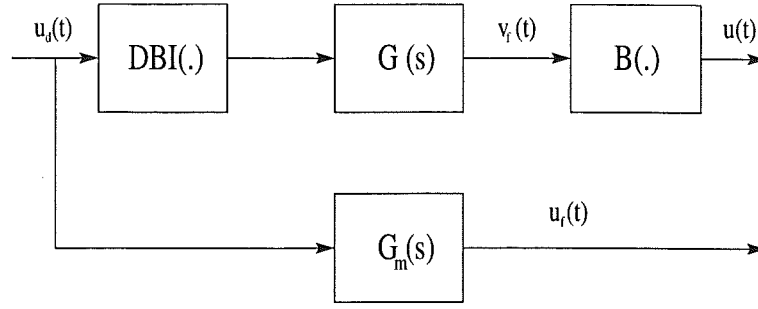


Figure 4.2 Backlash linearization

Then we have for the backlash output $u(t)$

$$u(t) = \chi_r(t)[v_f(t) - C_r] + \chi_l(t)[v_f(t) - C_l] + \chi_s(t)u_s$$

We can now consider the linearization error $\epsilon(t)$

$$\epsilon(t) \doteq u(t) - u_f(t)$$

Its expression follows immediately :

$$\epsilon(t) = (\chi_l + \chi_r)G(s)[\delta(t)] - (\chi_r C_r + \chi_l C_l) + \chi_s\{u_s - G(s)[u_d(t)]\}$$

Our aim is to choose $\delta(t)$ in order to minimize some positive definite functional of $\epsilon(t)$. In this way the "backlash linearization" purpose can be seen at all effects as a tracking problem. As it is known from linear control theory, whenever the relative degree of our plant is ≥ 1 it is not possible to achieve asymptotic tracking of discontinuous reference signals (as requested here).

An alternative is to define a reference model $G_m(s)$ of the same relative degree as the dynamical block $G(s)$, with unitary static gain. Then we control via a feedback the block $G(s)$ in order to have a close loop system transfer function equal to $G_m(s)$. Then we can put a backlash inverse in front of the dynamic block. This kind of backlash inverse would not provide asymptotic linearization of the backlash, still, if the reference model $G_m(s)$ is sufficiently ready, then it can prevent the backlash from operating in the dead-zone for too long time. The scheme of the dynamic backlash inverse is shown in Figure 4.3. We have by the time made the assumption that both the $G(s)$ output and its derivative are accessible. The two feedback blocks are the solutions of the following Diophantine equation:

$$\theta_v(s)R_g(s) + K_g\theta_z(s)Z_g(s) = \Omega(s)[R_g(s) - Z_g(s)R_{gm}(s)] \quad (4.1)$$

with

$$G_m(s) = \frac{K_{gm}}{R_{gm}(s)} \quad \theta_{bi} = \frac{K_{gm}}{K_g}$$

being θ_{bi} the backlash inverse slope or equivalently a constant gain just behind it. In this scheme we have a *switching mode signal*, that toggles when the derivative of the backlash input crosses zero. An equivalent way to implement the dynamic backlash inverse is shown in Figure 4.4 where the switching mode signal action has been replaced by a differential operator cascaded with a sign non-linearity.

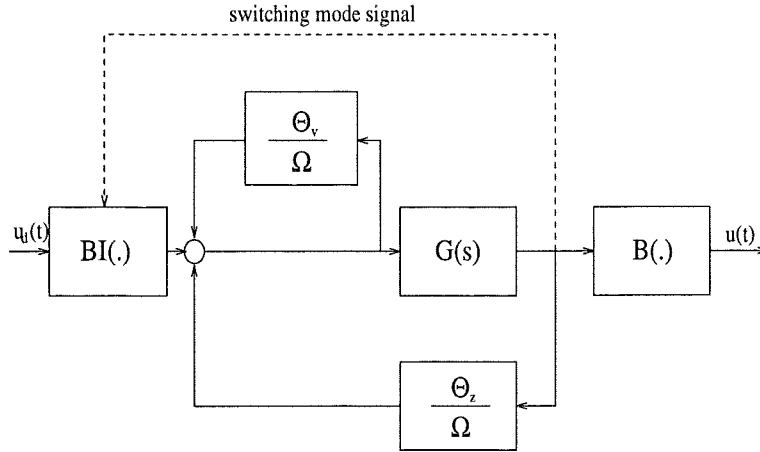


Figure 4.3 Dynamic backlash inverse

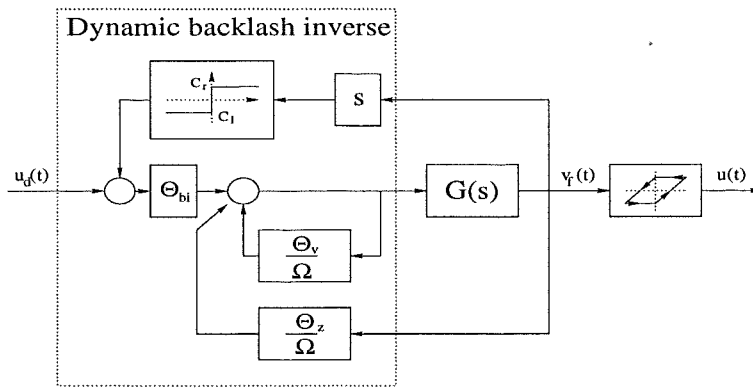


Figure 4.4 Equivalent of the dynamic backlash inverse

4.2. Plant and Controller structure

Let us consider now the plant structure shown in Figure 4.5. Since the backlash is preceded by the dynamical block $G(s)$ it is not possible anymore to achieve an exact backlash inversion; still we can use the dynamical inverse in order to reduce the backlash impact on the system, and then control the whole plant with standard linear control techniques. The closed-loop system is shown in Figure 4.6. If we compute the backlash inverse feedbacks according to equation 4.1, and we denote with $W_m(s) \doteq K_m/R_m(s)$ our reference model and let $\theta_r = K_m/K$ then the controller parameters are the solutions of

$$\theta_u(s)R(s) + K\theta_y(s)Z(s) = \Lambda(s)[R(s) - R_m(s)Z(s)] \quad (4.2)$$

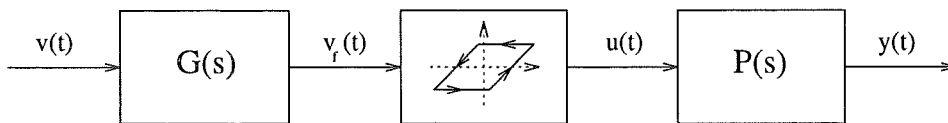


Figure 4.5 Plant structure

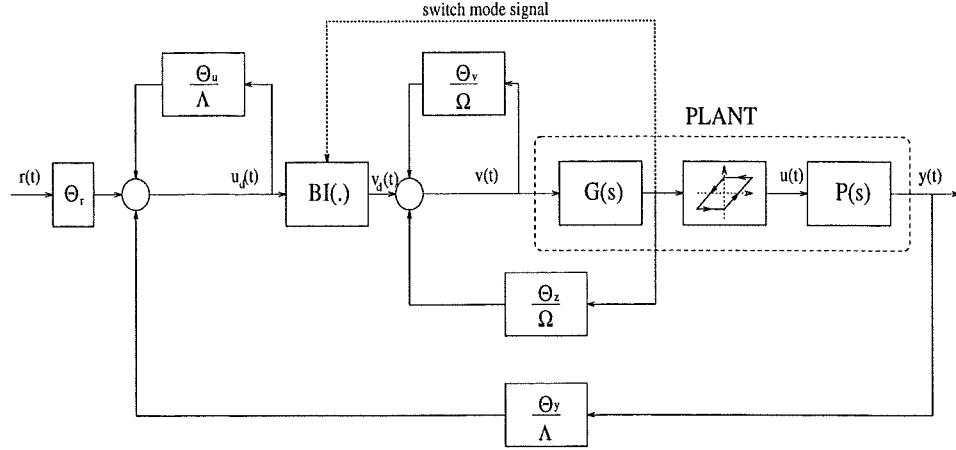


Figure 4.6 Closed-loop system

where

$$P(s) = K_p \frac{Z_p(s)}{R_p(s)} \quad G(s) = K_g \frac{Z_g(s)}{R_g(s)}$$

$$R(s) = R_{gm}(s)R_p(s) \quad Z(s) = Z_p(s) \quad K = K_{gm}K_p$$

4.3. Dynamic backlash inversion: implicit approach

Adaptive backlash inverse

We would like now to consider the problem of estimating the backlash in this new context. First of all it can be of some interest to see whether the Kokotovic algorithm can still be employed for this purpose. We can control the $G(s)$ function to some reference model $G_m(s)$ and then use the Kokotovic algorithm, trying to ignore in the adaptive laws the presence of the dynamic block $G_m(s)$.

In Figure 4.7 are shown the estimates of the backlash parameters. The two different plots refer to two different $G_m(s)$ chosen for the backlash inverse. In particular we have chosen $G_{m1}(s) = 5/(s + 5)$ and $G_{m2}(s) = 10/(s + 10)$ (backlash parameters: $C_r = 0.5$, $C_l = -0.5$), but still the estimates were very far from their matching values and obviously fluctuating, due to non exact backlash inversion.

It is quite intuitive that the convergence of Kokotovic algorithm can be improved for $G_m(s) = M/(s + M)$ just letting M tend to ∞ . Since this way of inverting the backlash does not make any physical sense we must try to find out a different adaptive algorithm. Let us consider the scheme shown in Figure 4.2. We have for the signals involved the following expressions:

$$u_d(t) = \hat{\chi}_r[v_d(t) - \hat{C}_r] + \hat{\chi}_l[v_d(t) - \hat{C}_l]$$

$$u(t) = \chi_r[v_f(t) - C_r] + \chi_l[v_f(t) - C_l] + \chi_s u_s$$

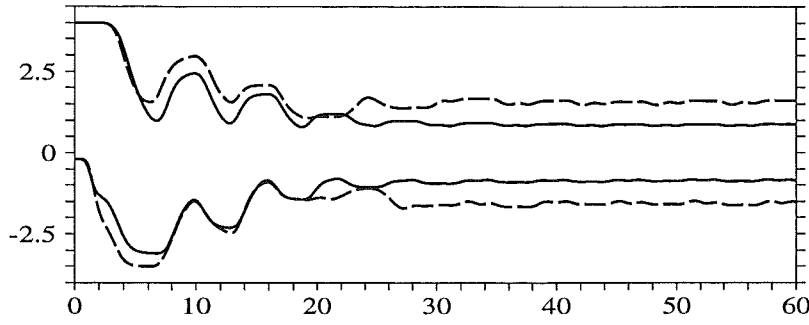


Figure 4.7 *Fluctuating backlash estimates*

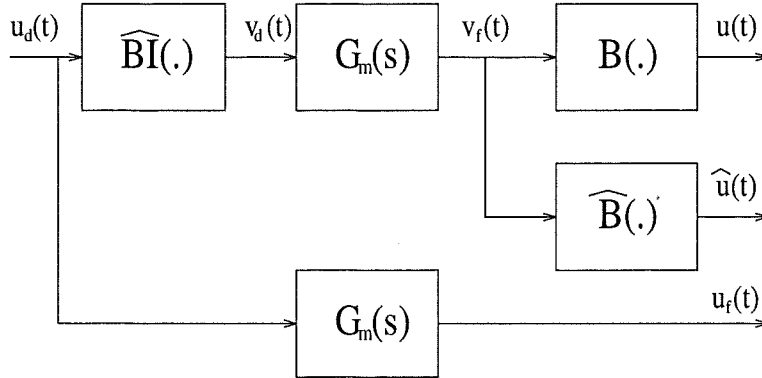


Figure 4.8 *Dynamic inverse signals*

Then subtracting one equation from the other

$$u(t) - u_d(t) = \hat{\chi}_r[\hat{C}_r - C_r] + \hat{\chi}_l[\hat{C}_l - C_l] + [v_f(t) - v_d(t)] + d_0(t)$$

where

$$d_0(t) = \chi_s u_s + (\chi_r - \hat{\chi}_r)[v_f(t) - C_r] + (\chi_l - \hat{\chi}_l)[v_f(t) - C_l]$$

Since we assumed $v_f(t)$ to be accessible, the quantity $[v_f(t) - v_d(t)]$ is known; we could then subtract from the output error the quantity $H(s)[v_f(t) - v(t)]$ and then use this decreased error to implement the adaptive law. Unfortunately, since we cannot achieve exact backlash inversion, is not true anymore that $d_0(t) \rightarrow 0$ as $\theta_b(t) \rightarrow \theta_b^*$. This implies that the estimates would not converge to a point because of adaptive loop excitation due to the noise $d_0(t)$. If we want to achieve asymptotic tuning of our estimates we need a parametrization of the output error that involves only vanishing disturbances. Let us consider now the scheme in Figure 4.8. The block $\hat{B}(\cdot)$ is the estimated backlash, then we have the following relations:

$$u(t) = \chi_r[v_f(t) - C_r] + \chi_l[v_f(t) - C_l] + \chi_s u_s$$

$$\hat{u}(t) = \hat{\chi}_{rb}[v_f(t) - \hat{C}_r] + \hat{\chi}_{lb}[v_f(t) - \hat{C}_l] + \hat{\chi}_{sb} u_{sb}$$

where we denoted with $\hat{\chi}_{\cdot b}$ the indicators functions of the estimated backlash. Let us now consider the difference $u(t) - u_f(t)$; we can split it into two contributes, namely $u(t) - \hat{u}(t)$ and $\hat{u}(t) - u_f(t)$. The last one is known, while the

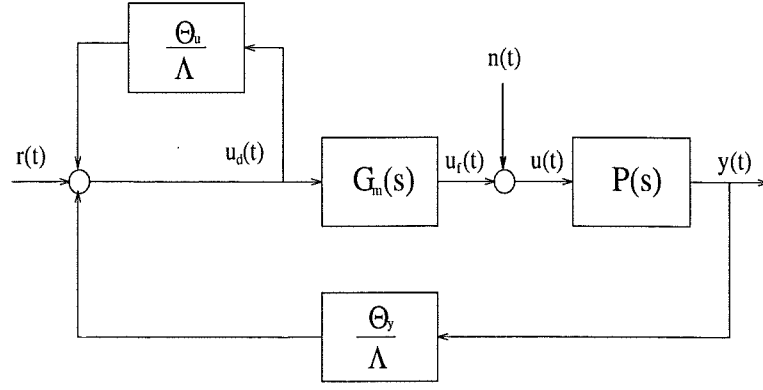


Figure 4.9 *Equivalent linear plant*

following relation holds for the first one:

$$u(t) - \hat{u}(t) = \hat{\chi}_{rb}[\hat{C}_r - C_r] + \hat{\chi}_{lb}[\hat{C}_l - C_l] + d_1(t)$$

where the disturbance $d_1(t)$ is now given by

$$d_1(t) = (\chi_r - \hat{\chi}_{rb})[v_f(t) - C_r] + (\chi_l - \hat{\chi}_{lb})[v_f(t) - C_l] + (\chi_s u_s - \hat{\chi}_{sb} u_{sb})$$

and most of all $d_1(t) \rightarrow 0$ as $\theta_b(t) \rightarrow \theta_b^*$. The control system can be seen as a linear plant with a bounded disturbance $n(t) \doteq u(t) - u_f(t)$ entering the loop (see Figure 4.9). We can now compute the transfer function $H(s)$ from $n(t)$ to $y(t)$.

$$H(s) = K_p \frac{R_{gm}(s)}{R_m(s)} \left(1 - \frac{\theta_u(s)}{\Lambda(s)} \right)$$

Then the output error expression is

$$e(t) = H(s)n(t)$$

We can then define what we call *ideal error* subtracting from $e(t)$ its known component.

$$e_i(t) \doteq e(t) - H(s)[\hat{u}(t) - u_f(t)]$$

Then we have for the ideal error the same expression that we had in Kokotovic algorithm for the output error, that is

$$e_i(t) = H(s) \left[\tilde{\theta}_b^T(t) \omega_b(t) + d_1(t) \right]$$

We can then define the auxiliary error $\xi(t)$ and the augmented error $\varepsilon_i(t)$ in the standard way

$$\zeta(t) \doteq H(s)[\omega_b(t)]$$

$$\xi(t) \doteq \tilde{\theta}_b(t)^T \zeta(t) - H(s)[\tilde{\theta}_b^T(t) \omega_b(t)]$$

$$\varepsilon_i(t) \doteq e_i(t) + \xi(t)$$

Then we can update the parameters estimate according to the following *gradient* algorithm.

$$\dot{\theta}_b(t) = -\Gamma \zeta(t) \frac{\varepsilon_i(t)}{1 + \zeta^T(t)\zeta(t)}$$

Once again it is not clear if this algorithm would provide asymptotic convergence of the estimates to their real values, but the dependence of the disturbance $d_1(t)$ on the estimates error and the simulations suggest that for sufficient rich signals we will have $e_i(t) \rightarrow 0$.

Simulation results

Example 10

In this example both $G(s)$ and $P(s)$ have unstable poles. Notice that the reference model for the dynamic block $G_m(s)$ has a bigger bandwidth than the plant reference model $W_m(s)$. This is in general an advisable choice since the internal control loop must satisfy quite severe requirements if we want to compensate the backlash in a satisfactory way. The first simulation refers to the following settings:

Plant transfer function	$P(s) = \frac{1}{(s-1.5)(s+1)}$
Dynamic block function	$G(s) = \frac{1}{s-1}$
Backlash parameters	$C_r = 2 \quad C_l = -2$
Plant reference model	$W_m(s) = \frac{M\omega^2}{(s+M)(s^2+2\xi\omega s+\omega^2)}$ $M = 5$ $\omega = 3$ $\xi = 0.7$
Dynamic block model	$G_m(s) = \frac{\lambda}{s+\lambda} \quad \lambda = 10$
Input signal	$r(t) = 5 \sin(2\pi\omega_0 t) \quad \omega_0 = 0.1$

As you can see in Figure 4.14 the backlash input is not discontinuous. Still it can prevent the backlash from operating in the dead-zone for too long time and the backlash output that results is almost a sinewave. In Figure 4.12 is shown the difference between the ideal error, that tends to zero, and the output error, that is essentially a filtered version of the backlash linearization error.

Example 11

The next simulations diagrams refer to a parameters setting equal to the one seen in Example 10. The only differences are in the input signal and in the backlash width.

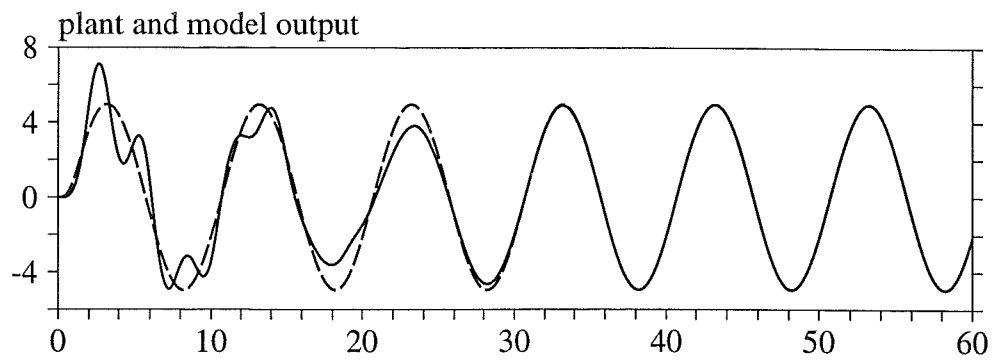


Figure 4.10 Simulation of Example 10

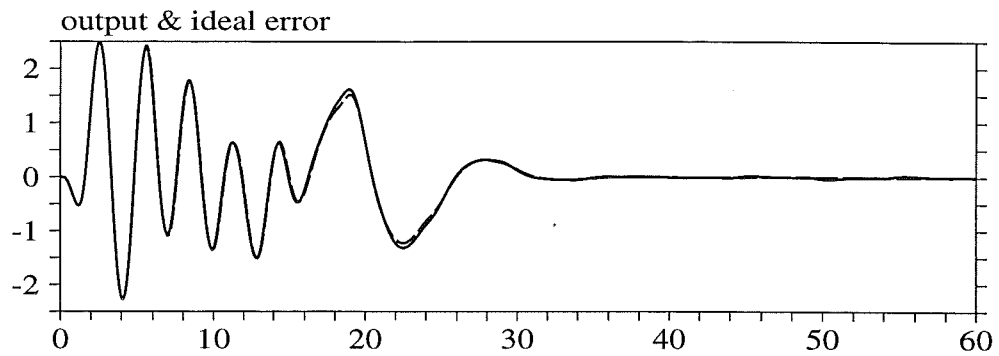


Figure 4.11 Simulation of Example 10

Input signal	<i>squarewave</i>	
	<i>frequency 0.1Hz</i>	
Backlash Parameters	<i>amplitude 5</i>	
	$C_r = 0.5$	$C_l = -0.5$

As you can see from Figure 4.16, though the estimates are tuned to their real values, an output error of a certain entity is still present, due to the non-perfect inversion of the backlash. In Figure 4.18 is shown the backlash input with the relative output (dashed line).

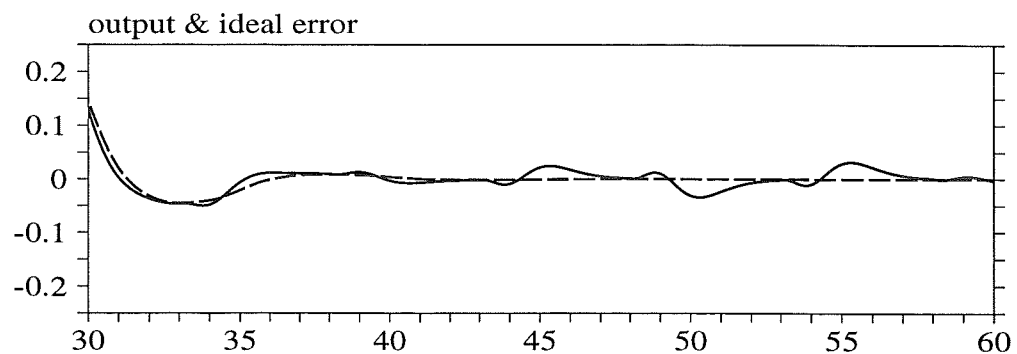


Figure 4.12 Simulation of Example 10

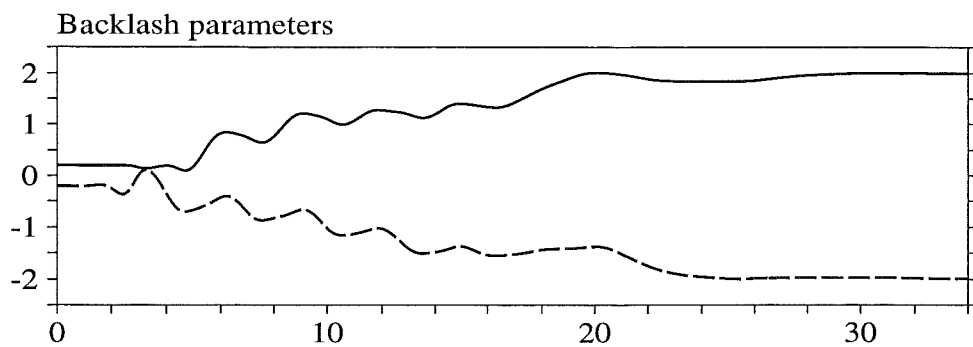


Figure 4.13 Simulation of Example 10

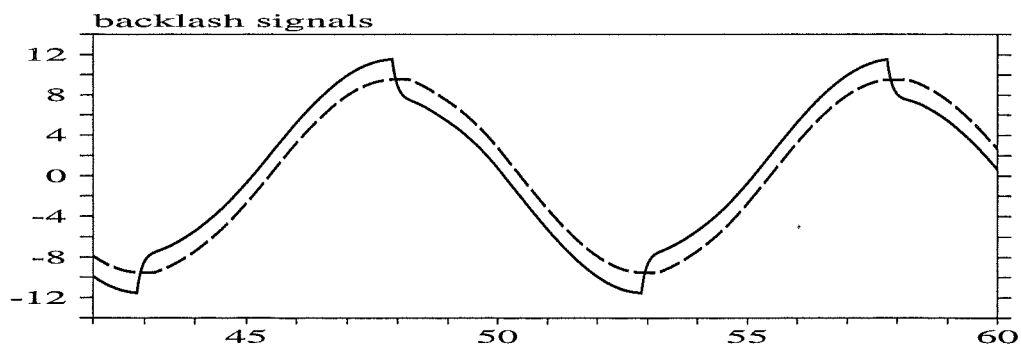


Figure 4.14 Simulation of Example 10

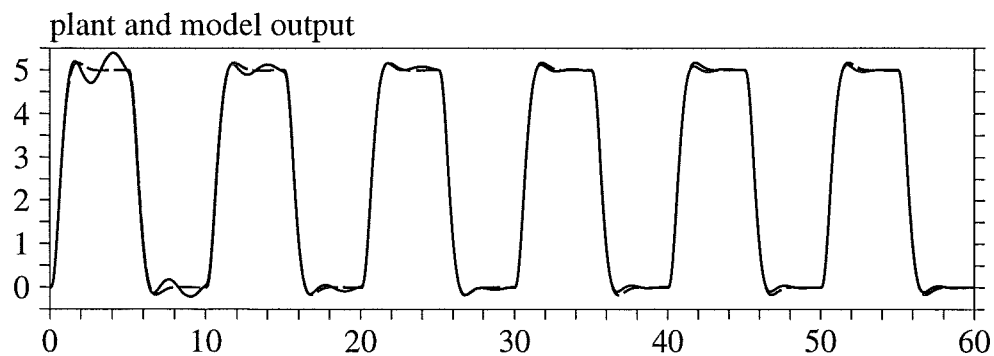


Figure 4.15 Simulation of Example 11

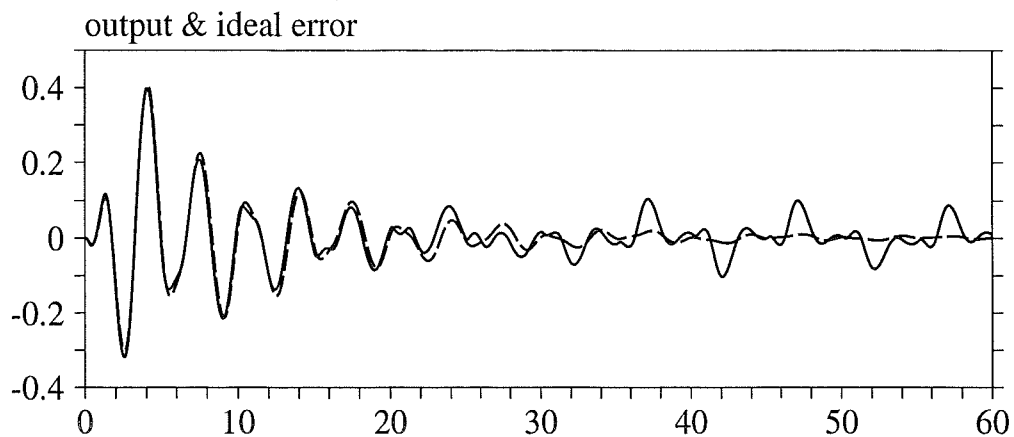


Figure 4.16 Simulation of Example 11

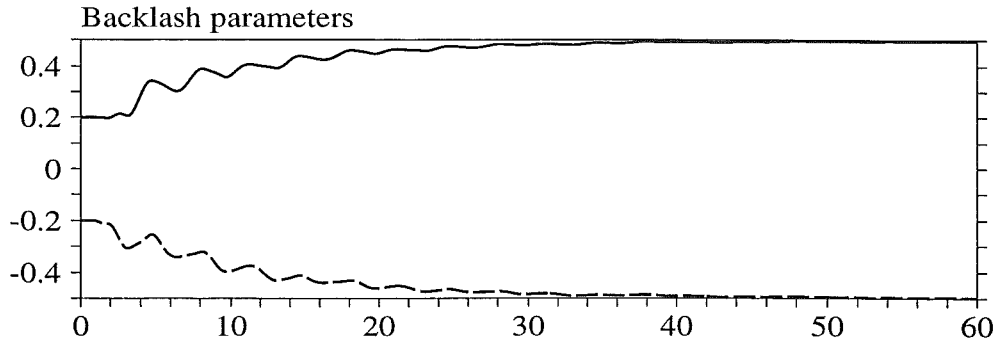


Figure 4.17 Simulation of Example 11

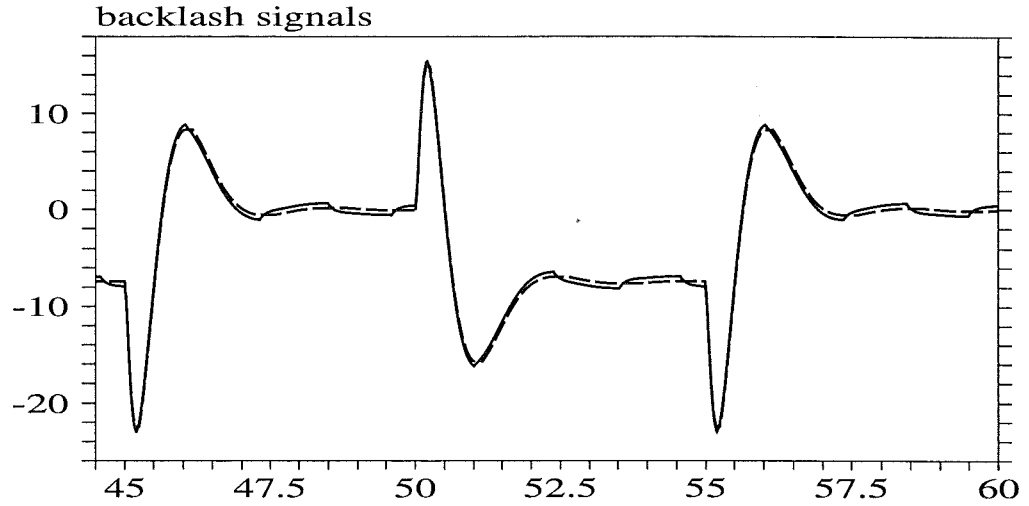


Figure 4.18 Simulation of Example 11

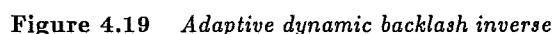
Unknown plant

We would like now to extend the previous algorithm to unknown plants. Let us consider at first an intermediate problem. Suppose to know only the transfer function $P(s)$. Since we assumed to have access to the output of the dynamical system $G(s)$ an adaptive regulator for this part of the plant can be implemented in a complete standard way with M.R.A.C. techniques, using a gradient or an R.L.S. algorithm as described in the previous chapter (see Figure 4.19). Once you have chosen a reference model $G_m(s)$ for the backlash inverse dynamics, then the project of the main loop feedbacks can be carried out solving as usual the Diophantine equation 4.2, since there are no unknown coefficients in it. The adaptive law for updating the backlash parameters can be implemented without any modification. In fact, the contribute given by the mismatched values of the controller parameters on the output error is subtracted and does not appear on the *ideal error* used for the backlash estimation. Let us see now in more detail how to implement an algorithm. If we denote with θ_v^* and θ_z^* the solutions of the following Diophantine equation:

$$\theta_v^T \vec{d}(s) R_g(s) + K_g \theta_z^T \vec{d}(s) Z_g(s) = \Omega(s) [R_g(s) - R_{gm}(s) Z_g(s)] \quad (4.3)$$

and let

$$\theta_{bi}^* = \frac{K_{gm}}{K_g}$$


$$\ddot{e}(t) = \frac{K_g}{R_{gm}(s)} \left\{ [\theta_v(t) - \theta_v^*]^T \frac{\ddot{a}(s)}{\Omega(s)} v(t) + [\theta_z(t) - \theta_z^*]^T \frac{\ddot{a}(s)}{\Omega(s)} v_f(t) + [\theta_{bi}(t) - \theta_{bi}^*] v_d(t) \right\} \quad (4.4)$$
$$\Theta_g(t) \doteq \begin{pmatrix} \theta_v(t) \\ \theta_z(t) \\ \theta_{b_i}(t) \end{pmatrix} \quad \Theta_g^* \doteq \begin{pmatrix} \theta_v^* \\ \theta_z^* \\ \theta_{b_i}^* \end{pmatrix} \quad \Omega_g(t) \doteq \begin{pmatrix} \omega_v(t) \\ \omega_z(t) \\ \omega_{b_i}(t) \end{pmatrix}$$
$$\omega_v(t) \doteq \frac{\vec{d}(s)}{\Omega(s)} v(t) \quad \omega_z(t) \doteq \frac{\vec{d}(s)}{\Omega(s)} v_f(t) \quad \omega_{bi}(t) \doteq v_d(t)$$
$$\check{e}(t) = \frac{K_g}{R_{gm}(s)} [\Theta_g(t) - \Theta_g^*]^T \Omega_g(t)$$

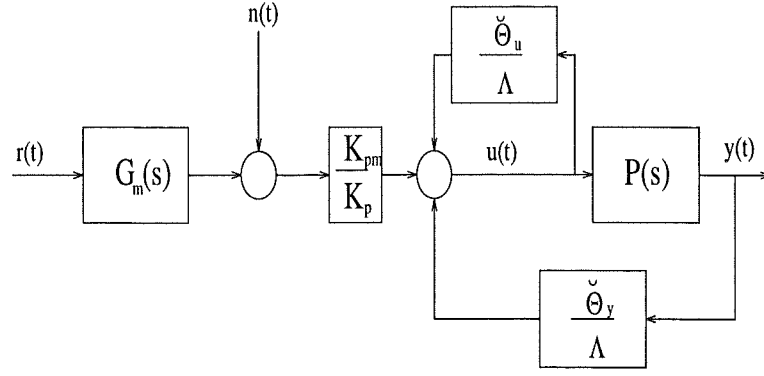


Figure 4.20 $P(s)$ model reference control

Then we can implement an augmented error gradient or RLS algorithm in the standard way

$$\begin{aligned}\zeta(t) &\doteq \frac{1}{R_{gm}(s)} [\Omega_g(t)] \\ \xi(t) &\doteq \Theta_g^T(t) \zeta(t) - \frac{1}{R_{gm}(s)} [\Theta_g^T(t) \Omega_g(t)] \\ \varepsilon(t) &\doteq \check{\varepsilon}(t) + k(t) \xi(t) \\ \dot{\Theta}_g &= -\text{sign}(K_g) \Gamma \zeta(t) \frac{\varepsilon(t)}{1 + \zeta^T(t) \zeta(t)} \\ \dot{k} &= -\gamma \xi(t) \frac{\varepsilon(t)}{1 + \zeta^T(t) \zeta(t)}\end{aligned}\tag{4.5}$$

Suppose now that both $G(s)$ and $P(s)$ are unknown. A straight way to implement an adaptive controller would be to tune the θ_y and θ_u parameters as already done in the previous chapter, just considering in the adaptive laws the ideal error instead of the output error. This kind of solution, though very simple, would lead to a high number of parameters. If we choose a reference model that admits the following factorization:

$$W_m(s) = G_m(s)P_m(s) = \frac{K_{gm}}{R_{gm}(s)} \frac{K_{pm}}{R_{pm}(s)}$$

then we can control separately the two $P(s)$ and $G(s)$ blocks to their reference models. Let us denote with $\check{\theta}_u^*$ and $\check{\theta}_y^*$ the solutions of the following reduced order (with respect to 4.2) diophantine equation:

$$\check{\theta}_u(s)R_p(s) + K_p\check{\theta}_y(s)Z_p(s) = \Lambda(s)[R_p(s) - R_{pm}(s)Z_p(s)]\tag{4.6}$$

where $\Lambda(s)$ is a stable polynomial of degree equal to the plant order. Then we could control $P(s)$ to its reference model $P_m(s)$, as shown in Figure 4.20. If we multiply both the members of 4.6 by $R_{gm}(s)$

$$\check{\theta}_u(s)R(s) + K\check{\theta}_y(s)\frac{R_{gm}(s)}{K_{gm}}Z(s) = \Lambda(s)[R(s) - R_m(s)Z(s)]$$

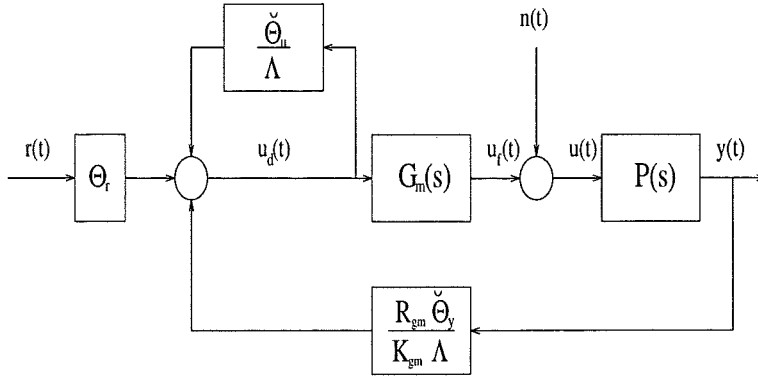


Figure 4.21 Feedbacks factorization

The previous equation implies that our plant can be controlled to the reference model $K_m/R_m(s)$ by the feedbacks shown in Figure 4.21 (with $\theta_r = K_{pm}/K_p$). With such a factorization we just need to estimate the parameters $\check{\theta}_u$ and $\check{\theta}_y$. If we suppose for a while $n(t) = 0$, then the output error expression will be

$$e(t) = \frac{K}{R_m(s)} \left\{ [\check{\theta}_u(t) - \check{\theta}_u^*]^T \frac{\vec{d}(s)}{\Lambda(s)} u(t) + [\check{\theta}_y(t) - \check{\theta}_y^*]^T \frac{\vec{d}(s)}{\Lambda(s)} \frac{R_{gm}(s)}{K_{gm}} y(t) + [\theta_r(t) - \theta_r^*] r(t) \right\}$$

and recalling the expressions of $R_m(s)$ and K

$$e(t) = K_p \left\{ \frac{K_{gm}}{R_m(s)} [\check{\theta}_u(t) - \check{\theta}_u^*]^T \frac{\vec{d}(s)}{\Lambda(s)} u(t) + \frac{K_{gm}}{R_m(s)} [\theta_r(t) - \theta_r^*] r(t) + \frac{1}{R_{pm}} [\check{\theta}_y(t) - \check{\theta}_y^*]^T \frac{\vec{d}(s)}{\Lambda(s)} y(t) \right\}$$

When $n(t) \neq 0$, we must add to the error expression the quantity, $H(s)n(t)$ as already seen.

$$e(t) = K_p \left\{ \frac{K_{gm}}{R_m(s)} [\check{\theta}_u(t) - \check{\theta}_u^*]^T \omega_u(t) + \frac{K_{gm}}{R_m(s)} [\theta_r(t) - \theta_r^*] \omega_r(t) + \frac{1}{R_{pm}(s)} [\check{\theta}_y(t) - \check{\theta}_y^*]^T \omega_y(t) + \frac{1}{R_{pm}(s)} \left(1 - \frac{\check{\theta}_u(s)}{\Lambda(s)} \right) [\theta_b(t) - \theta_b^*]^T \omega_b(t) \right\} + H(s)[\hat{u}(t) - u_f(t) + d_1(t)] \quad (4.7)$$

Then an adaptive algorithm can be implemented with the generalized augmented error technique.

$\Theta_1(t) \doteq \begin{pmatrix} \check{\theta}_u(t) \\ \theta_r(t) \end{pmatrix}$	$\Theta_2(t) \doteq \check{\theta}_y(t)$	$\Theta_3(t) \doteq \theta_b(t)$
$\Theta_1^* \doteq \begin{pmatrix} \check{\theta}_u^* \\ \theta_r^* \end{pmatrix}$	$\Theta_2^* \doteq \check{\theta}_y^*$	$\Theta_3^* \doteq \theta_b^*$
$\Omega_1(t) \doteq \begin{pmatrix} \omega_u(t) \\ \omega_r(t) \end{pmatrix}$	$\Omega_2(t) \doteq \omega_y(t)$	$\Omega_3(t) \doteq \omega_b(t)$
$\Phi_1(t) \doteq \Theta_1(t) - \Theta_1^*$	$\Phi_2(t) \doteq \Theta_2(t) - \Theta_2^*$	$\Phi_3(t) \doteq \Theta_3(t) - \Theta_3^*$
$W_1(s) \doteq \frac{K_{gm}}{R_m(s)}$	$W_2(s) \doteq \frac{1}{R_{pm}(s)}$	$W_3(s) \doteq \frac{\Lambda(s) - \check{\theta}_u^*(s)}{R_{pm}(s)\Lambda(s)}$

Notice that $W_3(s)$ depends on the vector $\check{\theta}_u^*$. This implies that in the adaptation law $\check{\theta}_u^*$ is replaced by its estimate at time t . With the previous notations the output error expression is

$$e(t) = K_p \left\{ \sum_{j=1..3} W_j(s) [\Phi_j^T(t) \Omega_j(t)] \right\} + H(s) [\hat{u}(t) - u_f(t) + d_1(t)] \quad (4.8)$$

We define the *ideal error* as

$$e_i(t) \doteq e(t) - k(t) J(s) [\hat{u}(t) - u_f(t)] \quad (4.9)$$

where $J(s) \doteq H(s)/K_p$. Then we can define the auxiliary errors in the standard way

$$\begin{aligned} \zeta_j(t) &\doteq W_j(s) \Omega_j(t) \\ \xi_j(t) &\doteq \Theta_j^T(t) \zeta_j(t) - W_j(s) [\Theta_j^T(t) \Omega_j(t)] \end{aligned} \quad \text{for } j = 1..3$$

$$\xi(t) \doteq \sum_{j=1..3} \xi_j(t) \quad \zeta(t) \doteq \begin{pmatrix} \zeta_1(t) \\ \zeta_2(t) \\ \zeta_3(t) \end{pmatrix}$$

The augmented ideal error is

$$\varepsilon_i(t) \doteq e_i(t) + k(t) \xi(t) \quad (4.10)$$

If we denote with $k(t) \doteq K_p + \varphi(t)$, and recalling the generalized augmented error expression, then the following equality holds:

$$\varepsilon_i(t) = K_p \left\{ \sum_{j=1..3} \Phi_j^T(t) \zeta_j(t) \right\} + \varphi(t) \left\{ \xi(t) - J(s) [\hat{u}(t) - u_f(t)] \right\} + H(s) d_1(t) \quad (4.11)$$

Our adaptive laws for adjusting Φ_j and φ are

$$\begin{aligned}\dot{\Phi}_j &= -\text{sign}(K_p) \zeta_j(t) \frac{\varepsilon_i(t)}{1 + \zeta^T(t)\zeta(t)} \quad \text{for } j = 1..3 \\ \dot{\varphi} &= -\varepsilon_i(t) \frac{\xi(t) - J(s)[\hat{u}(t) - u_f(t)]}{1 + \zeta^T(t)\zeta(t)}\end{aligned}\quad (4.12)$$

Simulation results

Example 12

In the algorithm presented in this section two different adaptive controllers are involved. The inner one is a standard linear MRAC; its estimates are shown in the “internal parameters estimates” plot of Figure 4.22 and are updated according to the *internal error* $\check{e}(t)$. The outer one updates both the backlash parameters and the feedback gains; its estimates are updated according to the ideal error evolution and are referred in the plots as “u feedback”, “y feedback” and “width and bias”. Figure 4.22 refers to the following model:

Plant transfer function	$P(s) = \frac{1}{s(s+1)}$
Dynamic block function	$G(s) = \frac{1}{s-0.5}$
Reference model 1	$P_m(s) = \frac{\omega^2}{s^2 + 2\omega\xi s + \omega^2} \quad \begin{matrix} \omega = 2 \\ \xi = 0.7 \end{matrix}$
Reference model 2	$G_m(s) = \frac{10}{s+10}$
Backlash parameters	$C_l = -2 \quad C_r = 2$
Adaptive algorithms	RLS for G(s) controller SG for Backlash and Plant

As already seen in Example 4 and 5, the convergence of the algorithm becomes very slow after the initial transient even if the estimates of the feedbacks parameters are still far from their matching values. Nevertheless the backlash width and bias estimates converge in general more rapidly and allow at least a partial backlash compensation.

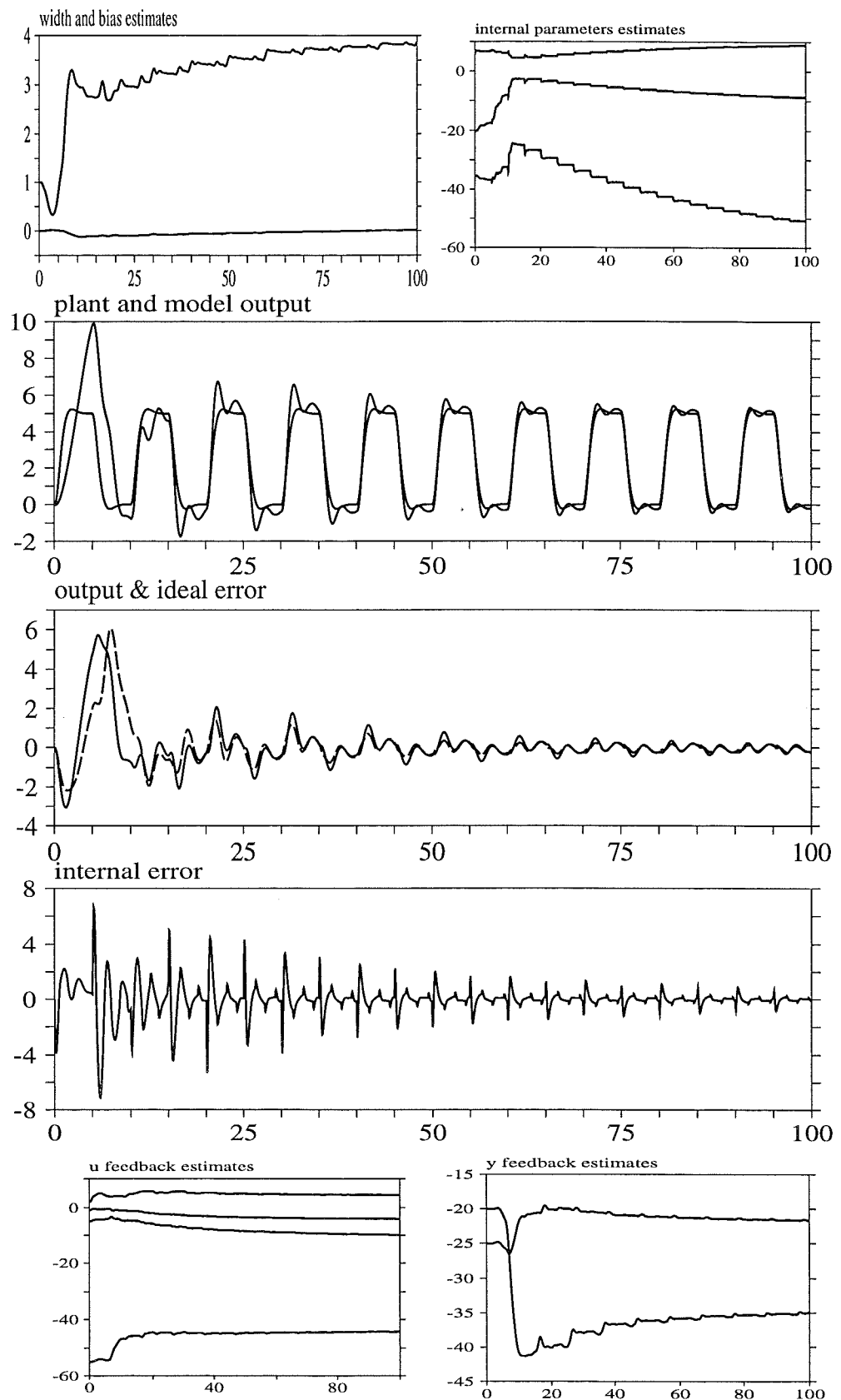


Figure 4.22 Simulation of Example 12

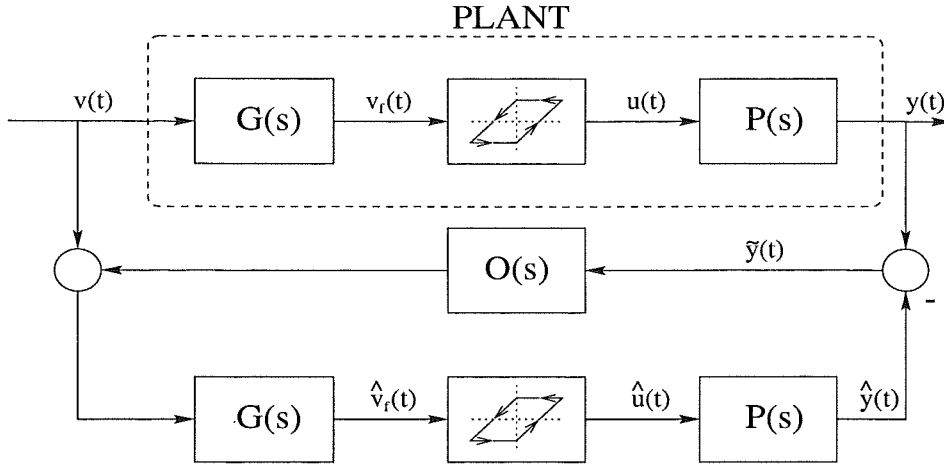


Figure 4.23 Non linear observer

4.4. Non linear observer

Deterministic plant observer: known backlash

In the previous paragraphs we always made the assumption that the input of the backlash was accessible. In order to remove that restriction we have to design an observer for our plant. In particular if the system $G(s)$ is stable, then we can observe its output with an open-loop observer. The algorithm described in the previous paragraphs (for the known plant case) can be directly extended to this situation. If the transfer function $G(s)$ is unstable or unknown we have to consider a more general scheme. Let us notice that the aim of asymptotic state observing is not achievable for an arbitrary input signal. Whenever the backlash is working in the *dead-zone* we loose all the information about its input and about the state evolution of $G(s)$. Still we can try to design a linear-like observer, including a backlash in our plant model. The observer structure is shown in Figure 4.23. We define $\tilde{u}(t)$, $\tilde{v}_f(t)$ and $\tilde{y}(t)$ as

$$\tilde{u}(t) \doteq u(t) - \hat{u}(t) \quad \tilde{v}_f(t) \doteq v_f(t) - \hat{v}_f(t) \quad \tilde{y}(t) \doteq y(t) - \hat{y}(t)$$

Then it follows from the observer scheme

$$\tilde{y}(t) = P(s) \tilde{u}(t)$$

$$\tilde{u}(t) = B[v_f(t)] - B[\hat{v}_f(t)]$$

If we denote with $d(t) \doteq B(v) - v + v_0$, it is easy to see that the following relationship holds:

$$|d(t)| \leq b$$

where $2b$ is as usual the backlash width and v_0 its bias. Then we have for $\tilde{u}(t)$

$$\tilde{u}(t) = \tilde{v}_f(t) + \tilde{d}(t)$$

Then if we write explicitly $\tilde{v}_f(t)$ as a function of $\tilde{y}(t)$ we have for the close loop system the following relation:

$$\tilde{u} = -\frac{G(s)O(s)P(s)}{1 + G(s)O(s)P(s)}\tilde{d}(t) \quad (4.13)$$

Then if we choose $O(s)$ in order to have in 4.13 a stable transfer function we will have a bounded observation error. The previous equation also suggest a possible criterion to design a good observer, that is trying to keep $|O(j\omega)|$ as low as possible for ω close to the reference frequency. It is quite interesting to see what kind of behavior we would expect from this observer with a first harmonic analysis. Let us assume to have

$$v_f(t) \doteq A \sin(\omega t)$$

$$\hat{v}_f(t) \doteq \hat{A} \sin(\omega t + \phi)$$

then, with a fasorial notation

$$\tilde{v}_f(t) = A - \hat{A}e^{j\phi}$$

We can use the backlash describing function to compute $\tilde{u}(t)$

$$\tilde{u}(t) = N(A)A - N(\hat{A})\hat{A}e^{j\phi}$$

Then recalling $\tilde{v}_f(t) = -G(j\omega)O(j\omega)P(j\omega)\tilde{u}(t)$ we have

$$-\frac{A - \hat{A}e^{j\phi}}{N(A)A - N(\hat{A})\hat{A}e^{j\phi}} = G(j\omega)O(j\omega)P(j\omega) \quad (4.14)$$

It is easy to see that when $b \rightarrow 0$ eqn. 4.14 reduces to the classical Nyquist expression to determine the closed-loop poles of the linear system $G(s)O(s)P(s)$ with a unitary feedback (since $N(\cdot) \rightarrow 1$). Let us now suppose for a while $\phi = 0$; we have

$$-\frac{A - \hat{A}}{N(A)A - N(\hat{A})\hat{A}} = G(j\omega)O(j\omega)P(j\omega)$$

If we pass to the limit for $\hat{A} \rightarrow A$ then the previous equation becomes

$$-\frac{1}{\frac{d}{dA}[N(A)A]} = G(j\omega)O(j\omega)P(j\omega) \quad (4.15)$$

Let us now consider what we have for $\hat{A} = A$. If we pass to the limit for $\phi \rightarrow 0$ then eqn. 4.14 yields

$$-\frac{1}{N(A)} = G(j\omega)O(j\omega)P(j\omega) \quad (4.16)$$

We can now see with a practical example what equations 4.15 and 4.16 suggest.

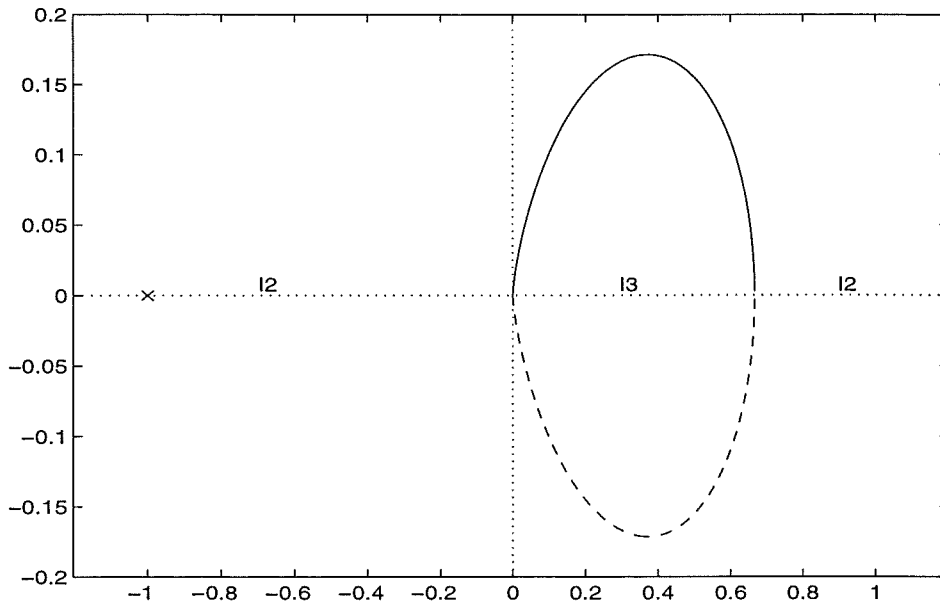


Figure 4.24 Nyquist diagram of $G(s)P(s)$

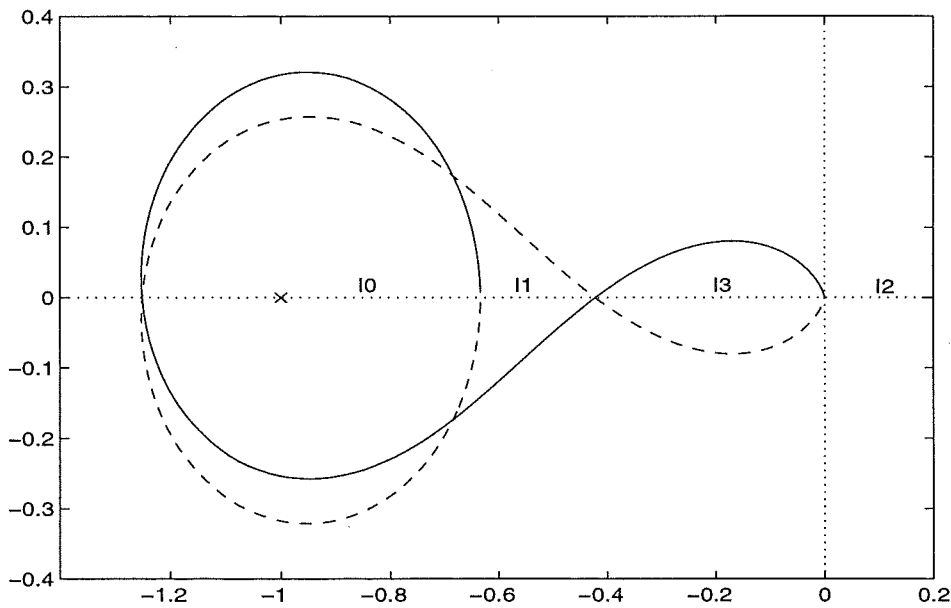


Figure 4.25 Nyquist diagram of $O(s)G(s)P(s)$

Let us consider the following transfer functions:

$$P(s) = \frac{1}{(s+1)(s-1.5)} \quad G(s) = \frac{1}{s-1}$$

The system $P(s)G(s)$ has two unstable poles. In order to stabilize it we have to find an $O(s)$ such that the Nyquist plot of $P(j\omega)G(j\omega)O(j\omega)$ chains twice the point -1 . We have chosen here $O(s) = (177s^2 + 121s - 55)/(s^2 + 11.5s + 58)$. The resulting Nyquist plot is shown in Figure 4.25. The two functions $-1/N(A)$ and $-1/\frac{d}{dA}[N(A)A]$ tend to -1 when $A \rightarrow \infty$, then the

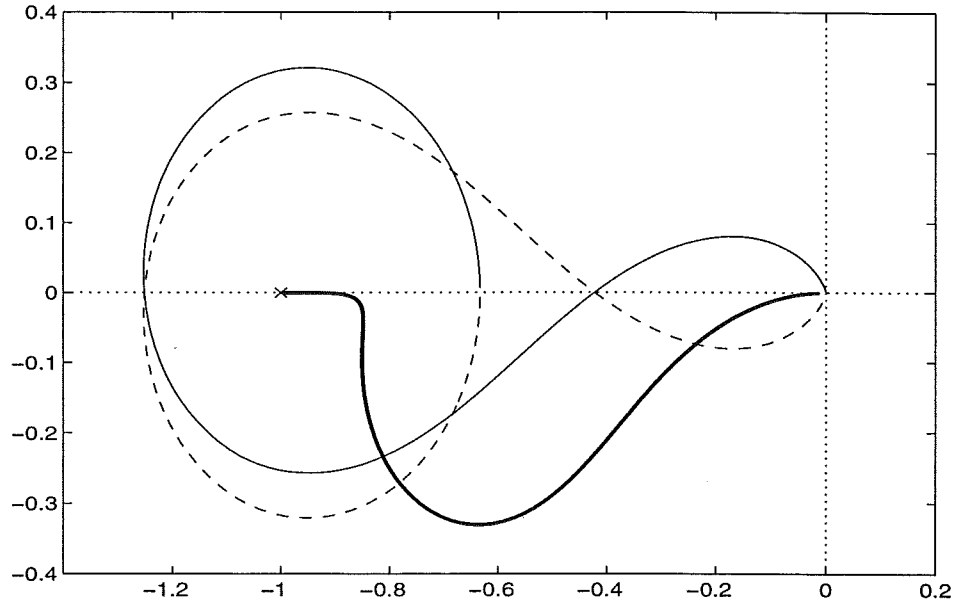


Figure 4.26 Nyquist plot of $-1/\frac{d}{dA}[N(A)A]$

system behavior tends to stability whenever the input signals amplitude is big compared to the backlash width. A rough estimate \bar{A} of the threshold value for the signal amplitude to guarantee a small observing error can be obtained plotting the graphs of the first members of eqns. 4.15 and 4.16 together with the Nyquist diagram of the loop-gain and choosing for \bar{A} the value

$$\bar{A} \doteq \max\{A1, A2\}$$

where $A1$ and $A2$ are the solutions of eqns. 4.15 and 4.16. The two diagrams are plotted in Figures 4.26 and 4.27. Simulations showed a fast convergence of the observing error to small values. In Figure 4.28 is shown the error evolution with a 15% ratio between the backlash width and the signal amplitude.

Adaptive observer: unknown backlash

Let us consider now the problem of estimating the backlash parameters within the observer scheme. If we substitute a backlash estimate in the observer we have for the closed-loop signals the following relations:

$$\begin{aligned}\tilde{y}(t) &= P(s) \tilde{u}(t) \\ \tilde{u}(t) &= B[v_f(t)] - \hat{B}[\hat{v}_f(t)] \\ \hat{v}_f(t) &= -G(s)O(s) \tilde{y}(t)\end{aligned}\tag{4.17}$$

If we recall the expression of the backlash output we obtain

$$\begin{aligned}B[v_f(t)] &= \chi_r(t)[v_f(t) - C_r] + \chi_l(t)[v_f(t) - C_l] + \chi_s(t)u_s \\ \hat{B}[\hat{v}_f(t)] &= \hat{\chi}_{rb}(t)[\hat{v}_f(t) - \hat{C}_r] + \hat{\chi}_{lb}(t)[\hat{v}_f(t) - \hat{C}_l] + \hat{\chi}_{sb}(t)\hat{u}_s\end{aligned}$$

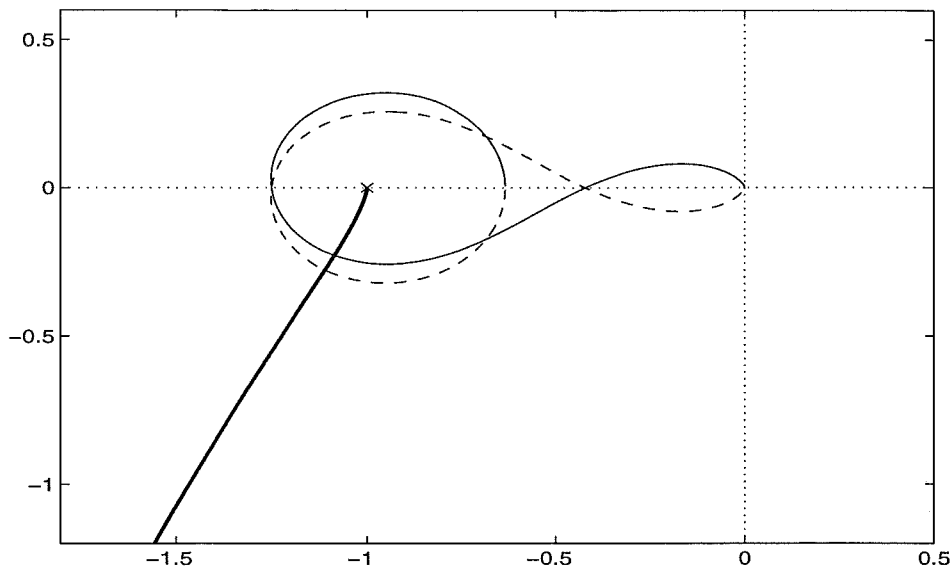


Figure 4.27 Nyquist plot of $-1/N(A)$

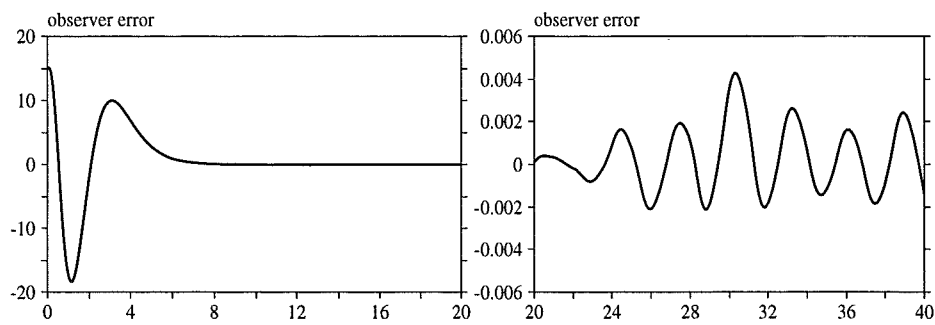


Figure 4.28 Observer simulation

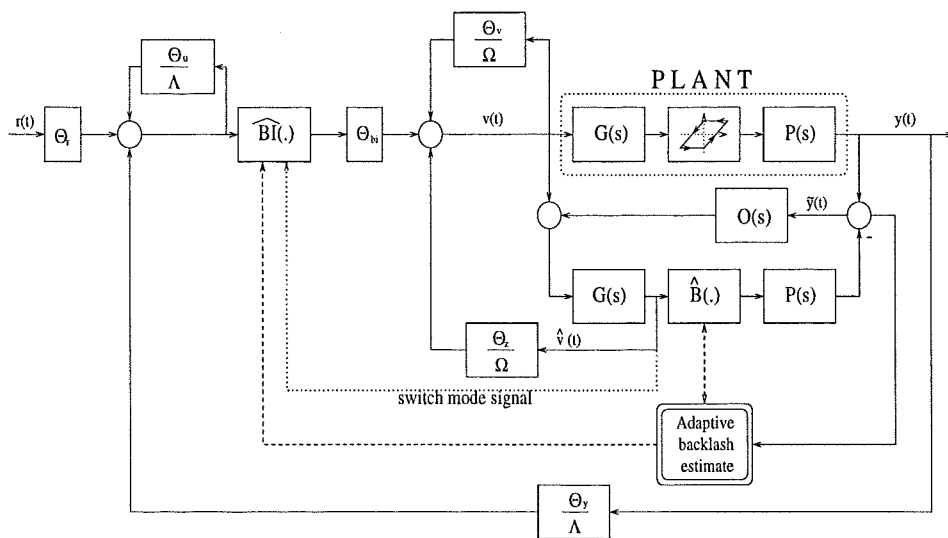


Figure 4.29 The structure of the adaptive controller

Then it follows for $\tilde{u}(t)$

$$\tilde{u}(t) = \hat{\chi}_{rb}(t)(\hat{C}_r - C_r) + \hat{\chi}_{lb}(t)(\hat{C}_l - C_l) + \tilde{v}_f(t) + d(t) \quad (4.18)$$

where $d(t)$ is a bounded disturbance defined as

$$d(t) = \chi_s u_s - \hat{\chi}_{sb} \hat{u}_s + [\hat{\chi}_{rb} - \chi_r][v_f(t) - C_r] + [\hat{\chi}_{lb} - \chi_l][v_f(t) - C_l] - \hat{\chi}_s \tilde{v}_f(t)$$

If we substitute $\tilde{u}(t)$ in 4.17 we have

$$\tilde{y}(t) = \frac{P(s)}{1 + P(s)G(s)O(s)} [(\theta_b(t) - \theta_b^*)^T \omega_b(t) + d(t)] \quad (4.19)$$

This parametrization of the observer error allows us to define an adaptation law for the backlash parameters. We can as usual implement a stochastic gradient or an RLS estimation law with the augmented error technique, in the following way:

$$\begin{aligned} T(s) &\doteq \frac{P(s)}{1 + P(s)G(s)O(s)} \\ \zeta_b(t) &\doteq T(s) \omega_b(t) \\ \xi(t) &\doteq \theta_b^T(t) \zeta_b(t) - T(s)[\theta_b^T(t) \omega_b(t)] \\ \varepsilon(t) &\doteq \tilde{y}(t) + \xi(t) \end{aligned}$$

Stochastic Gradient:

$$\dot{\theta}_b(t) = -\Gamma \zeta_b(t) \frac{\varepsilon(t)}{1 + \zeta_b^T \zeta_b}$$

Recursive Least Square:

$$\dot{\theta}_b(t) = -P(t) \zeta_b(t) \varepsilon(t)$$

$$\dot{P}(t) = \alpha P(t) - P(t) \zeta_b(t) \zeta_b^T(t) P(t)$$

Simulation results

Example 13

We are considering hereby a second order unstable system with a first order unstable dynamics in front of the backlash. The backlash effects are quite critical with respect to the amplitude of the signals involved. The simulation in fact showed big limit cycles around the reference in the initial transient, when there is not a proper backlash compensation. Figure 4.30 refers to the following settings:

Plant transfer function	$P(s) = \frac{1}{(s+1)(s-1.5)}$
Dynamic block function	$G(s) = \frac{1}{s-1}$
Plant reference model	$W_m(s) = \frac{5\omega^2}{(s+5)(s^2+2\xi\omega s+\omega^2)}$ $\xi = 0.7$ $\omega = 3$
Dynamic block model	$G_m(s) = \frac{10}{s+10}$
Feedback polynomials	$\Lambda(s) = (s+2)^3 \quad \Omega(s) = s+5$
Observer transfer function	$O(s) = \frac{177s^2+121s-55}{s^2+11.5s+58}$
Adaptive algorithm	Recursive Least Square
Backlash parameters	$C_r = 2.5 \quad C_l = -1.5$

Notice that the residual observation error always present when the dynamics of $G(s)$ are unstable does not compromise the convergence of the backlash parameters. Since we need an observer for the signal $v_f(t)$, this kind of approach is not extendible to the case of unknown plants and dynamics.

4.5. Dynamic backlash inversion: explicit approach

Plant estimate

Let us consider now the plant structure shown in Figure 4.31. We want to design an algorithm to estimate the whole system. Let us see the new notations¹ introduced²:

$$A(s) = s^n + a_1 s^{n-1} + a_2 s^{n-2} + \dots + a_n$$

$$B(s) = b_0 s^m + b_1 s^{m-1} + \dots + b_m$$

$$C(s) = s^p + c_1 s^{p-1} + c_2 s^{p-2} + \dots + c_p$$

$$D(s) = s^q + d_1 s^{q-1} + d_2 s^{q-2} + \dots + d_q$$

¹The notations are different from the previous chapters since a new kind of parametrization for the plants is needed.

²We have assumed without loss of generality $D(s)$ to be monic. It is always possible to include d_0 as a coefficient in front of $B(s)$, simply rescaling the backlash width.(see Figure 4.32)

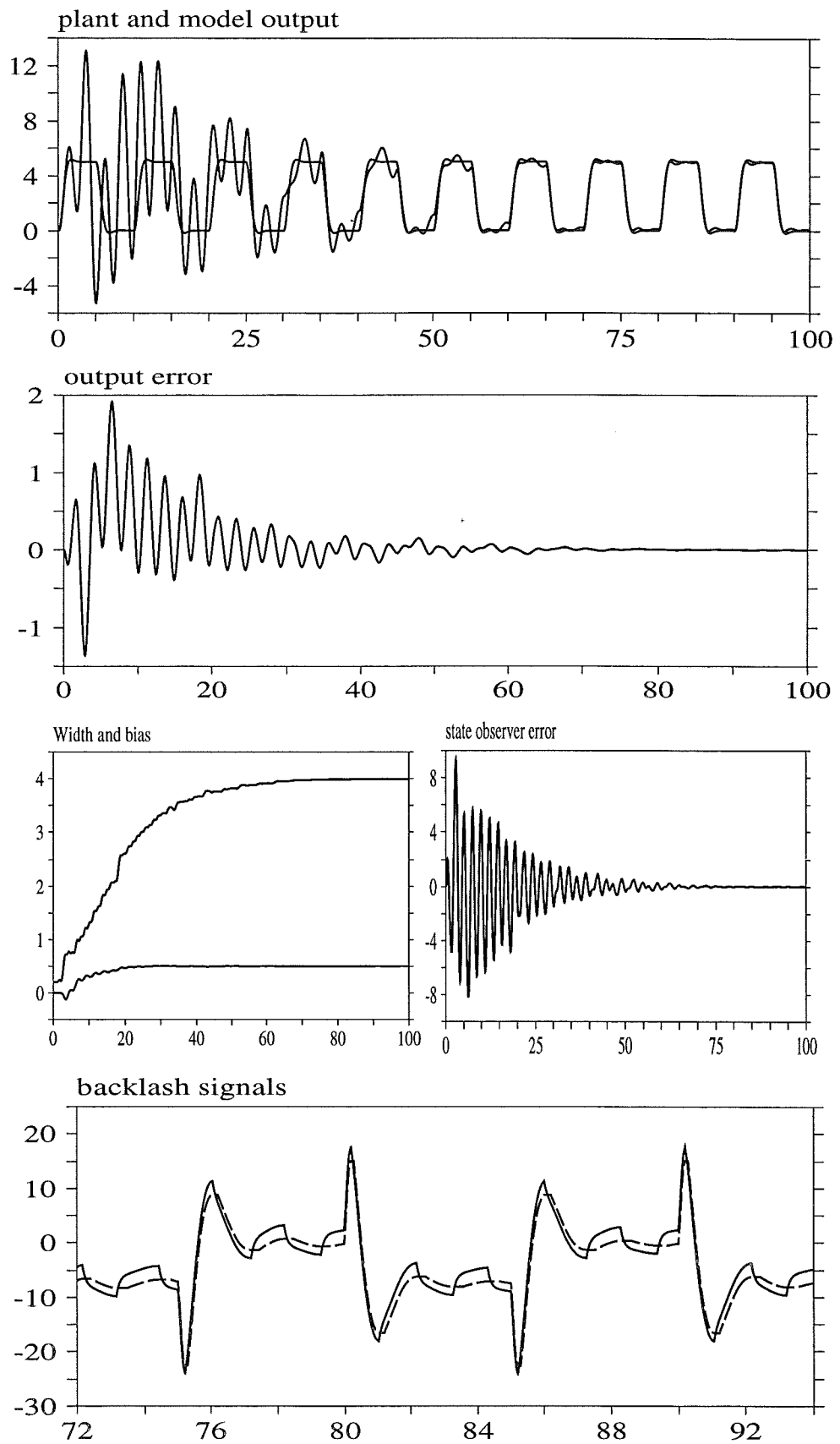


Figure 4.30 Simulation of Example 13

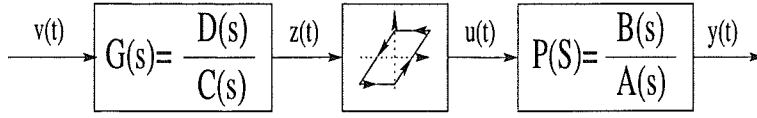


Figure 4.31 Plant structure

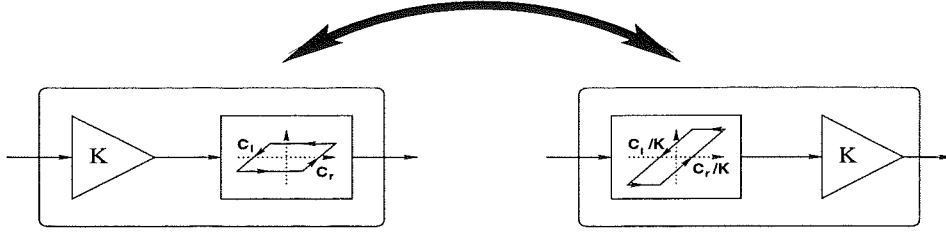


Figure 4.32 Backlash and gain commutation

Our plant equations are

$$\begin{aligned} A(s)y(t) &= B(s)u(t) \\ u(t) &= B[z(t)] \\ C(s)z(t) &= D(s)v(t) \end{aligned} \quad (4.20)$$

If we write the backlash output in terms of a width W and a bias z_0

$$u(t) = z(t) - z_0 + \frac{\chi_l(t) - \chi_r(t)}{2}W + \chi_s(t)[u_s - z(t)]$$

and we substitute its expression in eqn. 4.20, then we have the following equality:

$$AC(s)y(t) = BD(s)v(t) + BC(s) \left[\frac{\chi_l - \chi_r}{2}W - z_0 + \chi_s[u_s - z(t)] \right] \quad (4.21)$$

Since the signal $\rho(t) \doteq \frac{(\chi_l - \chi_r)}{2}$ is not assumed to be measurable, we will replace it with its estimate $\hat{\rho}(t)$, where

$$\hat{\rho}(t) \doteq \frac{\hat{\chi}_l - \hat{\chi}_r}{2}$$

We must now consider a stable polynomial $\Upsilon(s)$, with $\partial\Upsilon = p+n$. If we divide the two members by Υ and exploiting the equality

$$\frac{B(s)C(s)}{\Upsilon(s)}z_0 = \frac{b_m c_p}{\Upsilon(0)}z_0$$

we obtain

$$\frac{AC}{\Upsilon}(s)y(t) = \frac{BD}{\Upsilon}(s)v(t) - \frac{b_m c_p z_0}{\Upsilon(0)} + W \frac{BC}{\Upsilon}(s)\hat{\rho}(t) + d(t)$$

where we defined the bounded disturbance $d(t)$ as

$$d(t) \doteq \frac{B(s)C(s)}{\Upsilon(s)} [\chi_s(t)[u_s - z(t)] + W[\rho(t) - \hat{\rho}(t)]]$$

If we denote with $\Delta_i(s)$ the following transfer functions:

$$\Delta_i(s) \doteq \frac{s^i}{\Upsilon(s)} \quad \text{for } i = 0 \dots n+p$$

and we define the polynomials

$$\begin{aligned} A(s)C(s) &= s^{n+p} + \mathcal{A}C_1 s^{n+p-1} + \mathcal{A}C_2 s^{n+p-2} + \dots + \mathcal{A}C_{n+p} \\ B(s)D(s) &= \mathcal{B}D_0 s^{m+q} + \mathcal{B}D_1 s^{m+q-1} + \dots + \mathcal{B}D_{m+q} \\ B(s)C(s) &= \mathcal{B}C_0 s^{m+p} + \mathcal{B}C_1 s^{m+p-1} + \dots + \mathcal{B}C_{m+p} \end{aligned}$$

we have the following expression for $y_\Upsilon \doteq \Delta_{n+p}y(t)$:

$$\begin{aligned} y_\Upsilon = & -\mathcal{A}C_1 \Delta_{n+p-1}y - \mathcal{A}C_2 \Delta_{n+p-2}y - \dots - \mathcal{A}C_{n+p} \Delta_0 y + \\ & + \mathcal{B}D_0 \Delta_{m+q}v + \mathcal{B}D_1 \Delta_{m+q-1}v + \dots + \mathcal{B}D_{m+q} \Delta_0 v + \\ & + W\mathcal{B}C_0 \Delta_{m+p} \hat{\rho} + W\mathcal{B}C_1 \Delta_{m+p-1} \hat{\rho} + \dots + W\mathcal{B}C_{m+p} \Delta_0 \hat{\rho} + \quad (4.22) \\ & - \frac{b_m c_p z_0}{\Upsilon(0)} + d(t) \end{aligned}$$

The previous equation is (apart for the disturbance $d(t)$) a linear parametrization of the plant output. We can then define the following vectors:

$$\theta \doteq \begin{pmatrix} \mathcal{A}C_1 \\ \mathcal{A}C_2 \\ \vdots \\ \mathcal{A}C_{n+p} \\ \mathcal{B}D_0 \\ \mathcal{B}D_1 \\ \vdots \\ \mathcal{B}D_{m+q} \\ W\mathcal{B}C_0 \\ W\mathcal{B}C_1 \\ \vdots \\ W\mathcal{B}C_{m+p} \\ \frac{b_m c_p z_0}{\Upsilon(0)} \end{pmatrix} \quad \phi(t) \doteq \begin{pmatrix} -\Delta_{n+p-1}[y] \\ -\Delta_{n+p-2}[y] \\ \vdots \\ -\Delta_0[y] \\ \Delta_{m+q}[v] \\ \Delta_{m+q-1}[v] \\ \vdots \\ \Delta_0[v] \\ \Delta_{m+p}[\hat{\rho}] \\ \Delta_{m+p-1}[\hat{\rho}] \\ \vdots \\ \Delta_0[\hat{\rho}] \\ -1 \end{pmatrix}$$

Eqn. 4.22 can be rewritten as

$$y_\Upsilon = \theta^T \phi(t) + d(t) \quad (4.23)$$

We could now implement an RLS algorithm to estimate θ . The presence of the disturbance $d(t)$ would not allow an exact convergence of $\hat{\theta}(t)$ to the real values. If the requirements are not particularly severe it is possible that the estimates oscillations do not compromise the system behavior³. If we need a sharper convergence, we must try to observe the noise $d(t)$.

³It should be noticed that if the block $G(s)$ is controlled to a sufficiently ready model the noise $d(t)$ will be attenuated if it is active the backlash compensation; the residual noise that we have under matching conditions of the backlash parameters is caused by the inexact backlash inversion.

Parameters deconvolution

We need now to compute the plant parameters in order to design the controller and the observer. Since we assumed $C(s)$ and $D(s)$ to be monic, the two parameters WBC_0 and BD_0 can be seen, the first as an estimate of b_0W , the second as an estimate of b_0 , so we can define the width estimate as

$$\hat{w} \doteq \frac{WBC_0}{BD_0} \quad (4.24)$$

It is now quite evident that we can obtain an estimate of the product $B(s)C(s)$ as

$$BC_i \doteq \frac{WBC_i}{\hat{w}} \quad (4.25)$$

We have now to figure out a way to compute the estimates of the polynomials $A(s)$, $B(s)$, $C(s)$, $D(s)$ from the estimates of their products: $AC(s)$, $BC(s)$, $BD(s)$. One possible solution could be try to cancel the common factors from the polynomials $AC(s)$, $BC(s)$ and $BC(s)$, $BD(s)$; it is not sure whether this way to proceed would lead to good results for our control purposes, since it is not clear what kind of deconvolution we are performing under non-matching conditions. One different approach is to consider the following equalities

$$AC(s)B(s) - BC(s)A(s) = 0$$

$$BC(s)D(s) - BD(s)C(s) = 0$$

They are clearly satisfied under parameters matching conditions. We can then define the two polynomials $J_1(s)$, $J_2(s)$ as

$$J_1(s) \doteq AC(s)B(s) - BC(s)A(s)$$

$$J_2(s) \doteq BC(s)D(s) - BD(s)C(s)$$

We can then decide

$$[\hat{A}(s), \hat{B}(s)] = \arg \min_{A(s), B(s)} \aleph \{J_1(s)\}$$

$$[\hat{C}(s), \hat{D}(s)] = \arg \min_{C(s), D(s)} \aleph \{J_2(s)\}$$

where \aleph is a positive definite functional. In order to have a close solution to these problem we can choose a quadratic functional. If we define the polynomial $\Sigma(s)$, with $\partial\Sigma > \max\{\partial A(s)B(s)C(s), \partial B(s)C(s)D(s)\}$ in order to perform a low-pass filter action on $J(s)$, we can set

$$\aleph\{J\} \doteq \int_{-\infty}^{+\infty} \left| \frac{J(j\omega)}{\Sigma(j\omega)} \right|^2 d\omega \quad (4.26)$$

Let us consider the following vectors:

$$\theta_1 \doteq \begin{pmatrix} a_1 \\ a_2 \\ \cdot \\ \cdot \\ a_n \\ b_0 \\ b_1 \\ \cdot \\ \cdot \\ b_m \end{pmatrix} \quad \varphi_1(s) \doteq \begin{pmatrix} -\frac{BCs^{n-1}}{\Sigma} \\ -\frac{BCs^{n-2}}{\Sigma} \\ \cdot \\ \cdot \\ -\frac{BC}{\Sigma} \\ \frac{ACs^m}{\Sigma} \\ \frac{ACs^{m-1}}{\Sigma} \\ \cdot \\ \cdot \\ \frac{AC}{\Sigma} \end{pmatrix}$$

With the previous notations we have

$$\frac{J_1(s)}{\Sigma(s)} = \theta_1^T \varphi_1(s) - \frac{BCs^n}{\Sigma(s)}$$

Then our parameters value can be chosen solving the following linear system:

$$\left\{ \int_{-\infty}^{+\infty} \varphi_1(j\omega) \varphi_1(-j\omega)^T d\omega \right\} \theta_1 = \int_{-\infty}^{+\infty} \varphi_1(j\omega) \left(\frac{BCs^n}{\Sigma(s)} \right)_{s=-j\omega} d\omega \quad (4.27)$$

In the same way we have for $J_2(s)$

$$\frac{J_2(s)}{\Sigma(s)} = \theta_2^T \varphi_2(s) - \frac{BDs^p - BCs^q}{\Sigma(s)}$$

with the following notations:

$$\theta_2 \doteq \begin{pmatrix} c_1 \\ c_2 \\ \cdot \\ \cdot \\ c_p \\ d_1 \\ d_2 \\ \cdot \\ \cdot \\ d_q \end{pmatrix} \quad \varphi_2(s) \doteq \begin{pmatrix} -\frac{BDs^{p-1}}{\Sigma} \\ -\frac{BDs^{p-2}}{\Sigma} \\ \cdot \\ \cdot \\ -\frac{BD}{\Sigma} \\ \frac{BCs^{q-1}}{\Sigma} \\ \frac{BCs^{q-2}}{\Sigma} \\ \cdot \\ \cdot \\ \frac{BC}{\Sigma} \end{pmatrix}$$

Let us notice that eqn. 4.27 can be computed according to residues theory. All the integrals are of the following form:

$$\int_{-\infty}^{+\infty} \left(\frac{Q(s)}{\Sigma(s)\Sigma(-s)} \right)_{s=j\omega} d\omega$$

Since we have chosen the polynomial Σ we already know its zeros and we can easily compute a partial-fraction expansion of the ratio $Q(s)/(\Sigma(s)\Sigma(-s))$.

If we have chosen $\Sigma(s)$ with only simple zeros, we will have the following expression:

$$\frac{Q(s)}{\Sigma(s)\Sigma(-s)} = \sum_{i=1..\partial\Sigma} \left(\frac{r_i^+}{s-p_i} + \frac{r_i^-}{s+p_i} \right)$$

Integrating the previous equality

$$\int_{-\infty}^{+\infty} \left(\frac{Q(s)}{\Sigma(s)\Sigma(-s)} \right)_{s=j\omega} d\omega = \pi \sum_{i=1..\partial\Sigma} (r_i^- - r_i^+)$$

One possible drawback of the deconvolution discussed so far is the need to divide in eqns. 4.24 and 4.25 by quantities that we cannot guarantee to be different from zero. Besides we must be sure not to have over-parametrized our plant, otherwise we would get in 4.24 a ratio between quantities that may tend to zero. Whenever it is only known an upper limit for the plant order we must adopt a different kind of deconvolution. Using the same procedure we have previously described we can go through the following steps:

1. From \mathcal{AC} and $WBC \Rightarrow \hat{A}(s), \hat{W}B(s)$
2. From \mathcal{BD} and $WBC \Rightarrow \hat{D}(s), \hat{W}C(s)$
3. We compute the product $W^2BC \doteq \hat{W}B \times \hat{W}C$
4. Let $Q > 0 \in \mathbb{R}^{(m+p+1) \times (m+p+1)}$. We define ⁴ \hat{w} as

$$\hat{w} \doteq \arg \min_{w \in \mathbb{R}} \|W\vec{B}Cw - W^2\vec{B}C\|_Q^2$$

It follows from the definition

$$\hat{w} = \frac{W^2\vec{B}C^T Q W\vec{B}C}{W\vec{B}C^T Q W\vec{B}C}$$

Controller and Observer design

Our controller structure is shown in Figure 4.33. The controllers parameters can be set solving on line the two following Diophantine equations:

$$\begin{aligned} \check{\theta}_u(s)\hat{A}(s) + \check{\theta}_y(s)\hat{B}(s) &= \Lambda(s)\left[\hat{A}(s) - \frac{R_{pm}(s)\hat{B}(s)}{\hat{b}_0}\right] \\ \theta_v(s)\hat{C}(s) + \theta_z(s)\hat{D}(s) &= \Omega(s)\left[\hat{C}(s) - R_{gm}(s)\hat{D}(s)\right] \end{aligned}$$

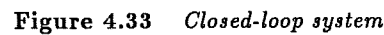
Let us notice that the previous equations are the same as 4.6 and 4.1 already seen (rewritten with the new plant notations). We can then set $\theta_y(s)$ according to

$$\theta_y(s) = \frac{R_{gm}(s)\check{\theta}_y(s)}{K_{gm}}$$

The two scalar gains θ_r and θ_{bi} are computed as

$$\theta_r = \frac{K_p r_n}{\hat{b}_0} \quad \theta_{bi} = K_{gm}$$

⁴We denote with $\vec{R}(s)$ the vector $(r_0, r_1, \dots, r_n)^T$, being $R(s) = r_0 s^n + r_1 s^{n-1} + \dots + r_n$


$$\frac{G(s)O(s)P(s)}{1 + G(s)O(s)P(s)}$$
$$\mathcal{AC}(s)O_D(s) + \mathcal{BD}(s)O_N(s) = \chi_{obs}(s)$$

Adaptive law

$$\hat{d}(t) = \frac{\mathcal{BC}(s)}{\Upsilon(s)} [\chi_{sb} [\hat{u}_s - \hat{z}(t)] + [\hat{\rho}_b - \hat{\rho}] \hat{w}]$$
$$e_i(t) \doteq y_{\mathcal{I}} - \phi(t)^T \hat{\theta}(t) - \hat{d}(t)$$
$$\frac{d}{dt} \hat{\theta}(t) = P(t) \phi(t) e_i(t) \quad (4.28)$$

75

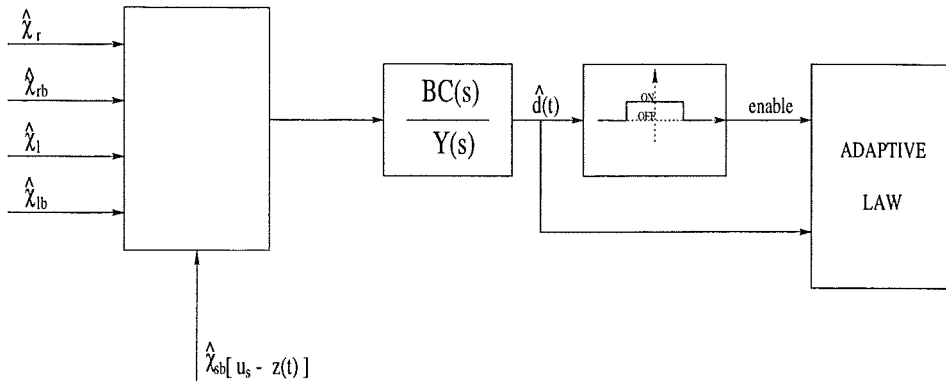


Figure 4.34 *Threshold disabling of the adaptive law*

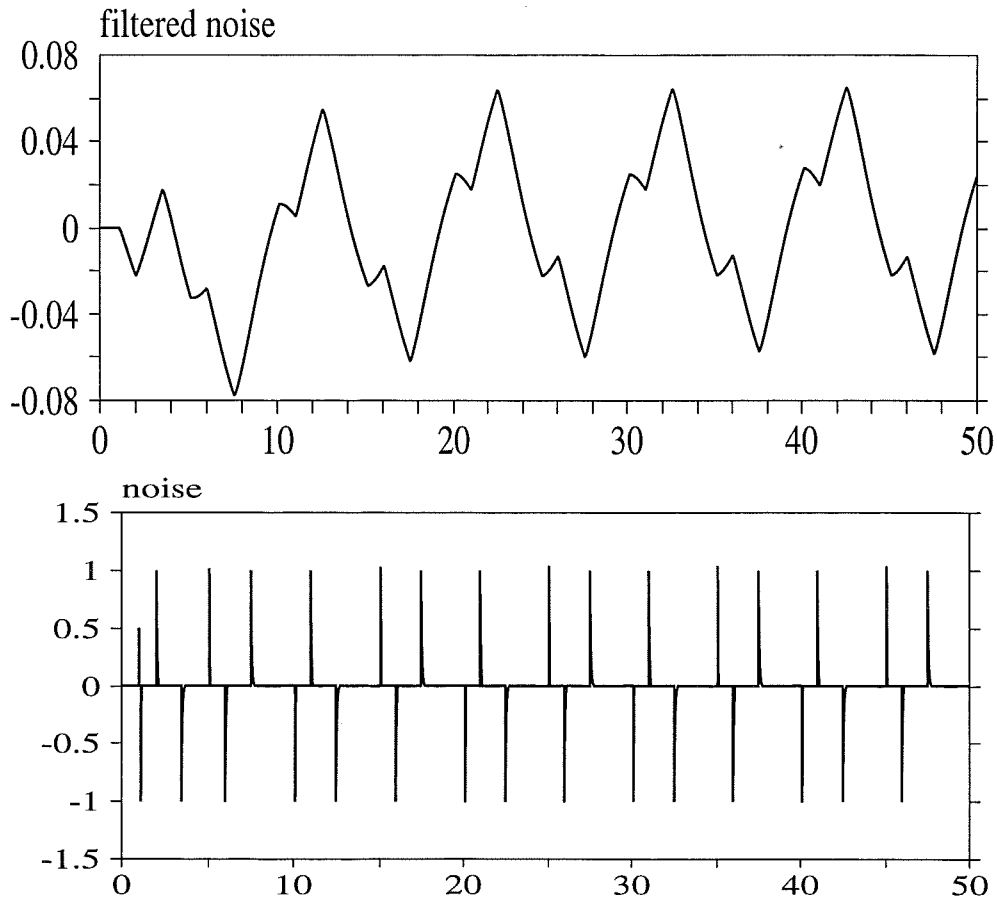


Figure 4.35 *Observed noise*

Let us notice that still a residual noise, due to the observation error, can excite the system. So it can be useful to have some kind of robustification for our algorithms. Besides whenever the estimated backlash works for too long time in the dead-zone, the estimated noise $\hat{d}(t)$ will grow up consistently and this can provoke a sudden estimates detuning. If we want to avoid this effect we must decide a threshold over which the updating of $\hat{\theta}$ is disabled. A plot of the residual parametrization noise is shown in Figure 4.35.

Simulation results

Example 14

This example take into consideration a quite critical situation where both the dynamic block and the plant are unstable. Besides, no a priori knowledge is assumed for the system poles since the parameters a_1 , a_2 and c_1 are initialized to zero. Notice that the plant parameters are updated only at discrete time events, while the width and the convoluted parameters have continuous time updating. Figures 4.36 and 4.37 refer to the following settings:

Plant transfer function	$P(s) = \frac{1}{s^2 + s - 1}$
Dynamic block function	$G(s) = \frac{1}{s - 0.5}$
Backlash parameters	$C_l = -0.5 \quad C_r = 0.5$
Reference model	$\frac{20\omega^2}{(s+20)(s^2+2\xi\omega s+\omega^2)} \quad \begin{matrix} \xi = 0.7 \\ \omega = 3 \end{matrix}$
Feedback polynomial	$\Lambda(s) = (s + 2)^3$
Forgetting factor	$\alpha = 0.1$
RLS polynomial	$\Upsilon(s) = (s + 0.5)^3$
Weight polynomial	$\Sigma(s) = (s + 0.5)(s + 1)(s + 2)(s + 3)$
Observer polynomial	$\chi_{obs}(s) = (s + 2)^5$

Notice that in the initial transient both the observer loop and the plant are unstable. Afterwards the convergence of the parameters becomes more precise and the observation error drops down quickly. Figures 4.37 also shows that in the time interval between approximately 10 sec. and 20 sec. the parameters estimates are constant. This is due to the threshold mechanism described in this section and illustrated in Figure 4.34.

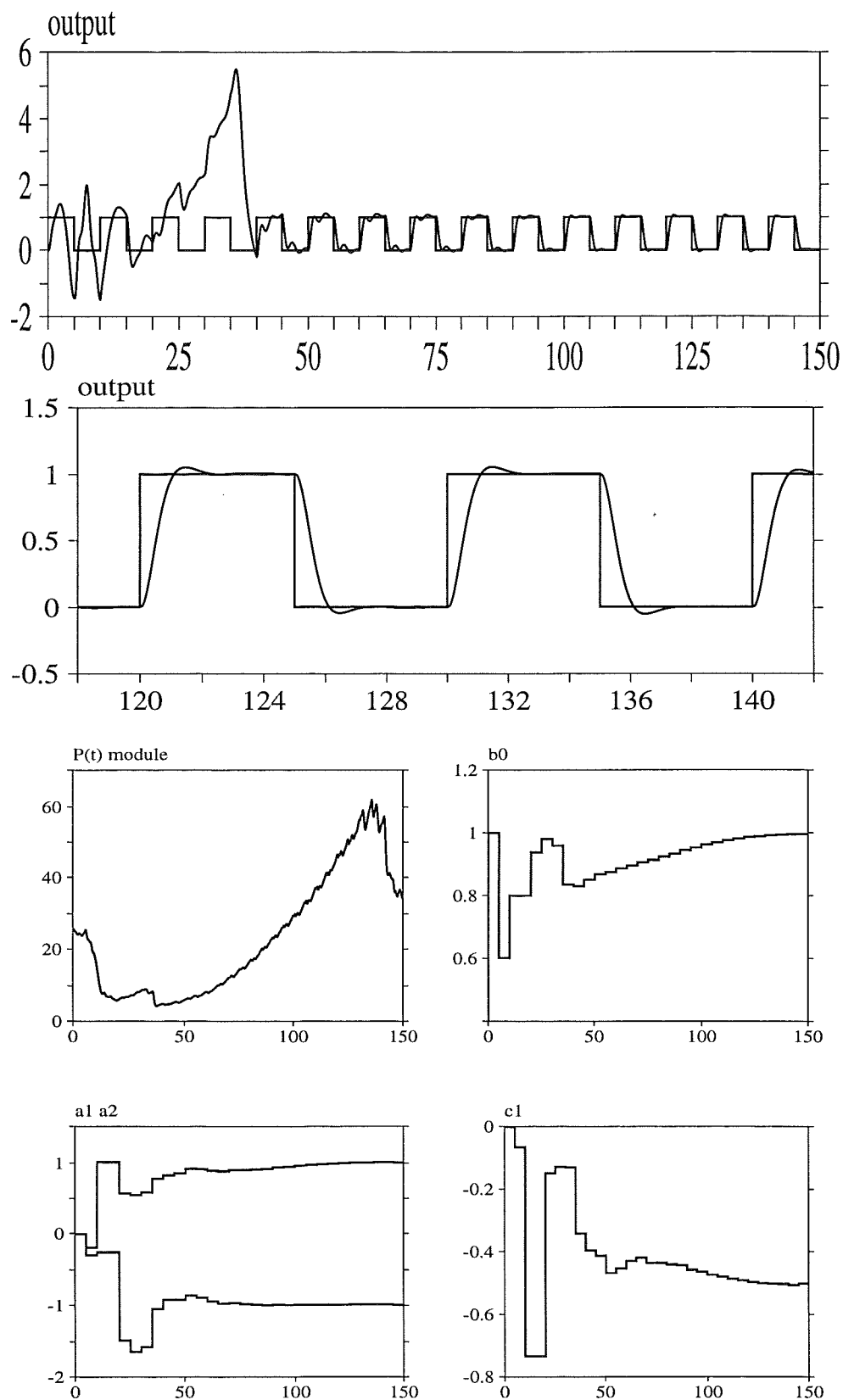


Figure 4.36 Simulation of Example 14

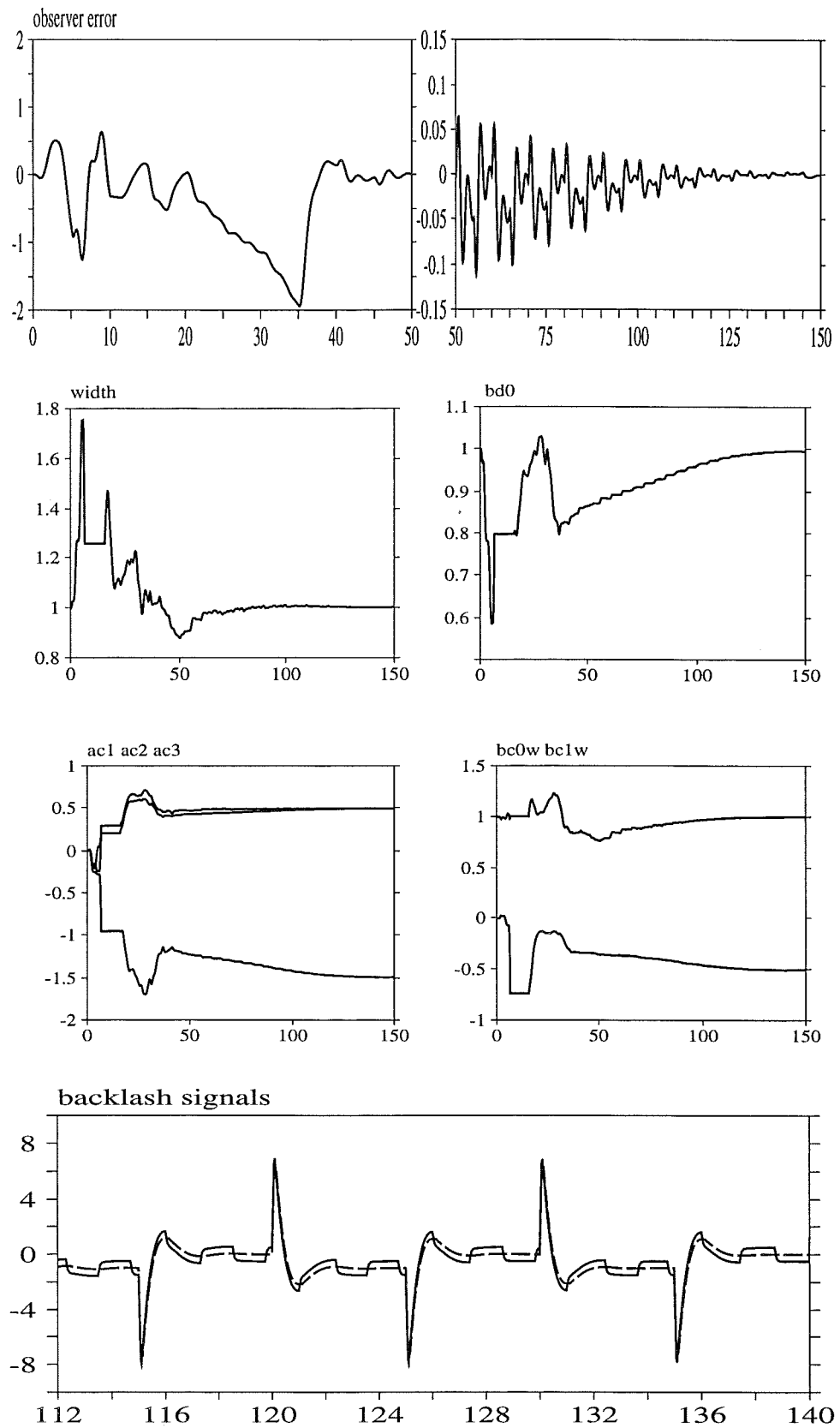


Figure 4.37 Simulation of Example 14

A. RLS continuous time implementation

Let us consider the standard exponential weighted RLS algorithm with forgetting factor α :

$$\begin{aligned} e(t) &= y(t) - \varphi^T(t)\hat{\theta}(t) \\ \frac{d}{dt}\hat{\theta}(t) &= P(t) \varphi(t) e(t) \\ \frac{d}{dt}P(t) &= \alpha P(t) - P(t) \varphi(t) \varphi^T(t) P(t) \end{aligned} \quad (\text{A.1})$$

The previous equations work properly only if the process is always excited. There are problems with the forgetting factor if the excitation is poor. If $P(t)\varphi(t)$ is close to zero for some amount of time, the matrix $P(t)$ will then grow up exponentially. This means that the estimates can abruptly detune whenever $P(t)\varphi(t)$ becomes different from zero. In a practical implementation we should avoid this kind situation. Let us consider the following matrix norm:

$$||P(t)|| \doteq \sqrt{\text{tr}(P^T P)}$$

Since our matrix is symmetric we will compute it as

$$||P(t)||^2 = \text{tr}(P^2)$$

In order to prevent $P(t)$ from windup we can write separately the equations of its norm and versor.

$$\frac{d}{dt}||P||^2 = 2 ||P|| \frac{d}{dt}||P|| \quad (\text{A.2})$$

If we recall the norm definition we obtain

$$\frac{d}{dt}\text{tr}(P^2) = 2\text{tr}(P\dot{P})$$

Substituting the expression of \dot{P} from eqn. A.1 we obtain

$$\frac{d}{dt}||P||^2 = 2 \left\{ \alpha ||P||^2 - \varphi^T P^3 \varphi \right\} \quad (\text{A.3})$$

Equating eqns. A.2 and A.3 we obtain

$$\frac{d}{dt}||P|| = \alpha ||P|| - \frac{\varphi^T P^3 \varphi}{||P||} \quad (\text{A.4})$$

Let us now define the versor Q of the matrix P

$$Q \doteq \frac{P}{||P||}$$

Deriving the previous equality we obtain

$$\frac{d}{dt}Q = \|P\| \left\{ (\varphi^T Q^3 \varphi) Q - Q \varphi \varphi^T Q \right\} \quad (\text{A.5})$$

We should notice here that only the norm equations depends explicitly from the forgetting factor α . If we want to prevent $\|P(t)\|$ from diverging exponentially we can modify eqn. A.4 in the following way:

$$\frac{d}{dt}\|P\| = \alpha \frac{\|P\|}{1 + \epsilon\|P\|} + \frac{\varphi^T P^3 \varphi}{\|P\|} \quad (\text{A.6})$$

where ϵ is a sufficiently small quantity. In this way even with poor excitation our matrix norm will grow up linearly with slope equal to $\frac{\alpha}{\epsilon}$. Let us notice in eqn. A.5 that

$$\|Q(t_0)\| = 1 \Rightarrow \|Q(t)\| = 1 \quad \forall t \geq t_0$$

Unfortunately the trajectories of eqn. A.5 with $\|Q(t)\| = 1$ are unstable. In order to have a proper evolution of our algorithm we can modify eqn. A.5 into the following:

$$\frac{d}{dt}Q = \|P\| \left\{ (\varphi^T Q^3 \varphi) Q - \|Q\|^2 Q \varphi \varphi^T Q \right\} \quad (\text{A.7})$$

If we combine eqns. A.6 and A.7 we obtain the RLS algorithm showed below:

$$e(t) = y(t) - \varphi^T \hat{\theta}$$

$$\frac{d}{dt}\hat{\theta} = \|P\| Q \varphi e(t)$$

(A.8)

$$\frac{d}{dt}\|P\| = \frac{\alpha\|P\|}{1 + \epsilon\|P\|} - (\varphi^T Q^3 \varphi)\|P\|^2$$

$$\frac{d}{dt}Q = \|P\| \left\{ (\varphi^T Q^3 \varphi) Q - \|P\|^2 Q \varphi \varphi^T Q \right\}$$

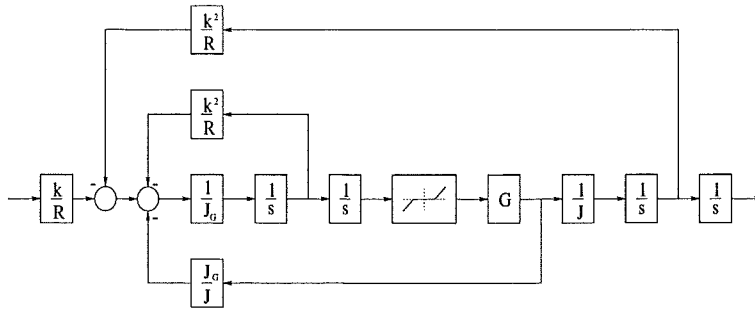


Figure B.1 Dynamic model of backlash ($G \rightarrow \infty$)

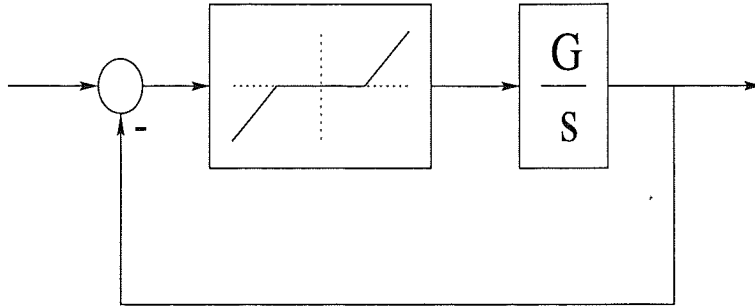


Figure B.2 Backlash approximation by dead-zone

B. Related works and future research

We would like to point out hereby some of the critical assumptions made throughout the present work and that, once removed, could constitute possible topics for a further research.

- The model of backlash we have considered is a static mathematical description of backlash phenomena. It is in some sense a zero-order approximation of what could be modeled in a very natural way as a fourth order system. A more complex backlash model, taking into account the inertial behavior of mechanical components is given in [6] (pages 206-209). Figure B.1 shows the mentioned backlash scheme. Results on how to approximate a static backlash operator by different non-linearities, such as dead-zones, are given in [4] (pages 90-93). In particular it is taken into consideration the backlash scheme of Figure B.2. This model tends to the static backlash if we let G tend to infinity.
- Still in [4] are given results about more general hysteresis operators and how to represent them in a canonical form via a backlash non-linearity. Figures B.3 and B.4 show some hysteresis operators and their canonical representation.
- A definition for *multidimensional* backlash is also presented in [4].
- In [3] the approach followed for backlash is also applied to other piecewise

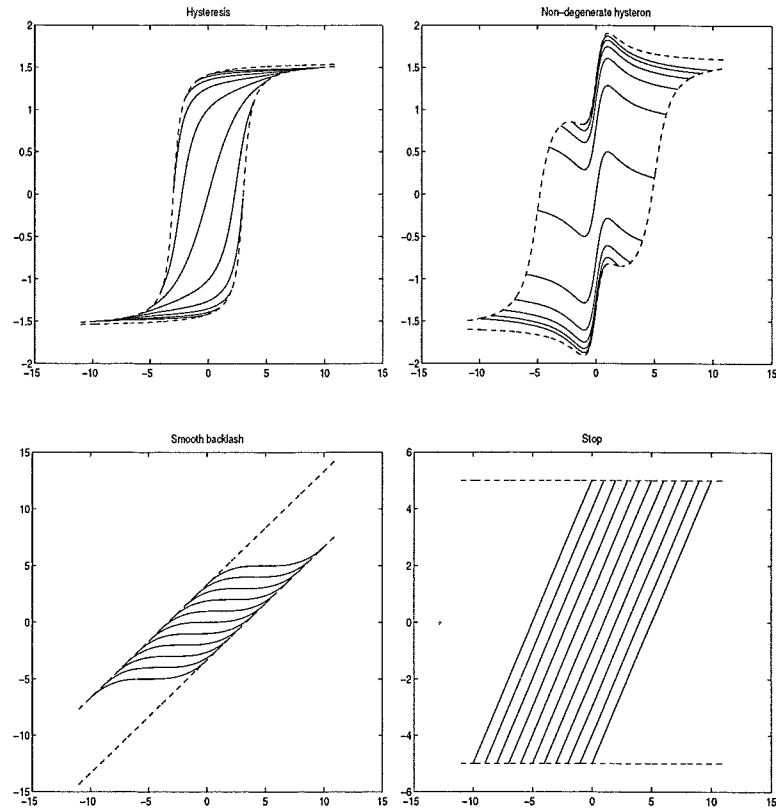


Figure B.3 *General hysteresis operators*

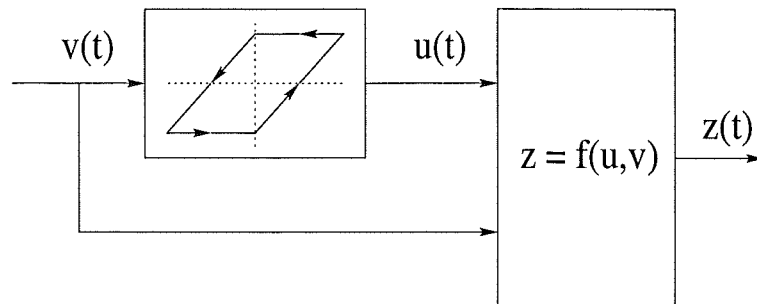


Figure B.4 *Canonical representation of hysteresis operators*

linear input-output characteristics, such as dead-zone or particular kinds of hysteresis non-linearities.

- It would be also interesting to remove the assumptions on the phase minimality of the plants and consider the problem of backlash inversion through *non-minimum phase* dynamic systems.
- In all the simulations we always assumed to be in the ideal situation in which there were no disturbances. In order to have algorithms that can possibly work for real systems we should pay a lot of attention to the robustification of the algorithms presented.

C. Bibliography

- [1] P. V. Kokotovic and G. Tao :
 "Continuous-Time Adaptive Control of Systems with Unknown Backlash"
 IEEE TRANSACTIONS ON AUTOMATIC CONTROL, VOL. 40, No.6,
 JUNE 1995
- [2] P. V. Kokotovic and G. Tao :
 "Adaptive Control of Systems with Backlash"
 Automatica, Vol. 29, No.2, 1993
- [3] P. V. Kokotovic and G. Tao :
 "Control of systems with actuator and sensor non-linearities"
 Addison Wesley 1996?
- [4] M. A. Krasnosel'skiĭ and A. V. Pokrovskiĭ :
 "Systems with Hysteresis"
 Springer-Verlag 1989 (Russian version 1983)
- [5] K. S. Narendra and A. M. Annaswamy :
 "Stable Adaptive Systems"
 Prentice Hall 1989
- [6] B. Friedland :
 "Advanced Control System Design"
 Prentice Hall 1996
- [7] J. E. Slotine and W. Li :
 "Applied Nonlinear Control"
 Prentice Hall 1991
- [8] E. Mosca :
 "Optimal, Predictive, and Adaptive Control"
 Prentice Hall 1995
- [9] K. J. Åström and B. Wittenmark :
 "Adaptive Control"
 Addison Wesley 1989